I INTRODUCTION

1.1 Reactivity of $[CpMo(CO)_n]_2$ [M = Cr, n =3 (1) or n = 2 (2); M=Mo, n=3 (3) or n=2 (4)]

1.1.1 Biscylopentadienyldichromiumhexacarbonyl, $[CpCr(CO)_3]_2$ (1)

Complex **1** was first synthesized in the late 1950's and reactivity studies in the 1960's by various research groups point to radical processes [1]. The X-ray crystal structure analysis by Adams, Collins, and Cotton in 1974 showed the presence of an unusually long Cr−Cr bond (3.281(1) Å) [2] which is much longer than that of its heavier congener molybdenum and tungsten analogues. This difference was attributed to steric repulsion between ligands in the two halves of the molecule. Cotton suggested that the dimer should readily dissociates into 17-electron $CpCr(CO)_3\cdot$ (**1A**) radicals (Eqn.1) and this was later established by (i) UV-VIS studies by McLain, which showed 10% dissociation to monomer radical **1A** at room temperature in a 10 mM solution [3]; (ii) ESR, UV-VIS and IR studies by Vahrenkamp [4]; and (iii) ESR and NMR studies by Goh *et* al [5]. The reactions of $[CpCr(CO)_3]_2$ with the homo- and hetero-polyatomic molecules of Groups 15 and 16 and diaryl dichalcogenides via a homolytic cleavage and aggregation pathways have been reviewed by Goh *et al*. The wide range of reactions of **1** includes recombination, atom abstraction, electron transfer, ligand association and rearrangement, which resembles intimately those of organic radicals [6]. Some of these reactions such as halogen abstraction, hydrogenation and acyl migratory insertion are important elementary steps in catalytic cycles. The high reactivity of **1** derives from the homolytic attack of **1A** on hydrogen [7], halogens and organic substracts eg, thiols [8], hydrogen sulfide [9], disulfides [10], organic halides [11a-b] and trialkyltin hydrides [12]. In addition, substitution [13] and disproportionation [11c] reactions of **1** are also well documented.

1 1A

…Eqn.(1)

1.1.2 Biscyclopentadienyldichromiumtetracarbonyl, $[CpCr(CO)_2]_2$ (2)

$[CpCr(CO)_2]_2$ (**2**) is the thermolytic congener of **1** (Eqn.2). Dimer **2** is less reactive compared to **1**. Its triply bonded Cr≡Cr bond distance in dimer **2** is shorter than 2.230(3) Å [14]. The short bond distance of **2** limits the tendency of homolytic metal-metal bond cleavage and thermal energy is needed to initiate a reaction with **2**.

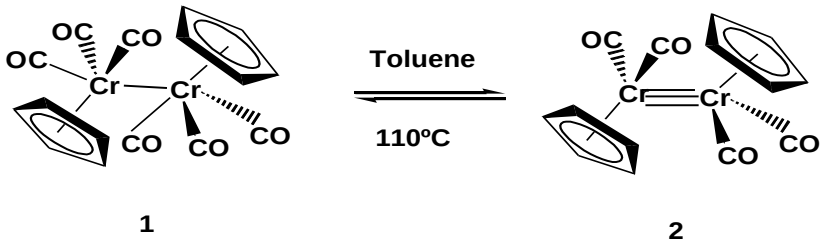

1 2

...Eqn.(2)

1.1.3 Biscyclopentadienyldimolybdenumhexacarbonyl, $[CpMo(CO)_3]_2$ (3)

Dimer **3** is less reactive when compared with its Cr analogue. A shorter bond length of the Mo-Mo bond (3.235(1) Å) decreases the reactivity of the complex [15a-b] and it does not give rise to the formation of the $17e^-$ radical species when it dissolves in the solution [16]. In general, **3** needs to be heated or photolyzed under UV irradiation to initiate a reaction (Eqn.3).

3 **3A**

… Eqn.(3)

1.1.4 Biscyclopentadienyldimolybdenumtetracarbonyl, $[CpMo(CO)_2]_2$ (4)

$[CpMo(CO)_2]_2$ (**4**) complex continues to attract interest and is a more reactive alternative to $Cp_2Mo_2(CO)_6$ (**3**) as a starting material in CpMo chemistry. **4** was first isolated by Job and Curtis from the photolysis of $CpMo(CO)_3GeMe_2(C_2H_3)$ [17]. Then, Ginley and Wrighton observed the formation of **4** during the photolysis of $Cp_2Mo_2(CO)_6$ (**3**) [18]. Later, Curtis *et al* reported that the thermolysis of $Cp_2Mo_2(CO)_6$ (**3**) at 100-120 ^oC in toluene or xylene solutions led to a formation of **4** (Eqn.4). Thermal formation of **4** proceed simultaneously with the rupture of the Mo-Mo bond of the $Cp_2Mo_2(CO)_6$ precursor. $[CpMo(CO)_2]_2$ (**4**) reacts with soft nucleophiles, e.g. phosphines and phosphites ; however, the presence of π-bond charge density in the complex allows **4** to react with many electrophilic reagents [19]. The structure of **4** was shown to have a linear Cp-Mo-Mo-Cp skeleton and four terminal carbonyls [20]. The terminal carbonyls are linear, as opposed to

the nonlinear M-CO structure usually associated with terminal carbonyls. It was proposed that these two classes of terminal carbonyls represent donor (linear) and acceptor (nonlinear) interactions.

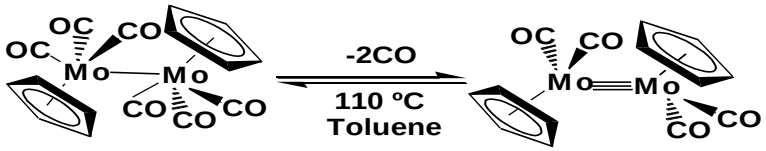

3 4

…Eqn.(4)

1.2 A review on the synthesis and reactivity of molybdenum and chromium with organochalcogenide ligands

1.2.1 Organochalcogenide derivatives of chromium complexes

King has synthesized $[Cp_2Cr_2(SCH_3)]$, a dark purple solid from the reaction of $[CpCr(CO)_3]_2Hg$ or $[CpCr(CO)_3]_2$(**1**) with dimethy disulfide in refluxing metylcyclohexane [21]. However, $[CpCr(CO)_3]_2$(**1**) gave a much better quality product compare to $[CpCr(CO)_3]_2Hg$. Due to insufficient inert atmosphere working facilities, the air sensitive $[Cp_2Cr_2(SCH_3)]$ decomposed easily even in a sealed vial flushed with nitrogen.

After two decades, due to the awareness of the rich chemistry of $[CpCr(CO)_3]_2$(**1**), Goh *et al.* continued to investigate the reactivity of **1** toward the chalcogens [22a-d] and later a more in-depth studies of **1** with a series of diphenyl dichalcogenide ligands, Ph_2E_2 (E=S[23], Se[24], Te[25]). Reaction of **1** with Ph_2S_2 at various temperature had afforded $[CpCr(CO)_2(SPH)]_2$, $[CpCr(CO)(SPh)]_2$ and $[CpCr(SPh)]_2S$ (Scheme 1). The known susceptibility of the S-S bond in organic disulfides to cleavage by nucleophilic, electrophilic, and radical processes [26], it is conceivable that

the initial step of this reaction involves the attack of the $CpCr(CO)_3\cdot$ radical towards the S-S bond of organic disulfide which resulting in thiolate-bridged dimers. Thermolysis studies showed that the degradation by stepwise decarbonylation of $[CpCr(CO)_2(SPH)]_2$ and $[CpCr(CO)(SPh)]_2$ to give $[CpCr(SPh)]_2S$ and ultimately to the cubane cluster, $Cp_4Cr_4S_4$.

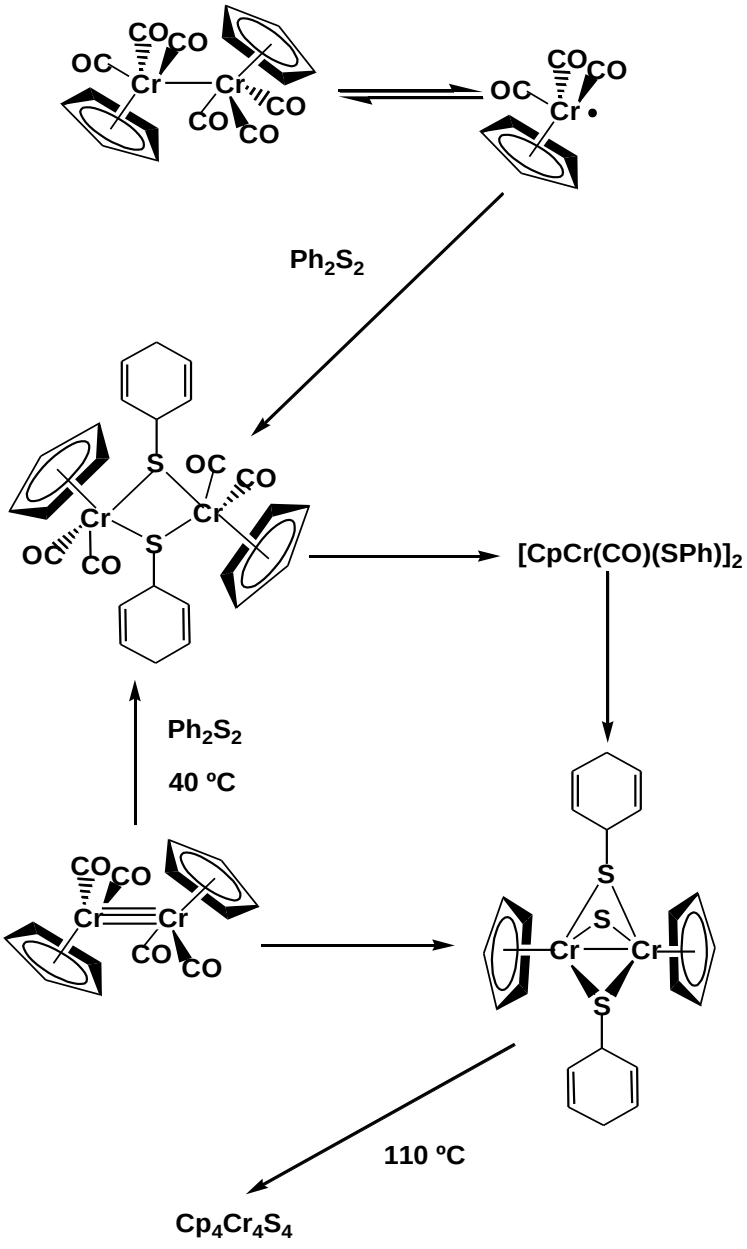

Scheme 1

Reaction of $[CpCr(CO)_3]_2$(**1**) with 1 molar equivalent of Ph_2Se_2 at ambient temperature had afforded $[CpCr(CO)_3SePh)]$ and $[CpCr(CO)_2(SePh)]_2$. At elevated temperatures, $[CpCr(CO)_3SePh)$ underwent decarbonylation with concomitant coupling to yield $[CpCr(CO)SePh]_2$ and finally $[CpCr(SePh)]_2Se$ (Scheme 2). The facile of the reaction originated from the 17e $[CpCr(CO)_3]$ radical species and the susceptibility of the Se-Se bond in Ph_2Se_2. It is noted that the mononuclear complex $[CpCr(CO)_3SPh]$, the sulfur analogue of $[CpCr(CO)_3SePh)]$, was not detected in the reaction of Ph_2S_2. Presumably, the higher electronegativity of S, compared to Se will result in a large δ^+ charge at the metal centre, and less π back bonding to the CO ligands, which therefore become less strongly bonded to the metal. Hence the ease of loss of CO from $[CpCr(CO)_3EPh]$ will concomitant dimerisation to form $[CpCr(CO)_2(SePh)]_2$ will he higher for E=S than for E=Se.

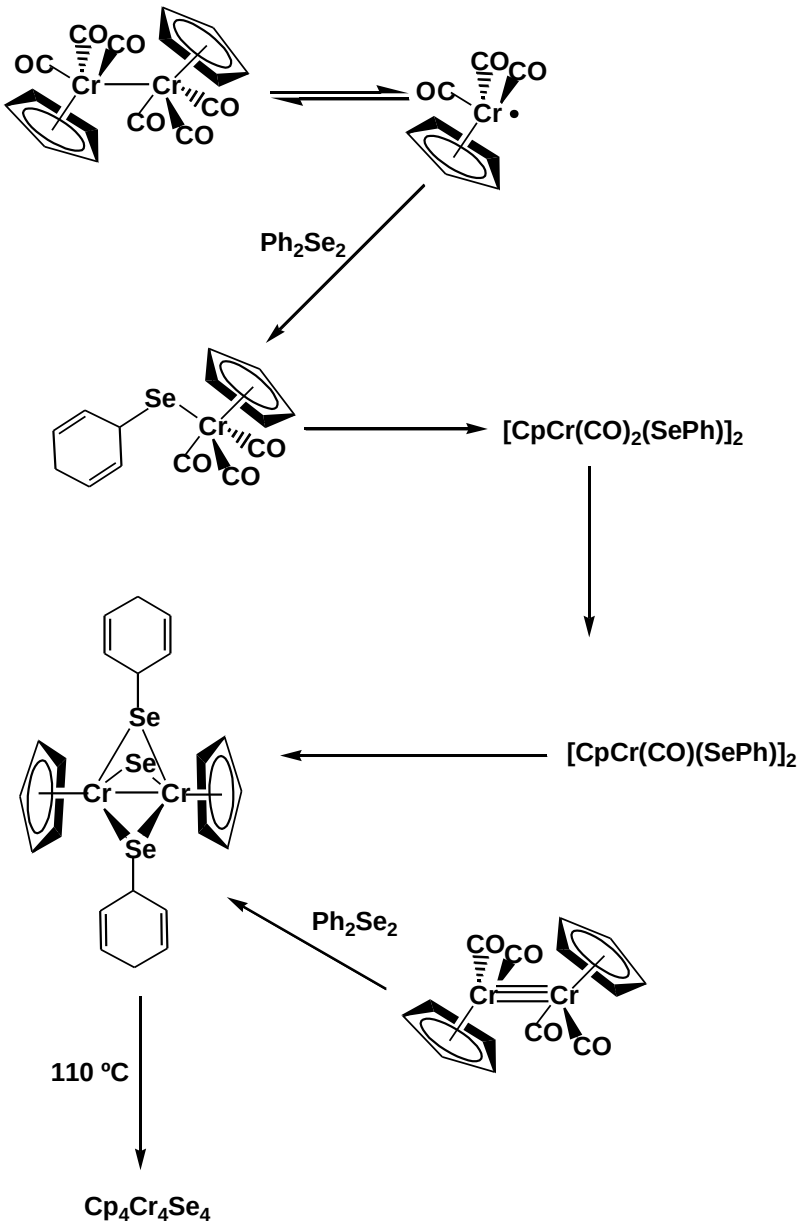
CO
CO
OC
Cr
Cr
CO
CO
CO
OC
Cr
Ph2Se2
Se
Cr
CO
CO
CO
[CpCr(CO)2(SePh)]2
[CpCr(CO)(SePh)]2
Se
Se
Cr
Cr
Se
Ph2Se2
CO
CO
Cr
Cr
CO
CO
110 ºC
Cp4Cr4Se4

Scheme 2

Another reaction of $[CpCr(CO)_3]_2$(**1**) with Ph_2Te_2 at ambient temperature had led to the isolation of $CpCr(CO)_3(TePh)$; where $[CpCr(CO)_2(TePh)]_2$ and $[CpCr(TePh)]_2Te$ were isolated at elevated temperature. From the thermolysis studies, it showed an interconversion between $CpCr(CO)_3(TePh)$ and $[CpCr(CO)_2(TePh)]_2$ followed by a slow total decarbonylation to $[CpCr(TePh)]_2Te$ (Scheme 3).

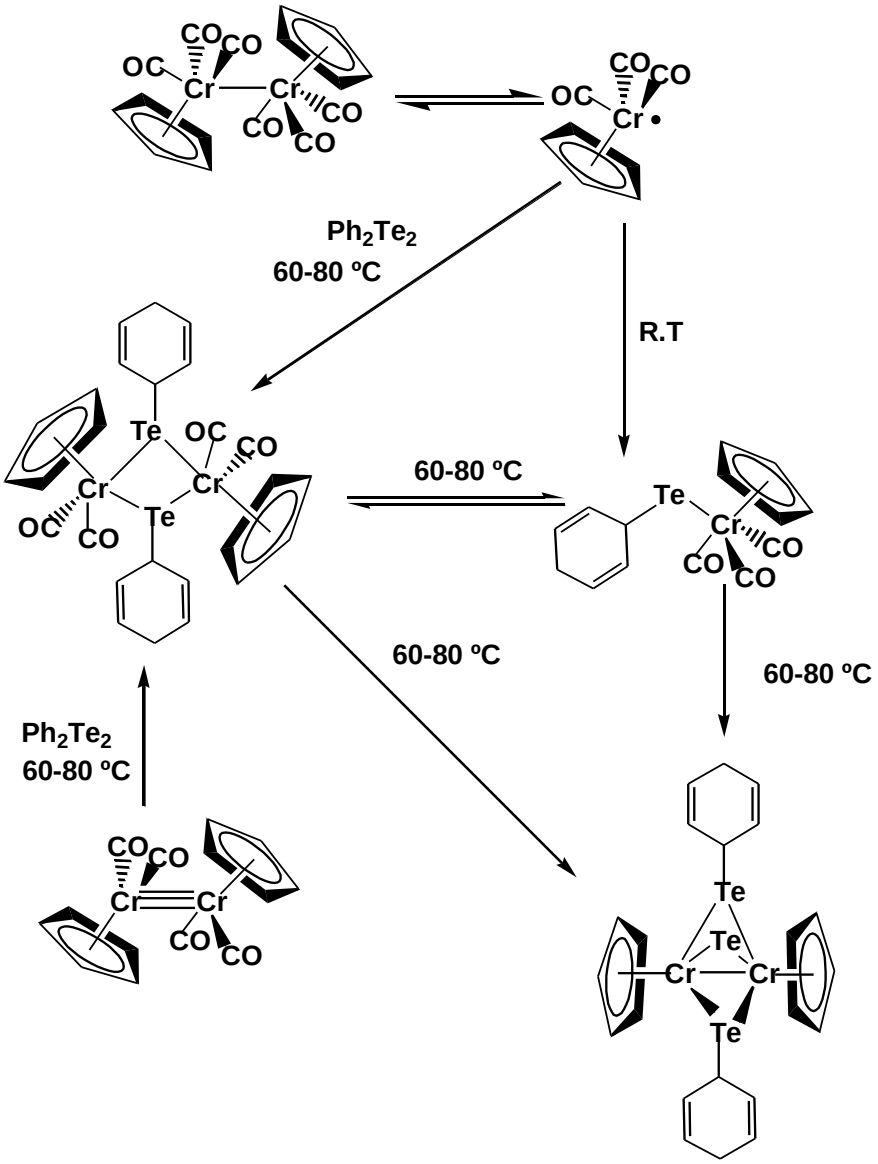

Scheme 3

1.2.2 Organochalcogenide derivatives of molybdenum complexes

In 1962, King investigated the reaction between $[CpMo(CO)_3]_2$(**3**) and dimethyl disulfide in refluxing methylcyclohexane for few hours. From the reaction, a brown solid $[CpMo(CH_3S)_2]_2$ was isolated. NMR and magnetic balance measurements indicated that $[CpMo(CH_3S)_2]_2$ is a diamagnetic compound. Insolubility of $[CpMo(CH_3S)_2]_2$ in organic solvents led to unsuccessful determination of molecular weight [21]. Under various reaction conditions, cyclopentadienylmolybdenum carbonyl derivatives and disulfides can form compounds of either the types $[CpMo(CO)_2SR]_2$ or $[CpMo(SR)_2]_2$.

However, Treichel *et al* also reported a similar reaction between $[CpMo(CO)_3]_2$ (**3**) and dimethyl disulfide at room temperature which led to the formation of brown crystalline $[CpMo(CO)_2SCH_3]_2$ [27]. Later, Treichel *et al* continued to study the reactivity of $[CpMo(CO)_3]_2$ (**3**) with cyclohexene sulfide in benzene solution. The following compounds were characterized: $[CpMo(CO)_2SC_6H_{11}]_2$, $[CpMo(CO)_3SC_6H_{11}]$, and a pair isomers of $[CpMoS_2C_6H_{10}]_2$ together with two uncharacterized products [28]. This finding agrees with the earlier hypotheses by King about the formation of derivatives with the general formula $[CpMo(CO)_2SR]_2$ or $[CpMo(SR)_2]_2$.

Several years later, Tillay *et al* used $[CpMo(CO)_3]_2$ (**3**) to react with aryl dichalcogenide ligands, Ph_2E_2 (E=S, Se, or Te) [29]. Reaction of **3** with diphenyl ditelluride afforded several complexes depending on the reaction conditions (Scheme 4). $[CpMo(CO)_2(TePh)]_2$ was obtained under rigorous conditions in refluxing benzene for 14 h. Formation of dinuclear $[CpMo(CO)_2(TePh)]_2$ complex appeared to proceed via initial formation of mononuclear $[CpMo(CO)_3(TePh)]$ in the reaction mixture, as was ascertained by monitoring the progress of the reaction by occasional withdrawal of samples for infrared examination. The mononuclear complex, $[CpMo(CO)_3(TePh)]$ was isolated by employing very mild reaction conditions which was stirring the reactants in benzene at 25 ^oC for 2.5 h.

Dinuclear $[CpMo(CO)_2(TePh)]_2$ was then formed when $[CpMo(CO)_3(TePh)]$ was thermally decomposed. However, the major product of the prolonged reaction of **3** and Ph_2Te_2 in refluxing xylene was the completely decarbonylated compound $[CpMo(TePh)_2]_x$.

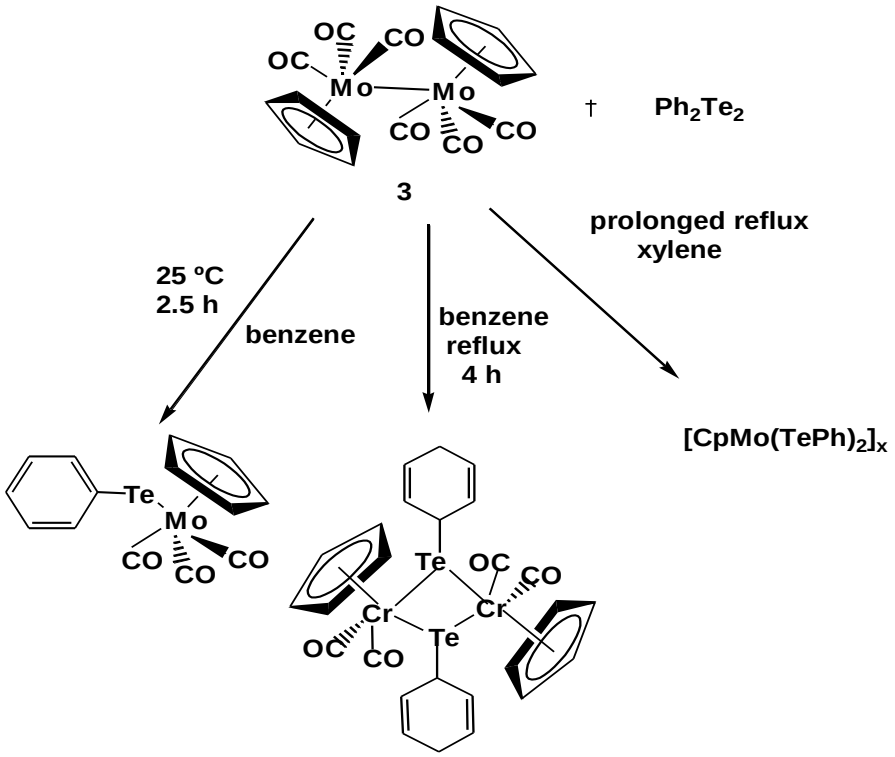

Scheme 4

Reaction of **3** with Ph_2Se_2 under milder condition afforded two complexes, mononuclear $[CpMo(CO)_3(SePh)]$ and a completely decarbonylated $[CpMo(SePh)_2]_x$. From the reaction mixtures, several other complexes including dinuclear $[CpMo(CO)_2(SePh)]_2$ was observed and there was evidence from the infrared monitoring (Scheme 5). When the reaction was stirred at 10 ºC for 2 h, the violet solid, $[CpMo(CO)_3(SePh)]$ was isolated out. In refluxing benzene for several hours, infrared sampling indicated that the selenium analog of $[CpMo(CO)_2(TePh)_2$ was present in solution. But, unlike the tellurium complex, $[CpMo(CO)_3(SePh)]$ transformed fairly rapidly into other carbonyl-containing complexes which was however, not isolated. After prolonged reaction, a very insoluble, amorphous product, $[CpMo(SePh)_2]_x$ was obtained.

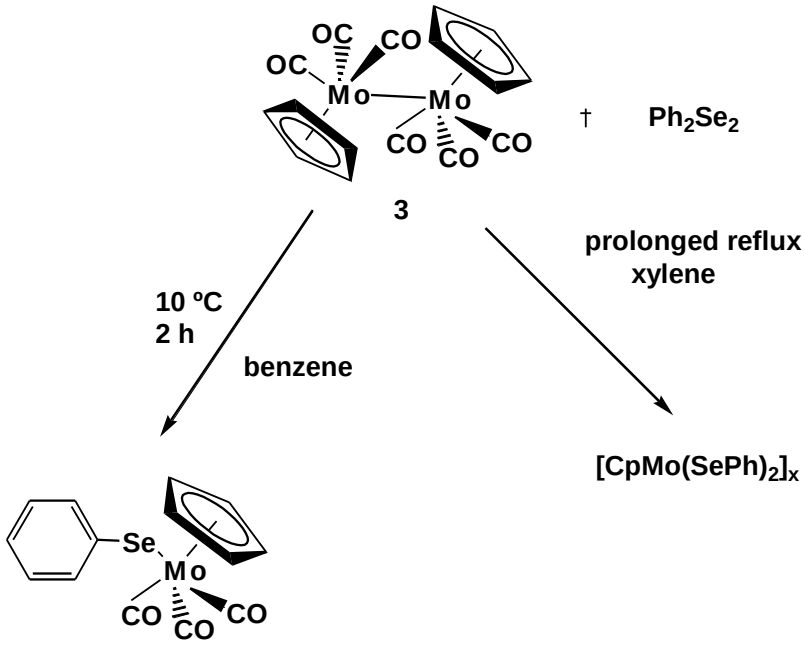

Scheme 5

Compare with the reactions of **3** with Ph_2Te_2 and Ph_2Se_2, its reaction with Ph_2S_2 was more rapid. However, only one product was isolated, the completely decarbonylated material $[CpMo(SPh)_2]_x$ (Eqn.5). Several carbonyl containing species were present in the reaction mixture from the infrared evidence. After the reactants had been stirred in benzene at 10 ºC for 10 min, the infrared spectrum of a withdrawn sample showed a sharp band at 2033 cm^{-1} , indicative of mononuclear $[CpMo(CO)_3(SPh)]$. Various attempts to enhance the concentration of this species failed; hence it could not be isolated. Infrared monitoring showed no evidence for the presence of dinuclear $[CpMo(CO)_2(SPh)]_2$ in the reaction mixtures.

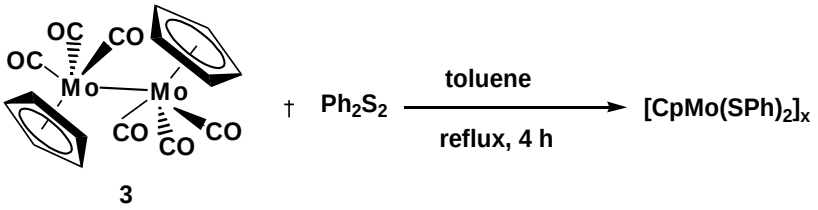

…Eqn.5

From the infrared data collected, it is suggested that π bonding between molybdenum and carbon monoxide is strongest in the tellurium complex, and the stabilities of $[CpMo(CO)_3EPh]$ (E : S, Se, Te) as observed in the preparative experiments indicate that the ability of the chalcogen to stabilize the mononuclear species decreases in the order E= Te > Se > S. Thus the greater "softness" of tellurium and selenium relative to sulfur results in a less positive charge on the molybdenum, and π bonding to CO is thereby enhanced. Decomposition of $[CpMo(CO)_3(EPh)]$ by loss of carbon monoxide to form $[CpMo(CO)_2(EPh)]_2$ therefore decreases in the order E : S > Se > Te.

In 1980's Benson *et al* is the first to report the X-ray structures of $[CpMo(CO)_2(SPh)]_2$ and $[CpMo(CO)(SBut)]_2$ [30] (Figure 1 & 2). From this finding, the complexes $[CpMo(CO)_2(SR)]_2$ (R= Me, Bu^t, Ph, *p*-tolyl), which do not contain metal-metal bonds, decarbonylate on heating to afford $[CpMo(CO)(SR)]_2$, which has a formal double metal-metal bond. Various isomers are possible for these complexes, based on *cis* or *trans* arrangements of the cyclopentadienyl ligands (with respect to the Mo_2S_2 ring) and on mutually *syn* or *anti* orientations of the R groups at sulphur. I.R and NMR spectra reveal that such isomers do exist, often interconverting rapidly on the NMR time-scale as a consequence of pyramidal sulfur inversion.

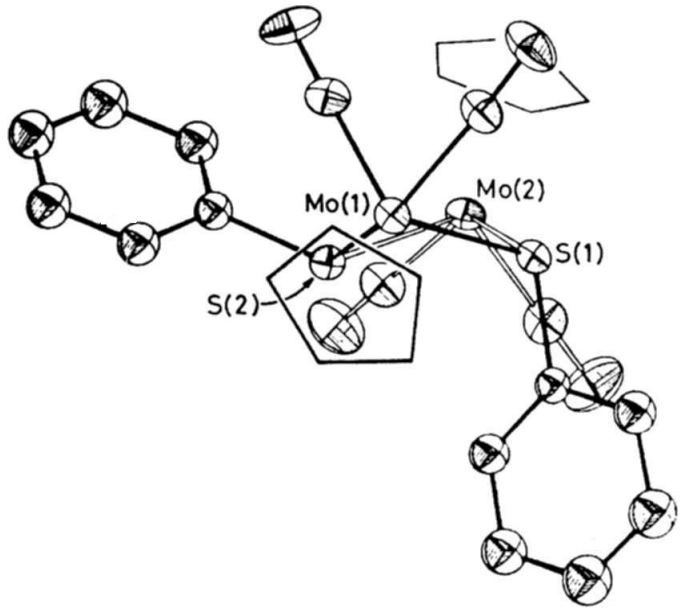

Figure 1. Molecular structure of $[CpMo(CO)_2(SPh)]_2$

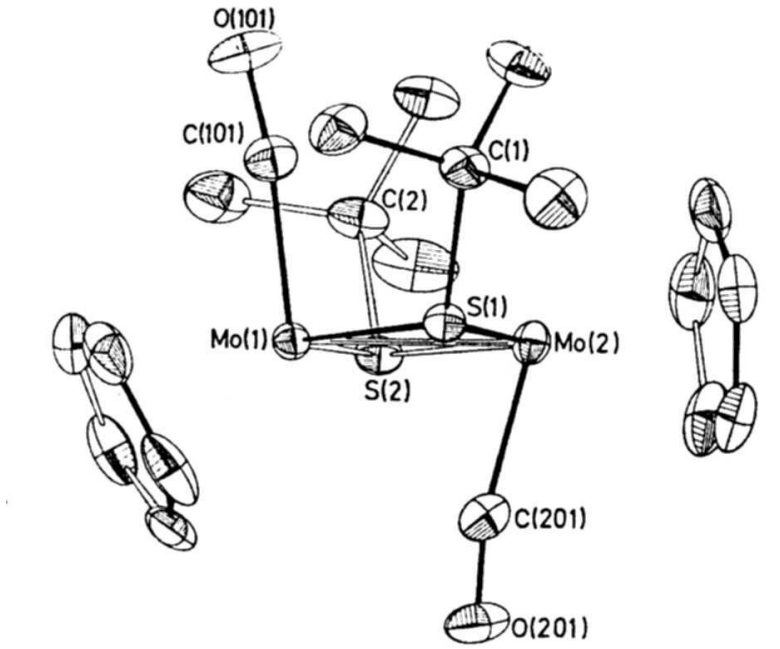

Figure 2. Molecular structure of $[CpMo(CO)(\mu\text{-}SBu^t)]_2$.

In 1990's, the synthesis and reactivity studies of organochalcogenide derivatives of molybdenum complexes continued to grow rapidly. Ziegler and his co-workers have synthesized a doubly-bridged complex, $[CpMo(CO)^2(\mu\text{-}SePh)]$, containing no metal-metal bond by reacting Mo dimer **4** with PhSeMgBr or PhSeLi [31]. Further investigation indicated that $[CpMo(CO)_2(\mu\text{-}SePh)]$ undergoes decarbonylation by reaction with selenium powder to produce a fourfold-bridged $[CpMo(\mu\text{-}Se)(\mu\text{-}SePh)]_2$ which contained a formal metal-metal double bond. The structures of $[CpMo(CO)_2(\mu\text{-}SePh)]$ and $[CpMo(\mu\text{-}Se)(\mu\text{-}SePh)]_2$ were shown in Figure 3 & 4. Ziegler's works has shown the presence of an alternative pathways to synthesize molybdenum organochalcogen derivatives with general formula of $[CpMo(CO)_2(\mu\text{-}SR)]_2$.

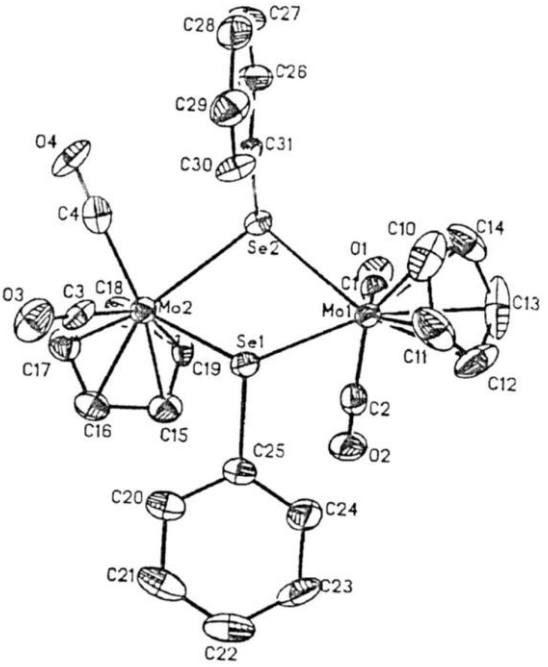

Figure 3. Molecular structure of $[CpMo(CO)_2(\mu\text{-}SePh)]_2$.

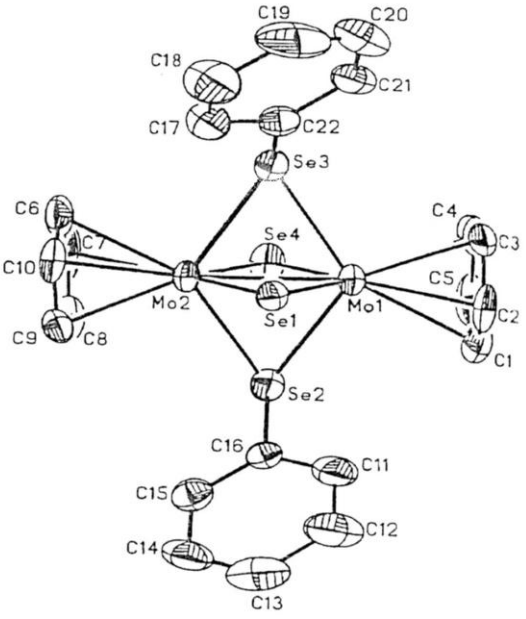

Figure 4. Molecular structure of $[CpMo(\mu\text{-}Se)(\mu\text{-}SePh)]$.

Song and co-workers have contributed a lot of important information in the area of organochalcogenide molybdenum reactivity studies. Song *et al.* have reported an alternative route to synthesize Mo=Mo doubly bonded complexes $[(\eta^5\text{-}RC_5H_4)Mo(CO)(\mu\text{-}SPh)]_2$ (R= H, MeCO) by the reaction of $[(\eta^5\text{-}RC_5H_4)Mo(CO)_2]_2$ with $(\mu\text{-}SPh)_2Fe_2(CO)_6$ [32]. Each of the complexes consists of two isomers which is *trans/anti* and *trans/syn*, in terms of the relative arrangement of the RC_5H_4 and CO ligands and the mutual orientation of the phenyl groups on the bridging sulfur atoms (Scheme 6).

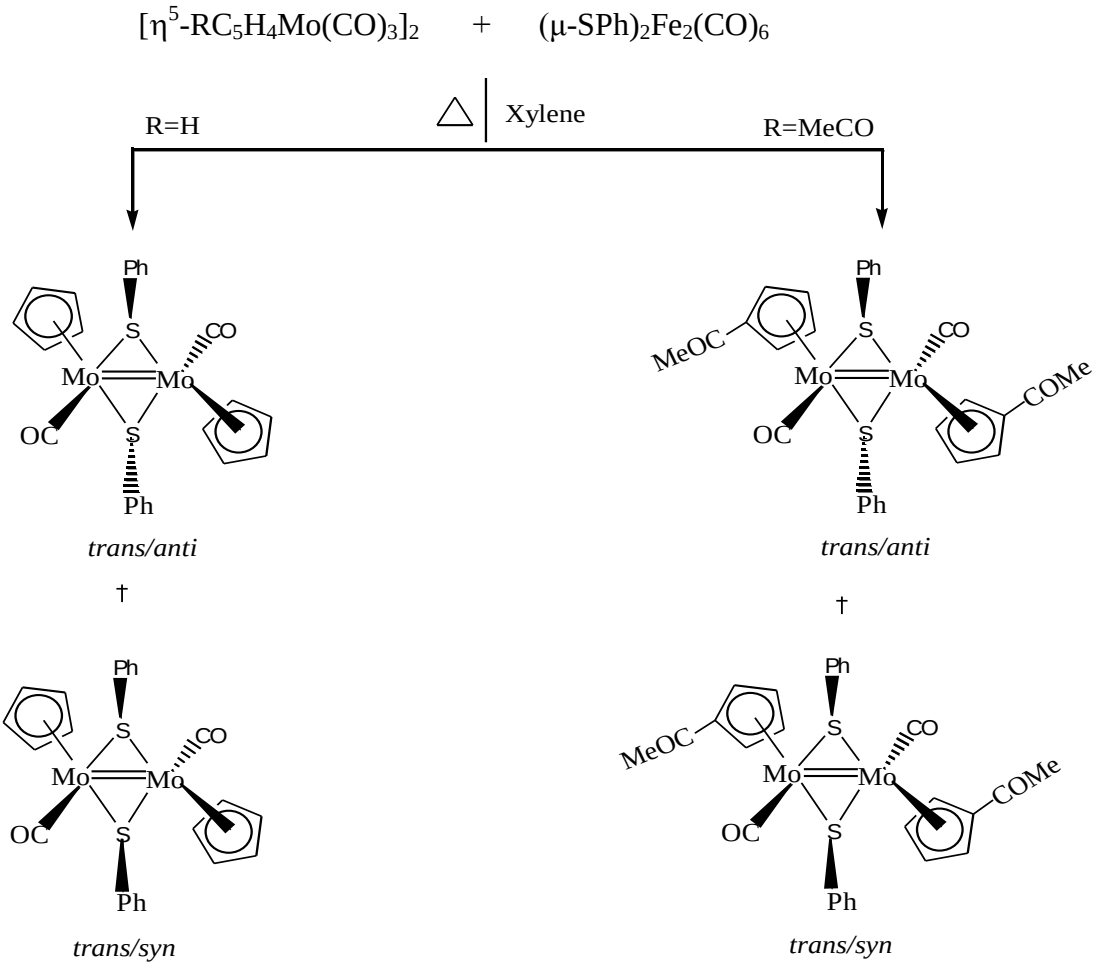

Scheme 6.

The two isomers with R= MeCO are convertible to each other by refluxing in xylene and their structures have been crystallographically determined by X-ray diffraction (Figure 5 & 6). The mechanism involves one of the Mo-S bonds coaxed to relax first to produce a transition state, in which two orbitals of the sulfur atom with lone electron pairs each may overlap with an empty d-orbital of the Mo atom, generated from the laxity of the Mo-S bond. Then, further rotation around the other Mo-S bond would accomplish this conversion.

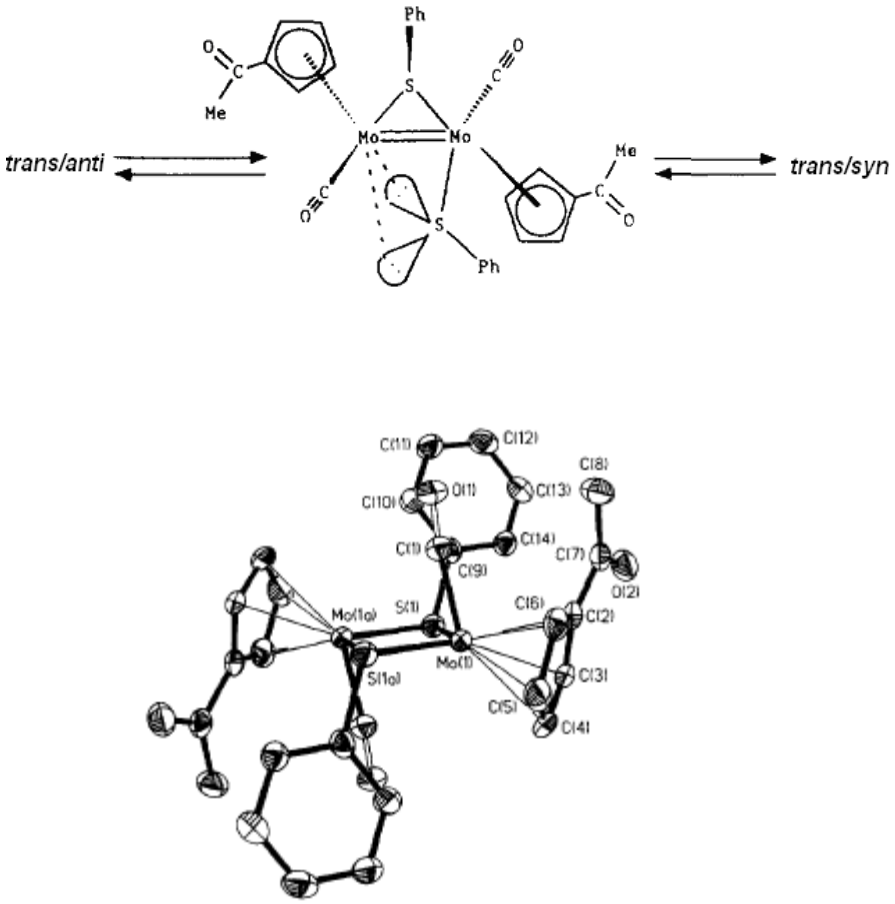

Figure 5. Molecular structure of *trans/anti*-[(η^5-$MeCOC_5H_4$)Mo(CO)(μ-SPh)]$_2$

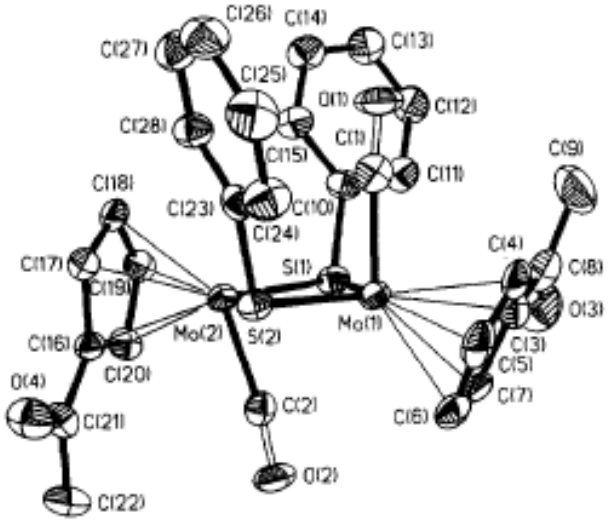

Figure 6. Molecular structure of *trans/syn*-[(η^5-$MeCOC_5H_4$)Mo(CO)(μ-SPh)]$_2$

Later Song continued to extend the studies of [(η^5-RC_5H_4)$Mo(CO)_2$]$_2$ (R= H, MeCO, MeO_2C, EtO_2C) with Ph_2Se_2 in refluxing toluene to afford the metal-metal doubly bonded isomers *trans/syn* and the *trans/anti*-[(η^5-RC_5H_4)$Mo(CO)_2$(μ-SePh)]$_2$ (Scheme 7) [33]. It was observed that two types of isomers for the Mo complexes have markedly different physical properties. For example,the *trans/syn* isomers are brown in color, whereas the *trans/anti* isomers are green.

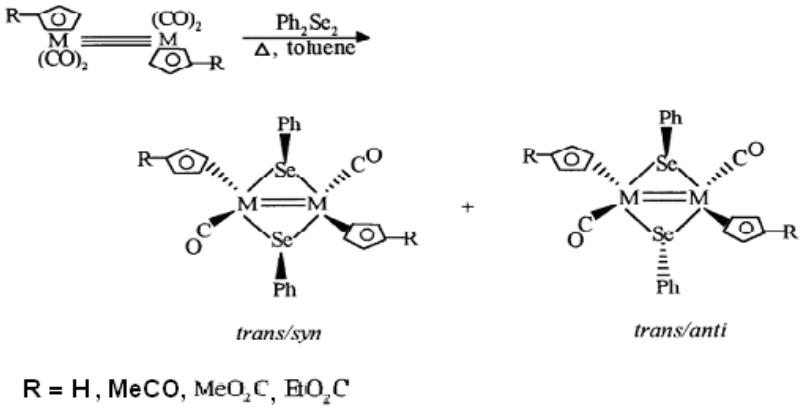

Scheme 7

Song *et al.* further investigated the reaction of $[(\eta^5\text{-}RC_5H_4)Mo(CO)_2]_2$ (R =H, Me_3Si, MeCO) with Ph_2Te_2 in refluxing toluene which resulted in the isolation of a series of doubly bridged complexes $[(\eta^5\text{-}RC_5H_4)Mo(CO)_2(\mu\text{-}TePh)]_2$ (R =H, Me_3Si, MeCO) [34]. However, when a similar reaction was repeated using $[(\eta^5\text{-}MeC_5H_4)Mo(CO)_2]_2$ as the precursor, not only the corresponding doubly bridged complex $[(\eta^5\text{-}MeC_5H_4)Mo(CO)_2(\mu\text{-}TePh)]_2$ was isolated but also an unexpected triply bridged complex $[(\eta^5\text{-}MeC_5H_4)_2Mo_2(CO)_4(\mu\text{-}TePh)_3]$. This observation indicated that the substituent R at the Cp ring has influence upon the type of reaction products (Scheme 8).

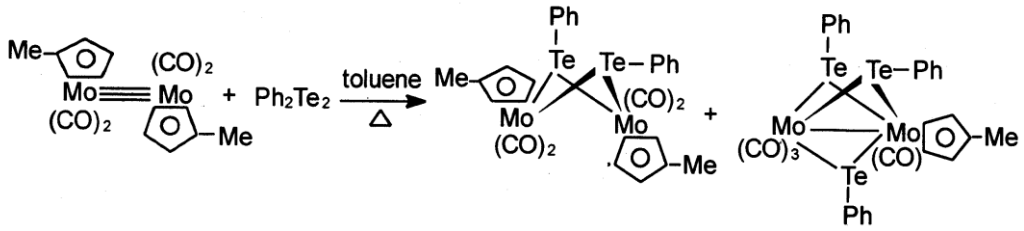

Scheme 8

Pétillon *et al.* have contributed an important study in the area of organochalcogenide derivatives of molybdenum complexes. In 1995, they reported the oxidative addition of thiols or selenoles across the Mo≡Mo centre of $[(\eta^5\text{-}Cp)Mo(CO)_2]_2$ (**4**) which gave complexes with bridging thiolate or selenate and hydride ligands $[Cp_2Mo_2(\mu\text{-}H)(\mu\text{-}ER)(CO)_4]$ (E=S, R=Me, tBu, Bz, Ph; E=Se, R=Ph) [36]. $[Cp_2Mo_2(\mu\text{-}H)(\mu\text{-}SMe)(CO)_4]$ was also formed from the reaction of $[Cp_2Mo_2(\mu\text{-}SMe)_2(CO)_4]$ with vanadocene $[VCp_2]$ with the possible involvement of a thioaldehyde, a hydride derivative of the vanadocene (Scheme 9)

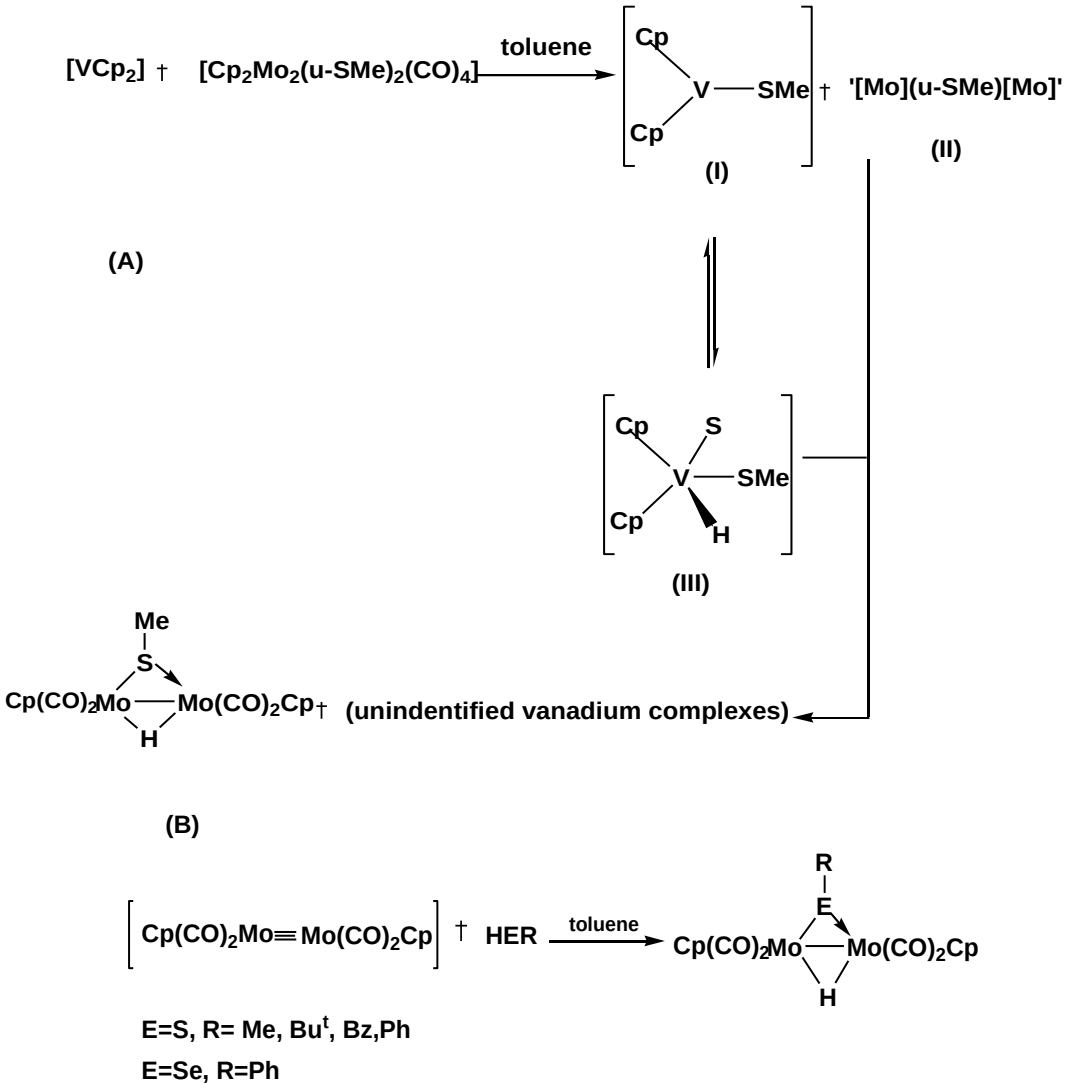

Scheme 9.

Petillon *et al.* continued to investigate the reaction of $[(\sigma^5\text{-}Cp^*)Mo(CO)_2]_2$ with MeSSMe, REER (ER= SPh, SeMe) and REH (ER=SBz, SePh) under various conditions to give corresponding products as shown in Scheme 9 [35].

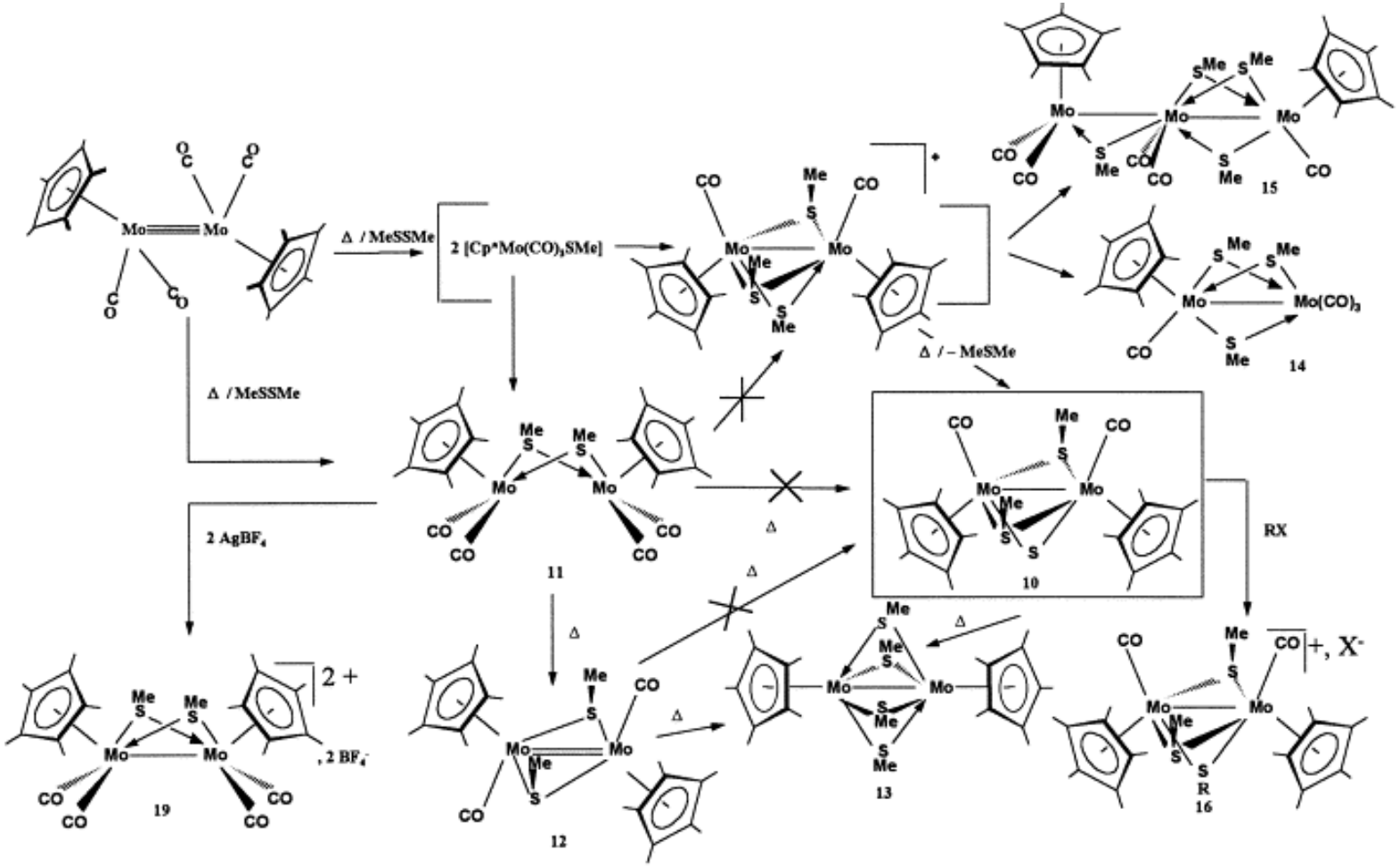

Scheme 10. Possible sequence of reactions ensuing from addition of 2 equivalent of REER or HER to $[(\eta^5\text{-Cp*})Mo(CO)_2]_2$.

1.3 OBJECTIVES

The project aims to investigate the reactivity of $[CpM(CO)_3]_2$ [M= Cr(**1**), Mo(**3**)] and their M≡M bonded $[CpM(CO)_2]_2$ [M= Cr(**2**), Mo(**4**)] towards aryl disulfides ligands (i) dicyclohexyl disulfide (ii) thienyl disulfide (Scheme 11).

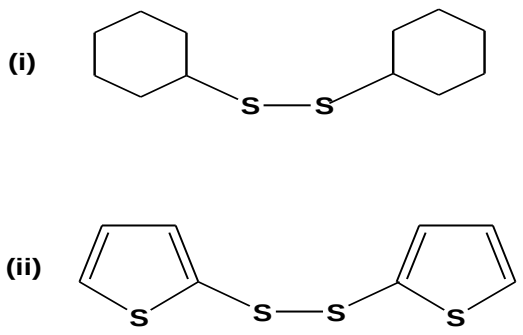

Scheme 11.

The study was directed to isolate novel complexes with possible potential in electrochemical study and as a comparative study between the behavior of Cr (**1** & **2**) and Mo (**3** & **4**).

II RESULTS AND DISCUSSION

2.1.1 Reaction of $[CpCr(CO)_3]_2$ (1) with an equimolar amount of Dicyclohexyl Disulfide

A deep green reaction mixture of $[CpCr(CO)_3]_2$ (**1**) with an equimolar amount of dicyclohexyl disulfide at 60 ºC was stirring vigorously for 60 h yielded $[CpCr(CO)_2]_2S$ (**5**) as the primary product, $[CpCr(SC_6H_{11})]_2S$ (**6**) as total decarbonylated product at 20.6 and 44.1 % yields, respectively.

2.1.2 Reaction of $[CpCr(CO)_2]_2$ (2) with an equimolar amount of Dicyclohexyl Disulfide

A stirred deep green reaction mixture of $[CpCr(CO)_2]_2$ (**2**) with an equimolar amount of dicyclohexyl disulfide had isolated out $[CpCr(CO)_2]_2S$ (**5**) and $[CpCr(SC_6H_{11})]_2S$ (**6**) at 7.5 and 32.7%, respectively.

2.1.3 Reaction of $[CpCr(CO)_2]_2$ S (5) with an equimolar amount of Dicyclohexyl Disulfide

Reaction of **5** with one mole equivalent of dicyclohexyl disulfide at elevated temperature produced **5** (13.3%), **6** (45.6 %) and $[Cp_4Cr_4S_4]$ (**7**) (4.7%).

2.1.4 Synthetic and Mechanistic pathways:

2.1.4.1 Formation of $[CpCr(SC_6H_{11})]_2S$ (6)

Reaction of $[CpCr(CO)_3]_2$ (**1**) with dicyclohexyl disulfide at 60 ºC for 60 h has led to the isolation of $[CpCr(CO)_2]_2$ S (**5**) and $[CpCr(SC_6H_{11})]_2S$ (**6**). The reaction of $[CpCr(CO)_2]_2$ (**2**) with dicyclohexyl disulfide at 110 ºC for 13 h gave **5** and **6** at 7.5 and 32.7 %, respectively. From the reaction, it is highly probable that **1** undergo dissociation into 17e radical species in solution as postulated in previous work carried out by Goh *et al.* with systems like Ph_2S_2 [23]. The S-S bond is known for its susceptibility to be cleavage by nucleophilic, electrophilic, and radical processes. It is conceivable that the

initial attack involves the radical attack on the dicyclohexyl disulfide which had led to the primary formation of **5** by sulfur insertion between two $CpCr(CO)_2$ fragments [37] followed by a total decarbonylation at elevated temperature to give **6.** After prolonged thermolysis, **6** was fully converted to a cubane-like cluster $Cp_4Cr_4S_4$. The synthetic and mechanistic pathways proposed for the above reactions are illustrated in Scheme 12.

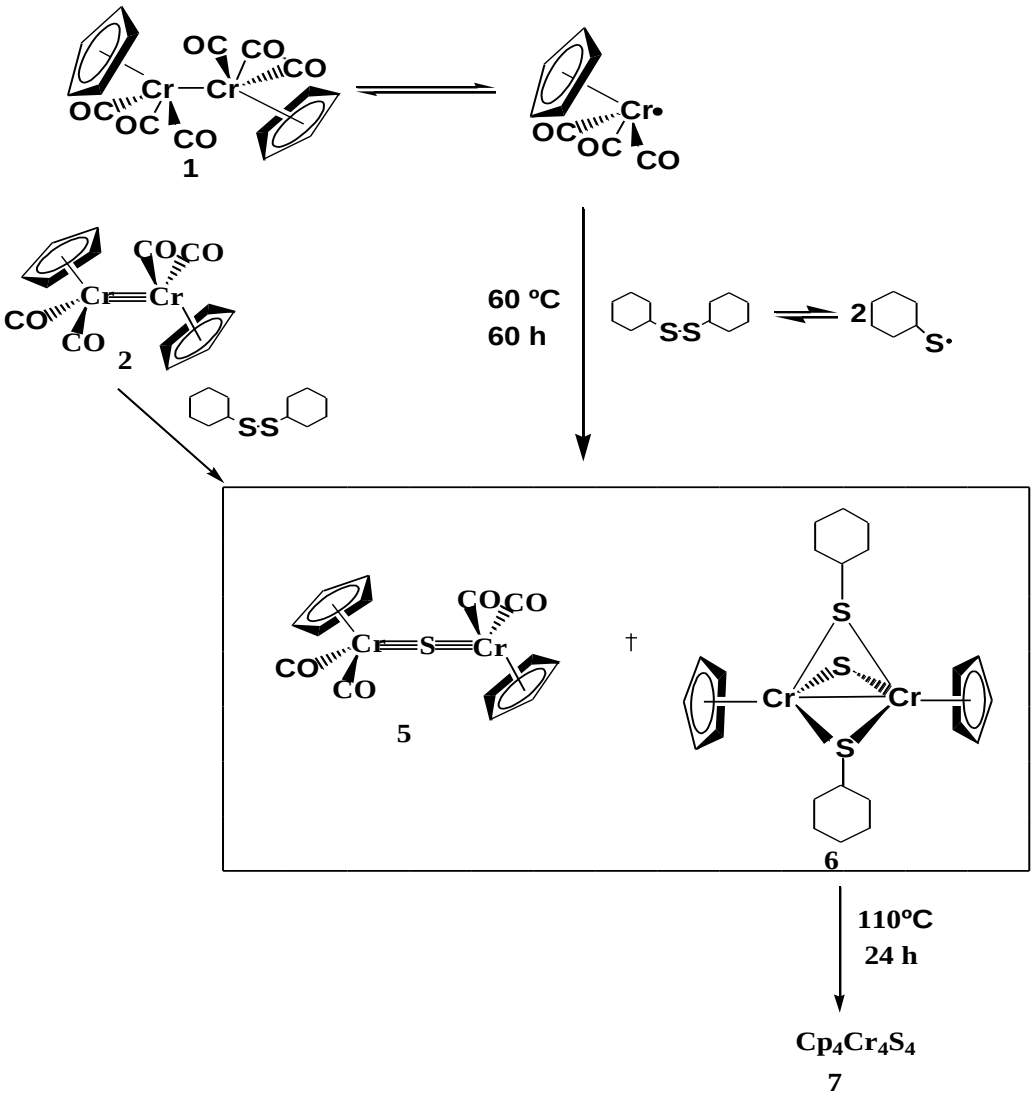

Scheme 12. Proposed synthetic pathway for the reaction of $[CpCr(CO)_3]_2$ (**1**) with Dicylohexyl Disulfide

2.1.5 Physical Properties of $[CpCr(SC_6H_{11})]_2S$ (6)

$[CpCr(SC_6H_{11})]_2S$ (**6**) exists as a dark purple crystalline solid. It is soluble in THF: ether mixture to give a purple colour solution. In the solid state **6** is stable at ambient temperature under an inert atmosphere for few days but stable at -28 ºC for prolonged period. In the solution state, **6** is stable at ambient temperature for few hours but can be kept longer at -28 ºC.

2.1.6 Spectra Characteristics

2.1.6.1 I.R. Spectrum

$[CpCr(SC_6H_{11})]_2S$ (6)

The I. R. spectrum nujol shows stretching frequencies at 1259m, 1093w, 1017w, 800m cm^{-1}. (refer to Appendix I)

2.1.6.2 NMR spectrum

$[CpCr(SC_6H_{11})]_2S$ (6)

Complex **6** is a paramagnetic complex**.** From the spectrum in benzene-d_6, it shows a broad peak at δ 14.09 (br, Cp, $v_{1/2}$ = 59 Hz) and -C_6H_{11} signal at δ 0.89-1.41. In the ^{13}C spectrum in benzene-d_6, the chemical shift for Cp is at δ 91.57; -C_6H_{11} at δ 27.60, 29.95, 38.46 and 40.02. The ^{13}C NMR resonances indicate that both the -C_6H_{11} ligands in **6** is unsymmetrical and with two symmetrical Cp ring lying at a parallel position to each other.

2.1.6.3 Mass spectra

$[CpCr(SC_6H_{11})]_2S$ (6)

The mass spectrum of **6** with its parent ion at m/z = 496 $[CpCr(SC_6H_{11})]_2S$ and its fragmentation ions are tabulated in Table 1.

Table 1. Electrospray ionization mass spectrum of $[CpCr(SC_6H_{11})]_2S$ (**6**)

m/z	Assignments
596	$[Cp_4Cr_4S_4]$
401	$[CpCr_4S_4]$
381	$[Cp_2Cr_2(SC_6H_{11})_2S]$
266	$[Cp_2Cr_2S]$
200	$[CpCr_2S]$
150	[CpCrS]

2.1.6.4 Molecular Structures

$[CpCr(SC_6H_{11})]_2S$ (6)

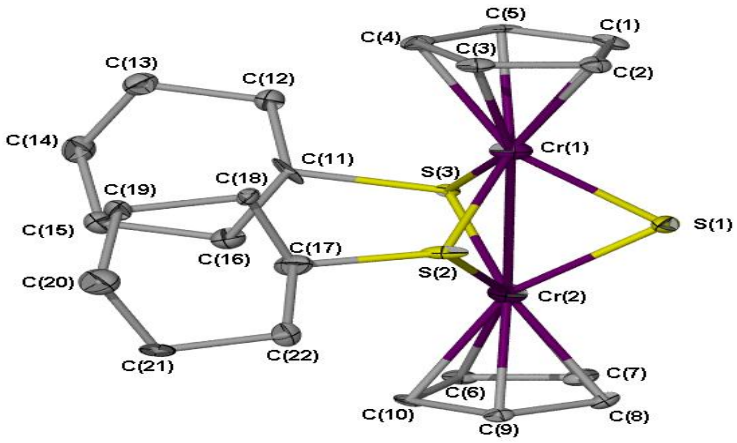

Figure 7. Molecular structure of $[CpCr(SC_6H_{11})]_2S$ (**6**).

$[CpCr(SC_6H_{11})]_2S$ (**6**) crystallized in the orthorhombic system with space group $Pna2_1$. The molecular structure of **6** is shown in figure 7 and its bond lengths and bond angles are tabulated in Table 2. Each Cr atom in **6** is in an elongated tetrahedral coordination environment with the Cp ligand occupying the apical position [23]. The Cr-S(thiolato) bond distances [2.342(3) Å] are significantly longer than the Cr-S(sulfido) distances [2.258(3) Å]. The angles between C(5)-Cr(1)-S(3) = 92.56(15) and C(9)-

Cr(2)-S(2) = 93.39(15) it indicates that both cyclohexyl moieties are in the axial position with the cyclopentadienyl group.

Table 2. Bond lengths [Å] and angles [º] for $[CpCr(SC_6H_{11})]_2S$ (**6**)

Bond lengths			
Cr(1)-C(3)	2.242(6)	Cr(2)-C(8)	2.220(6)
Cr(1)-C(4)	2.243(6)	Cr(2)-C(7)	2.228(6)
Cr(1)-C(2)	2.245(6)	Cr(2)-C(9)	2.235(6)
Cr(1)-C(5)	2.247(6)	Cr(2)-C(6)	2.249(6)
Cr(1)-S(1)	2.246(3)	Cr(2)-C(10)	2.253(6)
Cr(1)-C(1)	2.248(6)	Cr(2)-S(1)	2.258(3)
Cr(1)-S(3)	2.323(3)	Cr(2)-S(2)	2.320(3)
Cr(1)-S(2)	2.349(3)	Cr(2)-S(3)	2.342(3)
Bond angles			
C(3)-Cr(1)-C(4)	36.92(10)	C(10)-Cr(2)-S(2)	104.24(17)
C(3)-Cr(1)-S(1)	130.10(19)	S(1)-Cr(2)-S(2)	84.44(12)
C(3)-Cr(1)-C(1)	61.56(11)	C(8)-Cr(2)-S(3)	143.29(18)
C(2)-Cr(1)-C(1)	36.85(9)	C(9)-Cr(2)-S(3)	151.56(16)
C(5)-Cr(1)-S(3)	92.56(15)	C(6)-Cr(2)-S(3)	93.26(15)
S(1)-Cr(1)-S(3)	87.05(10)	C(10)-Cr(2)-S(3)	114.79(16)
C(1)-Cr(1)-S(3)	114.72(19)	S(1)-Cr(2)-S(3)	86.32(10)
C(3)-Cr(1)-S(2)	93.88(17)	S(2)-Cr(2)-S(3)	98.94(10)
S(1)-Cr(1)-S(2)	84.02(11)	C(9)-Cr(2)-Cr(1)	147.80(14)
C(1)-Cr(1)-S(2)	146.5(2)	S(3)-Cr(2)-Cr(1)	54.99(7)
S(3)-Cr(1)-S(2)	98.65(10)	Cr(1)-S(1)-Cr(2)	72.19(9)
C(3)-Cr(1)-Cr(2)	148.73(16)	C(17)-S(2)-Cr(2)	111.7(5)
S(1)-Cr(1)-Cr(2)	54.11(7)	C(17)-S(2)-Cr(1)	118.9(4)
C(8)-Cr(2)-C(7)	37.23(10)	Cr(2)-S(2)-Cr(1)	69.26(8)
C(9)-Cr(2)-C(6)	61.65(11)	C(8)-Cr(2)-S(1)	93.23(16)
C(9)-Cr(2)-S(1)	120.50(17)	C(11)-S(3)-Cr(1)	105.5(3)
C(8)-Cr(2)-S(2)	117.57(18)	C(11)-S(3)-Cr(2)	116.0(2)
C(7)-Cr(2)-S(2)	154.01(17)	Cr(1)-S(3)-Cr(2)	69.34(8)
C(9)-Cr(2)-S(2)	93.39(15	C(2)-C(1)-Cr(1)	71.4(2)
C(12)-C(11)-S(3)	107.0(5)	C(6)-C(7)-Cr(2)	72.3(2)

2.2 Studies of $[CpMo(CO)_2]_2$ (4) with Dicyclohexyl Disulfide

2.2.1 Reaction of $[CpMo(CO)_2]_2$ (4) with equimolar of Dicyclohexyl Disulfide

Reaction of $[CpMo(CO)_2]_2$ (**4**) with equimolar of Dicyclohexyl Disulfide at 70 ºC had led to the isolation of unreacted $[CpMo(CO)_2]_2$ (**4**) (18.5%), followed by a pair of isomeric products, dark green crystalline solids of *trans-syn* $[CpMo(CO)(SC_6H_{11})]_2$ (**8a**) (17.17% yield) and *trans-anti* $[CpMo(CO)(SC_6H_{11})]_2$ (**8b**) (12.83% yield), dark purple crystals of $[Cp_2Mo_2(CO)(O)(SC_6H_{11})_2]$ (**9**) (10.46 % yield) and dark brown crystalline solids of $[Cp_3Mo_3(CO)_4(\mu_3\text{-}O)(SC_6H_{11})]$ (**10**) (5.68% yield). In a similar reaction at 110ºC, unreacted $[CpMo(CO)_2]_2$ (**3**) (4% yield) was obtained, followed by the isolation of *trans-syn* $[CpMo(CO)(SC_6H_{11})]_2$ (**8a**) (16.09% yield) and *trans-anti*-$[CpMo(CO)(SC_6H_{11})]_2$ (**8b**) (16.74% yield), $[Cp_2Mo_2(CO)(O)(SC_6H_{11})_2]$ (**9**) (17.8%) and $[Cp_3Mo_3(CO)_4(\mu_3\text{-}O)(SC_6H_{11})]$ (**10**) (10.17%) at much greater yield. Thermolysis studies of *trans-anti* $[CpMo(CO)(SC_6H_{11})]_2$ (**8b**) at 70ºC for 10 h had shown that **8b** is slowly converting to trans-syn $[CpMo(CO)(SC_6H_{11})]_2$ (**8a**) together with $[Cp_2Mo_2(CO)(O)(SC_6H_{11})_2]$ (**9**) (7% yield) and $[Cp_3Mo_3(CO)_4(\mu_3\text{-}O)(SC_6H_{11})]$ (**10**) (4% yield). NMR tube reaction of **9** under similar condition for 10 h resulted $Cp_2Mo_2(CO)(O)(SC_6H_{11})_2]$ (**9**) (31%), $[Cp_3Mo_3(CO)_4(\mu_3\text{-}O)(SC_6H_{11})]$ (**10**) (27%). Likewise, thermolysis of **10** for 8 h had resulted a weak resonances of **10** (δ 4.87, 4.77 and 4.21). Total decomposition as indicated by the complete disappearance of the Cp resonances took place after 10 h. From the spectra, an organic fragment was left in the solution.

2.2.2 Synthetic and Mechanistic Pathways:

2.2.2.1 Formation of doubly bonded isomers *trans-syn/trans-anti* $[CpMo(CO)(SC_6H_{11})]_2$ (8), $[Cp_2Mo_2(CO)(O)(SC_6H_{11})_2]$ (9) and $[Cp_3Mo_3(CO)_4(\mu_3\text{-}O)(SC_6H_{11})]$ (10)

A major consequence of reactions involving organic disulfides (RSSR) is the susceptibility of their S-S linkage to be cleaved by nucleophilic, electrophilic or radical processes [42]. We believed that the reaction of $[CpMo(CO)_2]_2$ (**4**) with $(C_6H_{11}S)_2$ was initiated by cleavage of the S-S bond resulting in the formation of $C_6H_{11}S\cdot$ radicals. Subsequently, **4** underwent nucleophilic addition which has led to the formation of thiolate-bridged isomers *trans-syn/trans-anti* $Cp_2Mo_2(CO)_2(SC_6H_{11})_2$ (**8**) after decarbonylation. Both isomers **8a** and **8b** showed different physical properties. *Trans-syn* **8a** when in solution is yellowish brown and *trans-anti* **8b** is yellowish green. Similarly, this observed phenomenon is also shared by other *trans-syn/trans-anti* complexes of $[(RC_5H_4)M(CO)(\mu\text{-}ER')]$ [M= Mo or W; E= S, Se or Te; R= H, MeCO, MeO_2C, EtO_2C; R'= Me, Ph, Pr^i and Bu^t] [33-34]. Thermolysis studies indicated that **8** underwent stepwise decarbonylation and oxidation to afford **9** and **10**. An unexpected formation of a terminal and μ^3-oxo ligands in **9** and **10** was observed with moderate but reproducible yields under conditions supposedly anhydrous and oxygen-free. We assume that the bridging oxygen could originate from a CO ligand when all the reactions are conducted in supposedly anhydrous conditions [39]. The formation of **10** involves the loss of a $C_6H_{11}S$ moiety followed by the coordination of a $CpMo(CO)_2$ fragment, commonly encountered in this type of system. The synthetic and mechanistic pathways proposed for the above reactions are illustrated in Scheme 13.

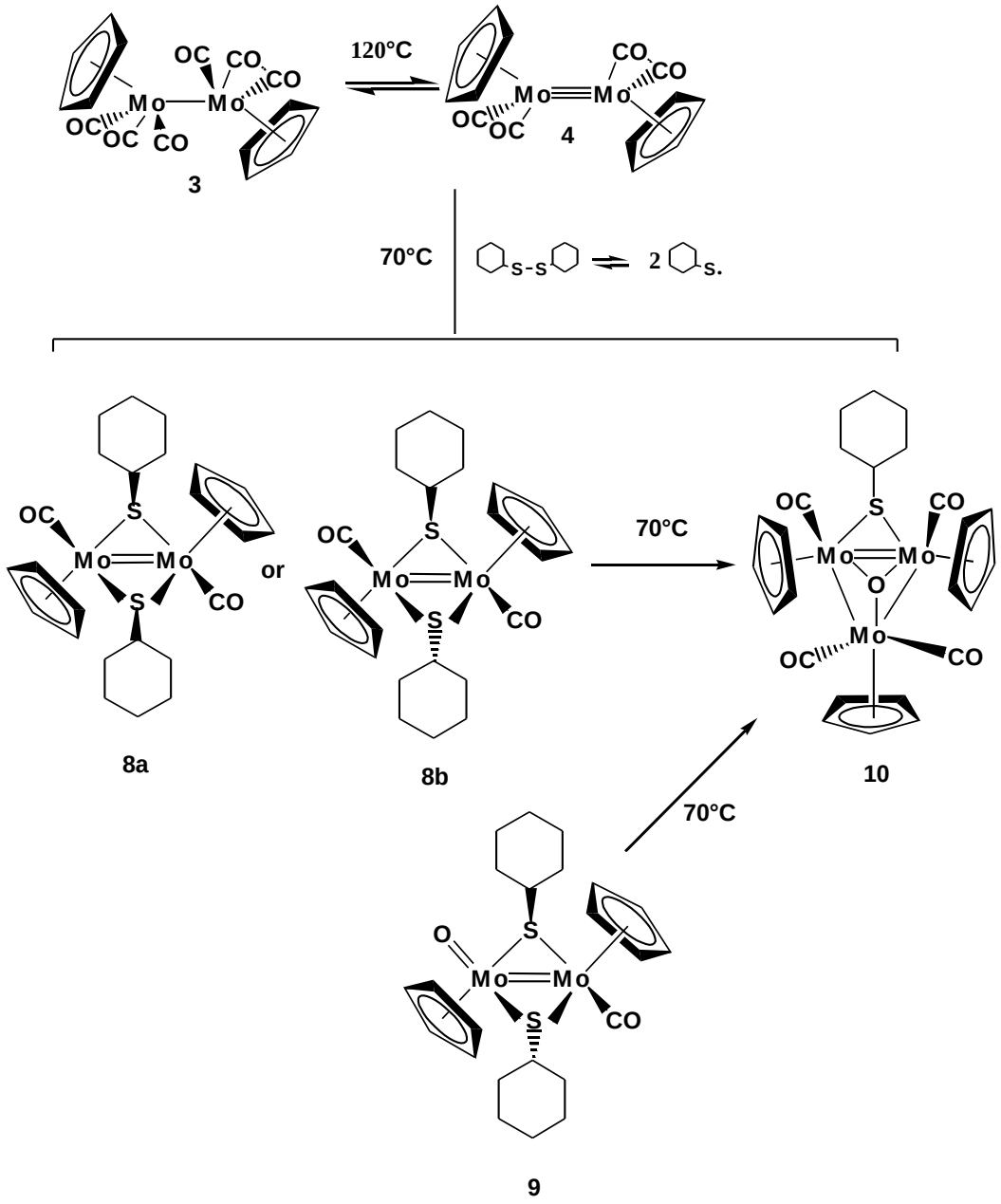

Scheme 13. Synthetic pathways of *trans-syn/trans-anti* $[CpMo(CO)(SC_6H_{11})]_2$ (**8a & b**), $[Cp_2Mo_2(CO)(O)(SC_6H_{11})_2]$ (**9**) and $[Cp_3Mo_3(CO)_4(\mu_3\text{-}O)(SC_6H_{11})]$ (**10**)

2.2.3 Physical Properties

***trans-syn* [CpMo(CO)(SC_6H_{11})]$_2$ (8a)**

8a exists as a dark yellowish brown crystalline solid. It is stable at ambient temperature as well as being stable for a couple of days at ambient temperature in solution under inert atmosphere. It is soluble in n-hexane/toluene mixture to give a yellowish brown solution.

***trans-anti* [CpMo(CO)(SC_6H_{11})]$_2$ (8b)**

8b exists as a dark green crystalline solid. It is soluble in THF/ether mixture to give a yellowish green solution. **8b** is stable at ambient temperature under inert atmosphere. In the solid state, it is air-stable for a couple of days at ambient temperature.

[Cp_2Mo_2(CO)(O)(SC_6H_{11})$_2$] (9)

[Cp_2Mo_2(CO)(O)(SC_6H_{11})$_2$] exists as a dark purple crystalline solid. It is soluble in a mixture of n-hexane/toluene to give a purple solution. In the solid state, it is stable at ambient temperature under an inert atmosphere. In solution, it is stable at room temperature under an inert atmosphere for a couple of days.

[$Cp_3Mo_3(CO)_4(\mu_3$-O)(SC_6H_{11})] (10)

10 exists as fine brown crystalline solids. It is soluble in toluene and other more polar solvents like ether and THF. It is stable in solution and solid state at ambient temperature for a couple of days.

2.2.4 Spectra Properties

2.2.4.1 I.R. Spectra

***trans-syn* [CpMo(CO)(SC_6H_{11})]$_2$ (8a)**

The I. R. spectrum in nujol shows ν_{CO} stretching frequencies at 1852vs, 1843vs; this indicates that the two ν_{CO} are not symmetrical. Other bands at 1255w, 1026w, 887m, 530w and 478w cm^{-1}. (refer to Appendix I)

***trans-anti* [CpMo(CO)(SC_6H_{11})]$_2$ (8b)**

The I.R. spectrum in nujol shows ν_{CO} stretching frequencies at 1858vs, 1819sh; it shows that this complex is symmetrical, with a strong band at 1858vs and 1819sh cm^{-1} at shoulder. Other bands at 1255w, 887w and 480w cm^{-1}. (refer to Appendix I)

[Cp_2Mo_2(CO)(O)(SC_6H_{11})$_2$] (9)

The I. R. spectrum in nujol shows ν_{CO} stretching frequencies at 1814s. Complex **10** containing monooxo groups (Mo=O) which υ(Mo=O) vibration is at 883s. The Mo=O stretching vibrations in I.R. spectrum has showed identical to those in the related oxo-bridged dinuclear complex [49]. Other bands at 1258m, 1186w, 996m, 816w and 788w cm^{-1} (refer to Appendix I).

[$Cp_3Mo_3(CO)_4(\mu_3\text{-}O)(SC_6H_{11})$] (10)

The I. R. spectrum in nujol shows ν_{CO} stretching frequencies at 1946m, 1927m, 1814m, 1759m; the complex is unsymmetrical. Other bands at 1096m, 821w and 723vw cm^{-1} (refer to Appendix I)

2.2.4.2 NMR spectrum

***trans-syn* [CpMo(CO)(SC_6H_{11})]$_2$ (8a)**

In the ^{1}H NMR spectrum (benzene-d_6), **8a** shows two Cp peaks at δ 5.05 and δ 4.95. It indicates that the two Cp rings are not symmetrical. For the -$C_6H_{11,}$ its chemical shift were recorded as multiplets at the region of δ 0.97- δ 1.68. In the ^{13}C NMR spectrum (benzene-d_6), two Cp peaks were recorded at δ 90.56, 90.91. For the - $C_6H_{11,}$ its chemical shift were at δ 26.98, δ 27.32, δ 37.40. The CO peak was recorded at δ 251.60.

***trans-anti* [CpMo(CO)(SC_6H_{11})]$_2$ (8b)**

In the ^{1}H NMR spectrum (benzene-d_6), **8b** shows only one Cp peaks at δ 5.12, it indicates that the two Cp rings are symmetrical. For the –C_6H_{11}**,** its chemical shift were recorded as multiplets at the region of δ 0.97-1.68. In the ^{13}C NMR spectrum (benzene-d_6), one Cp peak was recorded at δ 91.40. For the –$C_6H_{11,}$ its chemical shift were at δ 26.98, 27.32, 37.40. The CO peak was recorded at δ 250.22.

[Cp_2Mo_2(CO)(O)(SC_6H_{11})$_2$] (9)

The complex **9** is a diamagnetic and unsymmetrical compound. In the ^{1}H NMR spectrum (benzene-d_6), the Cp signals were assigned as δ 5.22, 5.78. The - C_6H_{11} peaks were recorded as multiplets at the region of δ 0.89- 0.97, δ 1.17- 1.29. In the ^{13}C NMR spectrum (benzene-d_6), the Cp peaks were recorded at δ 88.74, 106.90; the - C_6H_{11} peaks at δ 26.85, 27.65, 44.47. The CO peak was recorded at δ 242.48.

[$Cp_3Mo_3(CO)_4(\mu_3\text{-}O)(SC_6H_{11})$] (10)

The complex **10** is a trimer and unsymmetrical compound. In the ^1H NMR spectrum (benzene-d_6), the Cp signals were recorded as δ 4.87, 4.77 and 4.21. The –C_6H_{11} peaks were recorded in the region of δ 0.88- 0.97. In the ^{13}C NMR spectrum (benzene-d_6), the Cp signals were assigned as δ 111.22, 95.52 and 94.02. The -C_6H_{11} were recorded as δ 26.14 and 36.78. The CO peaks were recorded at δ 253.53, 269.95, 272.71 and 273.34.

2.2.4.3 Mass spectra

[$CpMo(CO)(SC_6H_{11})]_2$ (8b)

The mass spectrum of **8b** with its parent ion at m/z = 606 $[CpMo(CO)(SC_6H_{11})]_2$ and its fragmentation ions are tabulated in Table 3.

Table 3. Electrospray ionization mass spectrum of $[CpMo(CO)(SC_6H_{11})]_2$ (**8b**)

m/z	Assignment
554	$[Cp_2Mo_2(SC_6H_{11})_2]$
377	$[Cp_2Mo_2(CO)_2]$
320	$[Cp_2Mo_2]$
196	$[Mo_2S_2]$
198	$[(C_6H_{22})_2S]$
186	$[Mo_2]$
160	[CpMo]
83	$[(C_6H_{22})]$

[$Cp_2Mo_2(CO)(O)(SC_6H_{11})_2$] (9)

The mass spectrum of **9** with its parent ion at m/z = 594 [$(CpMoSC_6H_{11})_2CO(O)$] and its fragmentation ions are tabulated in Table 4.

Table 4. Electrospray ionization mass spectrum of [$Cp_2Mo_2(CO)(O)(SC_6H_{11})_2$] (**9**)

m/z	Assignments
578	[$Cp_2Mo_2(CO)(SC_6H_{11})_2$]
566	[$Cp_2Mo_2(O)(SC_6H_{11})_2$]
550	[$Cp_2Mo_2(SC_6H_{11})_2$]
479	[$Cp_2Mo_2(CO)(O)(SC_6H_{11})$]
364	[$Cp_2Mo_2(CO)(O)$]

[$Cp_3Mo_3(CO)_4(\mu^3\text{-}O)(SC_6H_{11})$] (10)

The mass spectrum of **10** with its parent ion at m/z = 723 [$Cp_3Mo_3(CO)_4(O)(SC_6H_{11})$] and its fragmentation ions are tabulated in Table 5.

Table 5. Electrospray ionization mass spectrum of [$Cp_3Mo_3(CO)_4(O)(SC_6H_{11})$] (**10**)

m/z	Assignments
692	[$Cp_3Mo_3(CO)_3(O)(SC_6H_{11})$]
669	[$Cp_3Mo_3(CO)_2(O)(SC_6H_{11})$]
640	[$Cp_3Mo_3(CO)(O)(SC_6H_{11})$]
610	[$Cp_3Mo_3(O)(SC_6H_{11})$]
496	[$Cp_3Mo_3(CO)_4$]
490	[$Cp_2Mo_2(CO)_2(SC_6H_{11})$]
232	[$CpMo(CO)_2(O)$]

2.2.4.4 Molecular Structures

***trans-anti* [CpMo(CO)(SC_6H_{11})]$_2$ (8b)**

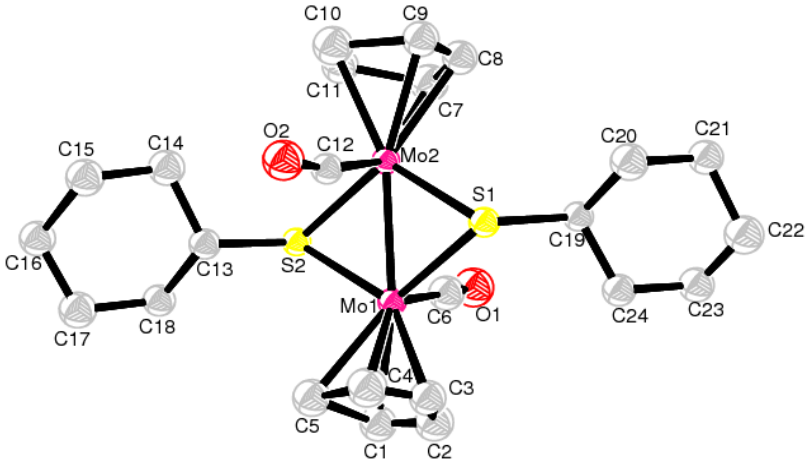

Figure 8. Molecular structure of *trans-anti* [CpMo(CO)(SC_6H_{11})]$_2$ (**8b**).

8b crystallized in the triclinic system with space group P(-1). The molecular structure of **8b** is shown in Figure 8 and its bond lengths and bond angles are tabulated in Table 6. Each Mo atom is in a coordination environment with both the cyclopentadienyl groups occupying the axial positions. It consists of two carbonyl moieties *trans* to each other while the two cyclohexylthiolate moieties are in the *trans-anti* positions with respect to Mo_2S_2 ring. Both the cyclohexylthiolate moieties bridge across the two CpMo(CO) fragments and form a butterfly core complex. The Mo-Mo bond distance of 2.5972(3) Å is comparable to other known Mo=Mo double bonded complexes [32-33].

Table 6. Bond lengths [Å] and angles [º] for $[CpMo(CO)(SC_6H_{11})]_2$ (**8b**)

Bond lengths

Mo(1)-S(2)	2.4214(6)
Mo(1)-S(1)	2.4236(6)
Mo(1)-Mo(2)	2.5972(3)
S(1)-Mo(2)	2.4214(6)
O(1)-C(6)	1.155(3)

Bond angles

C(6)-Mo(1)-C(5)	90.79(12)
C(6)-Mo(1)-C(1)	124.25(14)
C(6)-Mo(1)-C(2)	143.63(12)
C(1)-Mo(1)-S(2)	139.50(11)
C(1)-Mo(1)-S(1)	93.98(8)
S(2)-Mo(1)-S(1)	115.168(16)
C(1)-Mo(1)-Mo(2)	140.69(9)
S(2)-Mo(1)-Mo(2)	57.624(15)
S(1)-Mo(1)-Mo(2)	57.544(14)
C(7)-S(1)-Mo(2)	114.31(8)
C(7)-S(1)-Mo(1)	111.42(8)
Mo(2)-S(1)-Mo(1)	64.832(15)
O(1)-C(6)-Mo(1)	173.6(2)
C(12)-C(7)-S(1)	112.41(17)

[$Cp_2Mo_2(CO)(O)(SC_6H_{11})_2$] (9)

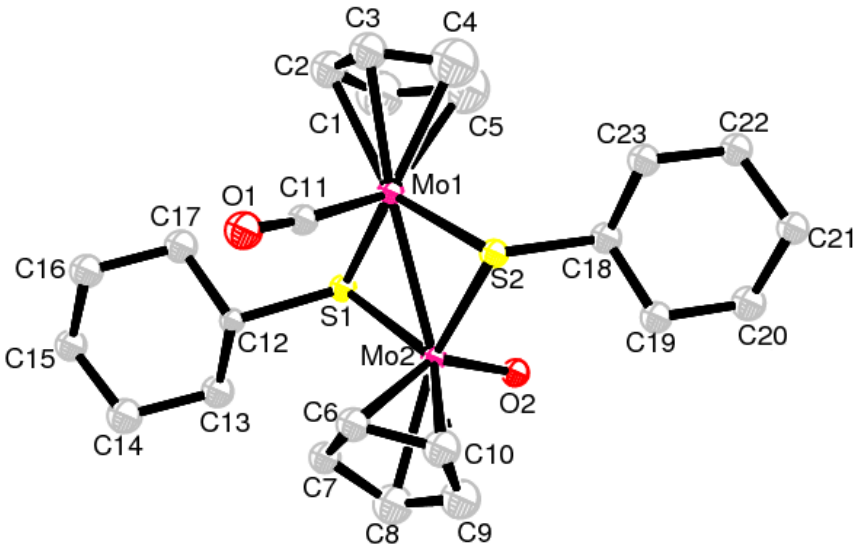

Figure 9. Molecular structure of [$Cp_2Mo_2(CO)(O)(SC_6H_{11})_2$] (**9**).

[$Cp_2Mo_2(CO)(O)(SC_6H_{11})_2$] (**9**) crystallized in monoclinic with space group P2(1). The molecular structure of **9** is shown in Figure 9 and its bond lengths and bond angles are tabulated in Table 6. It has similar features as [$CpMo(CO)(SC_6H_{11})]_2$ (**8**) except that one of the carbonyl is replaced by an oxygen atom. The highly electronegative oxygen atom distorts the position of the cyclopentadienyl ring adjacent to it. It causes the complex **9** to be highly unsymmetrical. The distance in Mo=O bond is 1.712(6) Å, which is quite similar in the related oxo-bridged dinuclear complex [50].

Table 7. Bond lengths [Å] and angles [º] for $[Cp_2Mo_2(CO)(O)(SC_6H_{11})_2]$ (**9**)

Bond lengths

Mo(2)-O(2)	1.712(6)
Mo(1)-S(1)	2.415(2)
Mo(1)-S(2)	2.434(2)
Mo(1)-Mo(2)	2.7321(10)
Mo(2)-S(1)	2.356(2)
Mo(2)-S(2)	2.381(2)

Bond angles

O(1)-Mo(1)-S(1)	98.2(2)	S(1)-Mo(2)-Mo(1)	56.09(5)
S(1)-Mo(1)-S(2)	108.28(8)	Mo(2)-S(1)-Mo(1)	69.85(7)
C(3)-Mo(1)-S(2)	103.38(16)	Mo(2)-S(2)-Mo(1)	69.14(7)
O(1)-Mo(1)-C(2)	131.3(2)	O(2)-Mo(2)-C(8)	104.0(3)
S(2)-Mo(1)-C(2)	80.23(13)	O(2)-Mo(2)-S(2)	89.9(3)
O(1)-Mo(1)-Mo(2)	111.27(18)	O(2)-Mo(2)-Mo(1)	87.4(3)
O(1)-Mo(1)-S(2)	101.0(2)	S(1)-Mo(2)-Mo(1)	56.09(5)
S(1)-Mo(1)-Mo(2)	54.06(6)	S(2)-Mo(2)-Mo(1)	56.35(6)
C(1)-Mo(1)-Mo(2)	139.14(15)	S(1)-Mo(2)-S(2)	112.14(8)
S(2)-Mo(1)-Mo(2)	54.51(5)	S(1)-Mo(2)-S(2)	112.14(8)

$[Cp_3Mo_3(CO)_4(\mu_3\text{-}O)(SC_6H_{11})]$ (10)

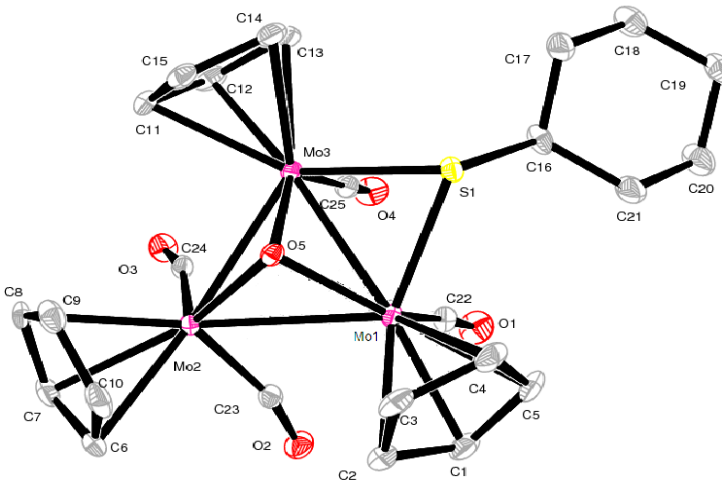

Figure 10. Molecular structure of $[Cp_3Mo_3(CO)_4(\mu_3\text{-}O)(SC_6H_{11})]$ (**10**).

10 crystallized in a monoclinic with space group P21/n. It has a triangulo-$Mo_3(\mu_3\text{-}O)$ core with a composite Mo-SC_6H_{11}-Mo and Mo-Mo double bond (2.8117(4) Å); and Mo-Mo bonds along the other two edges (2.8623(4) and 2.8621(4) Å). The molecular structure of **10** was found to posses a pseudo C_s-m geometry consisting of one $C_5H_5Mo(CO)_2$ fragment and two mirror-related $C_5H_5Mo(CO)$ fragments linked together by metal-metal bonds, by a trimetalcapped oxide atom, and by semibridging carbonyl interactions involving both carbonyl ligands of the $C_5H_5Mo(CO)_2$ fragment [39-40]. The molecular structure of **10** is shown in Figure 10 and its bond lengths and bond angles are tabulated in Table 8.

Table 8. Bond lengths [Å] and angles [º] for $[Cp_3Mo_3(CO)_4(\mu_3\text{-}O)(SC_6H_{11})]$ (**10**)

Bond lengths

Mo(1)-O(5)	2.0238(19)
Mo(1)-S(1)	2.4552(8)
Mo(1)-Mo(3)	2.8117(4)
Mo(1)-Mo(2)	2.8623(4)
Mo(2)-O(5)	2.028(2)
Mo(2)-Mo(3)	2.8621(4)
Mo(3)-O(5)	2.0180(19)
Mo(3)-S(1)	2.4662(8)
O(1)-C(22)	1.144(4)
O(2)-C(23)	1.179(4)
O(3)-C(24)	1.174(4)
O(4)-C(25)	1.146(4)

Bond angles

C(22)-Mo(1)-O(5)	133.12(11)	C(24)-Mo(2)-Mo(1)	103.85(9)
O(5)-Mo(1)-C(5)	140.84(10)	O(5)-Mo(2)-Mo(1)	45.00(5)
O(5)-Mo(1)-C(1)	138.99(10)	Mo(3)-Mo(2)-Mo(1)	58.835(9)
C(22)-Mo(1)-C(4)	119.86(12)	C(25)-Mo(3)-O(5)	131.09(10)
C(22)-Mo(1)-S(1)	91.65(9)	C(25)-Mo(3)-S(1)	92.21(9)
O(5)-Mo(1)-S(1)	77.01(6)	O(5)-Mo(3)-S(1)	76.85(6)
C(5)-Mo(1)-S(1)	97.22(9)	C(25)-Mo(3)-Mo(1)	88.65(8)
C(22)-Mo(1)-Mo(3)	90.33(9)	O(5)-Mo(3)-Mo(1)	46.01(5)
O(5)-Mo(1)-Mo(3)	45.84(5)	S(1)-Mo(3)-Mo(1)	54.975(18)
S(1)-Mo(1)-Mo(3)	55.342(19)	C(25)-Mo(3)-Mo(2)	102.38(9)

O(5)-Mo(1)-Mo(2)	45.11(6)	O(5)-Mo(3)-Mo(2)	45.12(6)
S(1)-Mo(1)-Mo(2)	113.54(2)	S(1)-Mo(3)-Mo(2)	113.194(19)
Mo(3)-Mo(1)-Mo(2)	60.580(9)	Mo(1)-Mo(3)-Mo(2)	60.585(9)
C(23)-Mo(2)-C(24)	84.87(12)	C(16)-S(1)-Mo(1)	115.61(10)
O(5)-Mo(2)-C(7)	147.29(10)	Mo(1)-S(1)-Mo(3)	69.68(2)
C(24)-Mo(2)-C(6)	123.83(12)	Mo(3)-O(5)-Mo(2)	90.05(8)
O(5)-Mo(2)-C(6)	126.00(10)	Mo(3)-O(5)-Mo(1)	88.16(8)
C(23)-Mo(2)-C(8)	132.59(12)	Mo(2)-O(5)-Mo(1)	89.89(8)
C(24)-Mo(2)-C(8)	88.54(12)	C(8)-C(9)-Mo(2)	71.89(17)
C(23)-Mo(2)-Mo(3)	102.41(9)	O(3)-C(24)-Mo(2)	164.2(2)
C(24)-Mo(2)-Mo(3)	64.18(9)	O(4)-C(25)-Mo(3)	174.5(3)
O(5)-Mo(2)-Mo(3)	44.83(5)		
C(7)-Mo(2)-Mo(3)	146.06(8)		
C(23)-Mo(2)-Mo(1)	64.17(9)		

2.3 Studies of $[CpCr(CO)_3]_2$ (1) with Thienyl Disulfide

2.3.1 Reaction of $[CpCr(CO)_3]_2$ (1) with an equimolar of Thienyl Disulfide

Reaction of $[CpCr(CO)_3]_2$ (**1**) with thienyl disulfide at room temperature for 2 h had led to the isolation of $CpCr(CO)_3H$ (**11**) as the primary products and $[CpCr(CO)_2]_2S$ (**5**) at 89.5%, 14.4 % respectively. Colour of the reaction changed spontaneously from deep green solution to orangy brown; effervescence was observed at the beginning of reaction. Reaction mixture changed to purple colour after 15 mins of vigorous stirring at 60 ºC yielded $[CpCr(CO)_2]_2S$ (**5**) and $[CpCr(S_2C_4H_3)]_2S$ (**12**) as a total decarbonylated product at 15.6 and 60.8%, respectively. Further thermolysis of **12** yielded $Cp_4Cr_4S_4$ as the final thermolyzed product.

2.3.2 Reaction of $[CpCr(CO)_2]_2$ (2) with an equimolar of Thienyl Disulfide

A deep green solution of $[CpCr(CO)_2]_2$ (**2**) was reacted with 1 mol equivalent of thienyl disulfide at elevated temperature with vigorous stirring for 3 h. Column chromatography of the resultant purple reaction mixture on silica gel led to the isolation of $[CpCr(CO)_2]_2S$ (**5**) (13.9%) and $[CpCr(S_2C_4H_3)]_2S$ (**12**) (57.8%).

2.3.3 Reaction of $[CpCr(CO)_2]_2S$ (5) with an equimolar of Thienyl Disulfide

The reaction of $[CpCr(CO)_2]_2S$ (**5**) with 1 mol equivalent of thienyl disulfide at elevated temperature, resulted in a greenish brown mixture. Column chromatography of the product mixture on silica gel led to the isolation of $[CpCr(CO)_2]_2S$ (**5**) (8 mg, 39.9%) and $[CpCr(S_2C_4H_3)]_2S$ (**12**) (5 mg, 16.1%).

2.3.4 Synthetic and Mechanistic Pathways:

2.3.4.1 Formation of $[CpCr(S_2C_4H_3)]_2S$ (12)

Reaction of $[CpCr(CO)_3]_2$ (**1**) with one mole equivalent of thienyl disulfide at ambient temperature produced an orangy brown solution. Two products $CpCr(CO)_3H$ (**11**) (89.5%) and $[CpCr(CO)_2]_2S$ (**5**) (14.4%) were eluted out *via* column chromatography. It is postulated that the reaction involves the 17e radicals $CpCr(CO)_3\cdot$ generated from the facile thermal dissociation of the Cr-Cr bond of **1** [22]. Formation of the hydride, $CpCr(CO)_3H$ (**11**) probably originates from the Cp ligand via thermal C-H bond activation [38]. At ambient temperature, NMR monitoring of the reaction reveal that **11** is the main product at the beginning of the reaction. The relative amount of **11** was found to vary according to experimental conditions. At higher temperature, **11** was consumed almost completely [39] in the presence of thienyl disulfide. Apparently, the ligand underwent desulfuration which gave rise to sulfur insertion into **1** to form $[CpCr(CO)_2]_2S$ (**5**) [37]. Prolonged heating led to total decarbonylation to form $[CpCr(S_2C_4H_3)]_2S$ (**12**) (60.8%), and finally the cubane $Cp_4Cr_4S_4$. The synthetic and mechanistic pathways proposed for the above reactions are illustrated in Scheme 14.

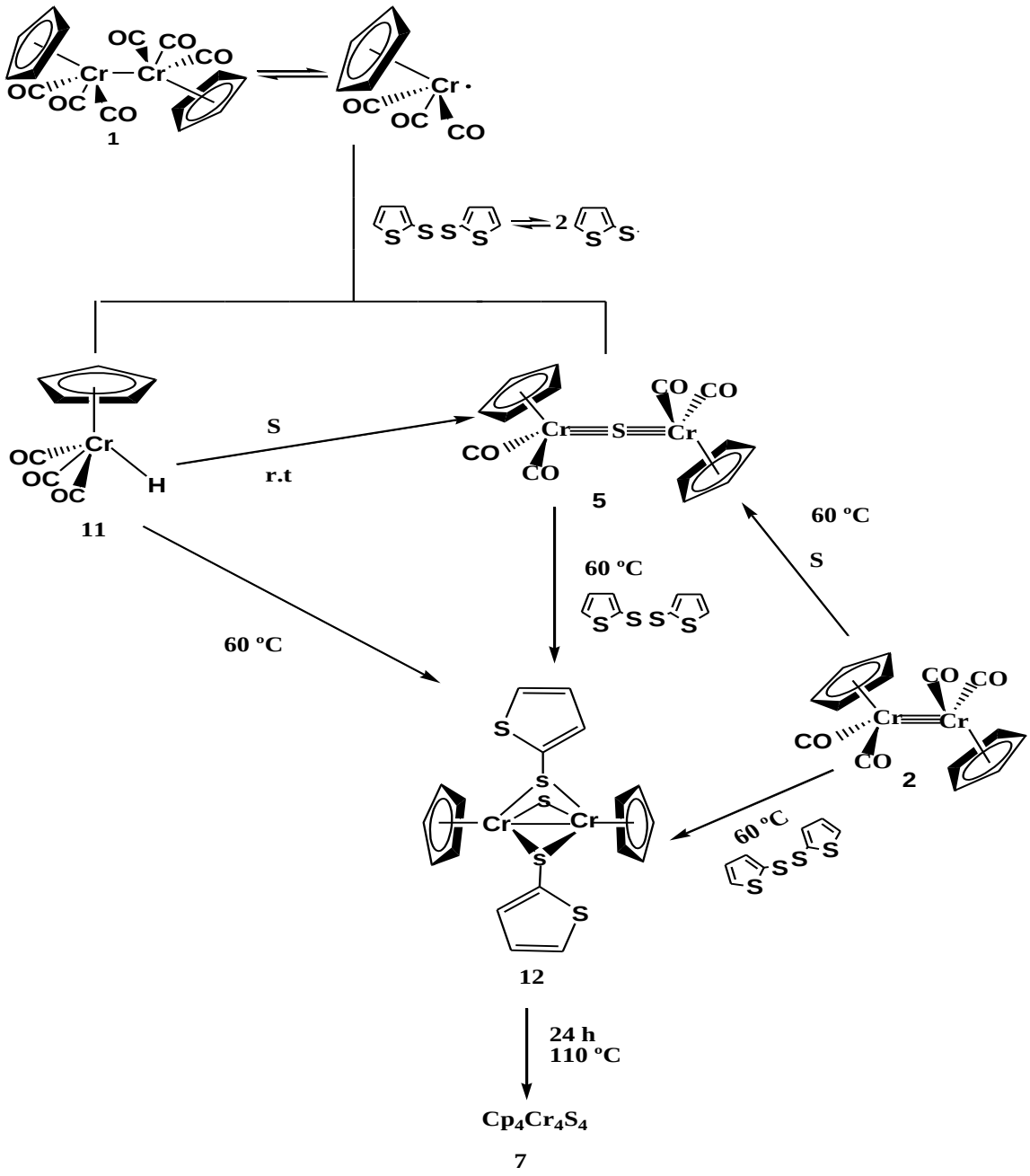

Scheme 14. Proposed Synthetic pathway for the reaction of $[CpCr(CO)_3]_2$ (**1**) with Thienyl Disulfide

2.3.5 Physical Properties

[CpCr($S_2C_4H_3$)]$_2$S (12)

12 exist as dark purple fine crystalline solids which are air-stable for extended periods at ambient temperature. It is soluble in both ether and THF. In the solution state it is fairly stable at room temperature under inert atmosphere.

2.3.6 Spectra Properties

2.3.6.1 I.R. Spectrum

[CpCr($S_2C_4H_3$)]$_2$S (12)

The I.R. spectrum in nujol shows ν_{CO} stretching frequencies at 1052w, 1015w, 839vw, 804 m and 722w cm^{-1} (refer to Appendix I).

2.3.6.2 NMR Spectrum

[CpCr($S_2C_4H_3$)]$_2$S (12)

Complex **12** is a paramagnetic complex**.** From the spectrum in benzene-d_6, it shows a broad peak at δ 12.72 (br, Cp, $v_{1/2}$ = 30 Hz) and -$S_2C_4H_3$ signal at δ 7.12, δ 7.36. In the ^{13}C spectrum in benzene-d_6, the chemical shift for Cp is at δ 101.04; -$S_2C_4H_3$ at δ131.24, δ 132.83, δ 134.84 and δ 135.12.

2.3.6.3 Mass Spectra

$[CpCr(S_2C_4H_3)]_2S$ (12)

The mass spectrum of **12** with its parent ion at m/z = 501 $[CpCr(S_2C_4H_3)]_2S$ and its fragmentation ions are tabulated in Table 9.

Table 9. Electrospray ionization mass spectrum of $[CpCr(S_2C_4H_3)]_2S$ (**12**)

m/z	Assignments
597	$[Cp_4Cr_4S_4]$
401	$[CpCr_4S_4]$
385	$[Cp_2Cr_2(S_2C_4H_3)_2S]$
266	$[Cp_2Cr_2S]$
200	$[CpCr_2S]$
150	[CpCrS]

2.3.6.4 Molecular Structures

$[CpCr(S_2C_4H_3)]_2S$ (12)

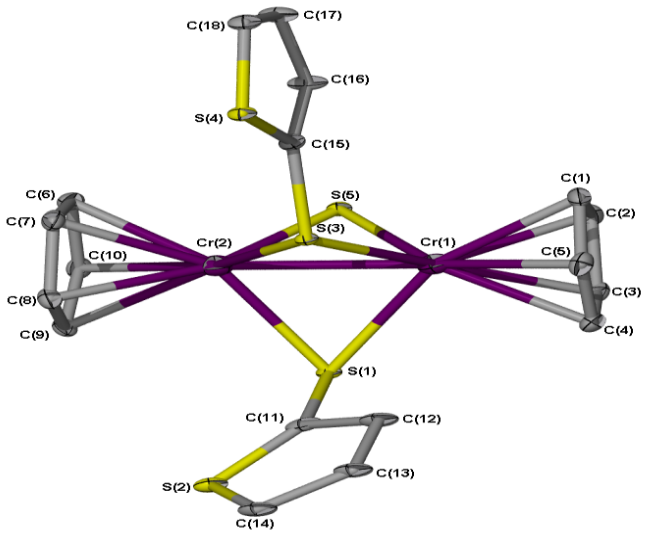

Figure 11. Molecular structure of $[CpCr(S_2C_4H_3)]_2S$ (**12**)

12 crystallized in the monoclinic system with space group P21/n. The Cr-S (thiolato) bond distances [2.3661(1) Å] are significantly longer than the Cr-S (sulfido) distances [2.258(1) Å]. From the angles S(1)…S(3)…C(15)= 146.40 and S(1)…S(3)…C(6)= 73.91º, it show that the two thienyl group are attached to the thiolate bridges in an equatorial-axial configuration [23].

Table 10. Bond lengths [Å] and angles [º] for $[CpCr(S_2C_4H_3)]_2S$ (**12**)

Bond lengths [Å]

Cr(1)-S(5)	2.2575(11)	S(1)-C(11)	1.763(4)
Cr(1)-S(3)	2.3680(11)	S(3)-C(15)	1.768(4)
Cr(1)-S(1)	2.3835(12)	S(4)-C(18)	1.702(4)
Cr(1)-Cr(2)	2.6703(9)	S(4)-C(15)	1.725(4)
Cr(2)-S(5)	2.2525(12)	C(11)-S(2)	1.666(5)
Cr(2)-S(1)	2.3659(11)	S(2)-C(14)	1.682(5)
Cr(2)-S(3)	2.3777(12)		

Bond angles

C(1)-Cr(1)-S(5)	112.14(13)	S(1)-Cr(2)-S(3)	87.11(4)
C(3)-Cr(1)-S(3)	155.87(13)	C(10)-Cr(2)-Cr(1)	145.90(12)
S(5)-Cr(1)-S(3)	96.87(4)	S(5)-Cr(2)-Cr(1)	53.78(3)
C(3)-Cr(1)-S(1)	102.35(12)	S(1)-Cr(2)-Cr(1)	56.10(3)
S(5)-Cr(1)-S(1)	86.54(4)	S(3)-Cr(2)-Cr(1)	55.59(3)
C(3)-Cr(1)-Cr(2)	146.69(12)	C(11)-S(1)-Cr(2)	106.28(12)
S(5)-Cr(1)-Cr(2)	53.61(3)	C(11)-S(1)-Cr(1)	111.46(14)
S(3)-Cr(1)-Cr(2)	55.93(3)	Cr(2)-S(1)-Cr(1)	68.42(3)
S(1)-Cr(1)-Cr(2)	55.48(3)	C(15)-S(3)-Cr(1)	111.19(14)
C(10)-Cr(2)-S(5)	96.77(12)	C(15)-S(3)-Cr(2)	106.42(14)
C(8)-Cr(2)-S(5)	156.23(13)	Cr(1)-S(3)-Cr(2)	68.48(3)
C(6)-Cr(2)-S(1)	149.60(13)	Cr(2)-S(5)-Cr(1)	72.61(4)
S(5)-Cr(2)-S(1)	87.08(4)	C(12)-C(11)-S(1)	122.0(4)
C(10)-Cr(2)-S(3)	156.86(12)	C(16)-C(15)-S(3)	132.0(3)
C(8)-Cr(2)-S(3)	101.23(12)	S(4)-C(15)-S(3)	117.2(2)
S(5)-Cr(2)-S(3)	96.73(4)		

2.4 Studies of $[CpMo(CO)_2]_2$ (4) with Thienyl Disulfide

2.4.1 Reaction of $[CpMo(CO)_2]_2$ (4) with one mole equivalent of Thienyl Disulfide

Reaction of $[CpMo(CO)_2]_2$ (**4**) with one equimolar of thienyl disulfide at 70 ºC for 4 h resulted in a dark brownish red reaction mixture. Column chromatography of the dark brownish red reaction mixture led to the isolation of unreacted $[CpMo(CO)_2]_2$ (**3**) (37 mg, 12.33%), followed by a pair of isomeric products, dark green crystalline solids of *trans-syn* $[CpMo(CO)(C_4H_3S_2)]_2$ (**13a**) (17.66%) and *trans-anti* $[CpMo(CO)(C_4H_3S_2)]_2$ (**13b**) (14.76%) and purple crystalline solids of $[CpMo(O)(C_4H_3S_2)]_2O$ (**14**) (6.37%). In the reaction of **4** with one equimolar of thienyl disulfide at 110 ºC, unreacted $[CpMo(CO)_2]_2$ (**3**) (13 mg, 4.33%), *trans-syn* $[CpMo(CO)(C_4H_3S_2)]_2$ (**13a**) (12.84%), *trans-anti* $[CpMo(CO)(C_4H_3S_2)]_2$ (**13b**) (15.20%) and $[CpMo(O)(C_4H_3S_2)]_2O$ (**14**) (7.28%) were isolated. Thermolysis of **13** (racemic mixture**)** after 9 h showed that the resultant solution degrades slowly to **14** (14.3%) together with unconverted **13b** (33%) together its *trans-syn* isomer **13a** (9%). Thermolytic studies of **14** under similar condition for 22 h resulted in 9.7% yield of **14** together with some uncharacterized dark brown precipitates.

2.4.2 Synthetic and Mechanistic Pathways:

2.4.2.1 Formation of *trans-syn/trans-anti* $[CpMo(CO)(C_4H_3S_2)]_2$ (13) and $[CpMo(O)(C_4H_3S_2)]_2O$ (14)

$[CpMo(CO)_2]_2$ (**4**) is known to react with REER (E= S, Se ,Te; R= Me, Et, Ph) [23-25, 22, 27-30, 32-33] under different reaction conditions. For the reaction of **4** with $(C_4H_3S)_2S_2$, it is postulated that the $(C_4H_3S)_2S\cdot$ moiety undergoes oxidation addition to the M≡M bonds to form the thiolato-bridged isomers *trans-syn/trans-anti* $[CpMo(CO)(C_4H_3S_2)]_2$ (**13**). Both isomers showed markedly different physical properties. The *trans-syn* isomer is yellowish brown in colour whereas the *trans-anti* isomer is yellowish green. This observed phenomenon is also shared by other *trans-syn/trans-anti* complexes of $[(RC_5H_4)M(CO)(\mu\text{-}ER')]$ [M= Mo or W; E= S, Se or Te; R= H, MeCO, MeO_2C, EtO_2C; R'= Me, Ph, Pr^i and Bu^t] [32-33].

Thermolytic NMR tube reactions of **13** has yielded $[CpMo(O)(C_4H_3S_2)]_2O$ (**14**) (14.3% yield). It is conceivable that the formation of the oxo-bridged species **14** had co-crystallized with **13** [30]. The synthetic and mechanistic pathways proposed for the above reactions are illustrated in Scheme 15.

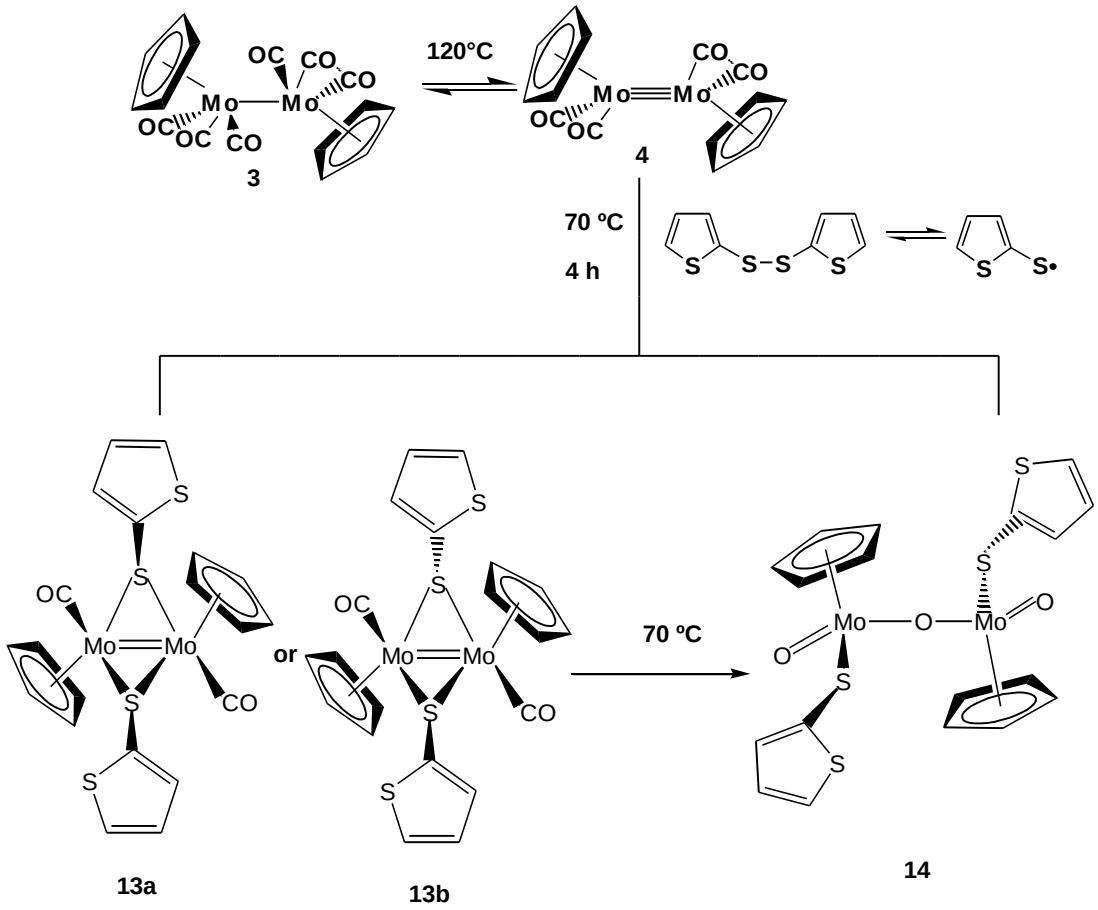

Scheme 15. Proposed synthetic pathway for the reaction of $[CpMo(CO)_2]_2$ (**4**) with Thienyl disulfide.

2.4.3 Physical Properties

***trans-syn* [CpMo(CO)($C_4H_3S_2$)]$_2$ (13a)**

Complex **13a** is a dark yellowish brown crystalline solid. It is stable at ambient temperature under an inert atmosphere; it is air-stable for extended periods at ambient temperature. It is soluble in n-hexane/toluene mixture to give a yellowish brown solution.

***trans-anti* [CpMo(CO)($C_4H_3S_2$)]$_2$ (13b)**

13b exists as a dark green crystalline solid. It is soluble in ether/THF mixture to give a yellowish green solution. It is stable at ambient temperature under an inert atmosphere as well as air for an extended period of time.

[CpMo(O)($C_4H_3S_2$)]$_2$O (14)

14 is a purple crystalline solids. It is stable at ambient temperature under an inert atmosphere. It is slightly soluble in toluene but is more easily soluble in ether to give a pinkish purple solution.

2.4.4 Spectra Properties

2.4.4.1 I.R. Spectra

***trans-syn* [CpMo(CO)($C_4H_3S_2$)]$_2$ (13a)**

The I.R. spectrum in nujol shows ν_{CO} stretching frequencies at 1830s, 1865s this indicates that the two ν_{CO} are not symmetrical; other bands, 1418w, 1218w, 1210vw, 1062w, 807w and 694w cm^{-1}. (refer to Appendix 1)

***trans-anti* [CpMo(CO)($C_4H_3S_2$)]$_2$ (13b)**

The I.R. spectrum in nujol shows ν_{CO} stretching frequencies at 1909vs, it shows that this complex is symmetrical with a strong band at 1909vs cm^{-1}. Other bands 1418w, 1218w, 1210vw, 1062w, 807w, 694w cm^{-1}. (refer to Appendix 1)

[CpMo(O)($C_4H_3S_2$)]$_2$O (14)

The I.R. spectrum in nujol shows stretching frequencies at 1060w, 809, 723w and 701w cm^{-1}. (refer to Appendix 1)

2.4.4.2 NMR Spectra

***trans-syn* [CpMo(CO)($C_4H_3S_2$)]$_2$ (13a)**

Complex **13a** is an unsymmetrical molybdenum dimer. The Cp rings were recorded as δ 4.92 and 5.31 in the ^{1}H NMR (Benzene-d_6). The -$C_4H_3S_2$ ring signals are at δ 6.69, 6.78, 6.90 and 7.02 as multiplet. In the ^{13}C NMR (Benzene-d_6), the Cp ring signals were assigned as δ 92.45, 92.48; -$C_4H_3S_2$ ring signals are at δ126.26, 127.88, 129.67 and 130.06. CO signal were recorded as δ 245.65, 246.73.

***trans-anti* [CpMo(CO)($C_4H_3S_2$)]$_2$ (13b)**

Complex **13b** is a symmetrical molybdenum dimer. The Cp rings were recorded as δ 5.09 in the ^{1}H NMR (Benzene-d_6). The -$C_4H_3S_2$ ring signals are at δ 6.69, 6.78, 6.90 and 7.02 as multiplet. In the ^{13}C NMR (Benzene-d_6), the Cp ring signal was assigned as δ 91.75; -$C_4H_3S_2$ ring signals are at δ126.26, 127.88, 129.67 and 130.06. CO signal was recorded as δ 242.09.

[CpMo(O)($C_4H_3S_2$)]$_2$O (14)

Complex **14** is an oxo-bridged species. From the ^{1}H NMR (Benzene-d_6) of **14** shows a single peak at δ 4.79, 4.95 in 2: 1 intensity ratio, which can be attributed to the two equivalent of Cp ligands. The -$C_4H_3S_2$ ring signals are at δ7.03, 7.12, and 7.70. In the ^{13}C NMR (Benzene-d_6), the Cp ring signals were recorded as δ 91.48 and 95.51; The -$C_4H_3S_2$ ring signals are at δ 135.10, 135.40, 130.57 and 128.63.

2.4.4.3 Mass Spectra

[CpMo(CO)($C_4H_3S_2$)]$_2$ (13b)

The mass spectrum of **13b** with its parent ion at m/z = 606 [CpMo(CO)($C_4H_3S_2$)]$_2$ and its fragmentation ions are tabulated in Table 11.

Table 11. Electrospray ionization mass spectrum of [CpMo(CO)($C_4H_3S_2$)]$_2$ (**13b**)

m/z	Assignments
577	[$Cp_2Mo_2(CO)(C_4H_3S_2)_2$]
551	[$Cp_2Mo_2(C_4H_3S_2)_2$]
491	[$Cp_2Mo_2(CO)_2(C_4H_3S_2)$]
464	[$Cp_2Mo_2(CO)(C_4H_3S_2)_2$]
437	[$Cp_2Mo_2(C_4H_3S_2)_2$]
377	[$Cp_2Mo_2(CO)_2$]

[CpMo(O)($C_4H_3S_2$)]$_2$O (14)

The mass spectrum of **14** with its parent ion at m/z = 598 [CpMo(O)($C_4H_3S_2$)]$_2$O and its fragmentation ions are tabulated in Table 12.

Table 12. Electrospray ionization mass spectrum of [CpMo(O)($C_4H_3S_2$)]$_2$O (**14**)

m/z	Assignments
598	[Cp_2Mo_2(O)($C_4H_3S_2$)]$_2$O
368	[$Cp_2Mo_2O_3$]
307	[CpMo(O)$_2$($C_4H_3S_2$)]
291	[CpMo(O)($C_4H_3S_2$)]

2.4.4.4 Molecular Structures

[CpMo(CO)($C_4H_3S_2$)]$_2$ (13b)

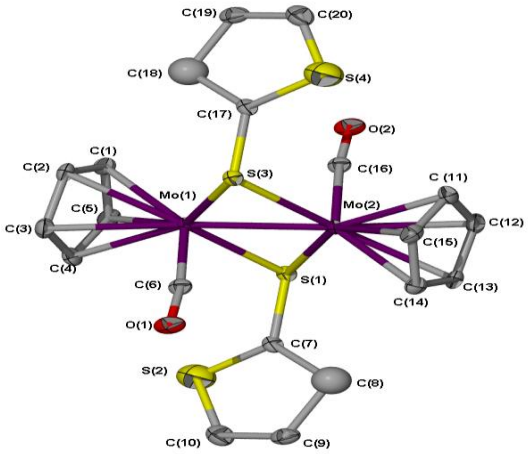

Figure 12. Molecular structure of [CpMo(CO)($C_4H_3S_2$)]$_2$ (**13b**)

13b crystallized in monoclinic with space group P2(1)/c. It consists of a planar Mo_2S_2 ring system with two substituted cyclopentadienyl and two carbonyl ligands are in a *trans* arrangement. However, the two dithienyl rings lie in the anti positions with respect to the Mo_2S_2 ring. Mo-Mo distance has shortened to

2.6009(3) Å, which indicates the Mo=Mo double bond to achieve an 18 electron configuration [35-36].

Table 13. Bond lengths [Å] and angles [º] for $[CpMo(CO)(C_4H_3S_2)]_2$ (**13b**)

Bond lengths	
Mo(1)-S(3)	2.4247(5)
Mo(1)-Mo(2)	2.6009(3)
S(3)-Mo(2)	2.4247(5)
O(1)-C(6)	1.162(3)
Bond angles	
C(5)-Mo(1)-S(3)	83.83(7)
S(3)-Mo(1)-S(1)	115.266(14)
S(3)-Mo(1)-Mo(2)	57.801(13)
Mo(2)-S(1)-Mo(1)	64.734(14)
O(1)-C(6)-Mo(1)	173.1(2)

$[CpMo(O)(C_4H_3S_2)]_2O$ (14)

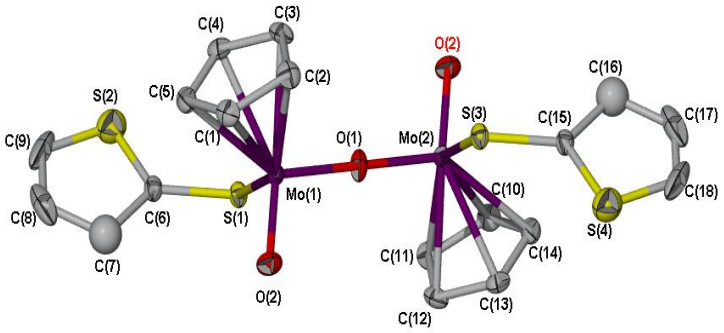

Figure 13. Molecular structure of $[CpMo(O)(C_4H_3S_2)]_2O$ (**14**)

14 crystallized in a monoclinic with space group P2(1)/c. It consists of an oxo-bridged dimolybdenum unit (Mo-O-Mo) and also attached to each Mo atom are a Cp ligand and a terminally bonded oxo group. The bridging oxygen atom resides on a crystallographic inversion centre and the Mo(1)-O(1)-Mo(2) is centrosymmetric. Both cyclopentadienyl ring resonances at δ 4.79, 4.95 in a 2:1 intensity ratio ; an evidence of

diamagnetism which implies delocalization *via* molybdenum-oxygen *d-p* orbital overlap in a three centre Mo(1)-O(1)-Mo(2) interaction [30].

Table 14. Bond lengths [Å] and angles [º] for $[CpMo(O)(C_4H_3S_2)]_2O$ (**14**)

Bond lengths	
Mo(1)-O(2)	1.6977(16)
Mo(1)-O(1)	1.83(4)
Bond angles	
O(2)-Mo(1)-O(1)	104.7(8)
O(1)-Mo(1)-C(5)	97.5(13)
O(1)-Mo(1)-S(1)	105.76(6)
O(2)-Mo(1)-S(1)	88.1(13)
O(2)-Mo(1)-C(1)	143.51(8)
Mo(1)-O(1)-Mo(2)	171.6(15)

2.5 Coordination of the (μ-S) ligand to $Fe(CO)_3$ fragments from $Fe(CO)_9$

2.5.1 The reaction of $[CpCr(S_2C_4H_3)]_2S$ (12) with 2 mole equivalent of $Fe(CO)_9$

A heterogeneous mixture of $[CpCr(S_2C_4H_3)]_2S$ (**12**) with 2 mole equivalent of $Fe(CO)_9$ undergoes a facile reaction in THF under an atmosphere of CO at ambient temperature for 15 h to give a brownish purple solution. Isolation using column chromatography yielded $[Cp_2Cr_2(S_2C_4H_3)]S_2[Fe(CO)_3]$ (**15**) as dark crystalline brownish purple crystals (34.18%) and an uncharacterized dark brown precipitate (12 mg) (Scheme 16).

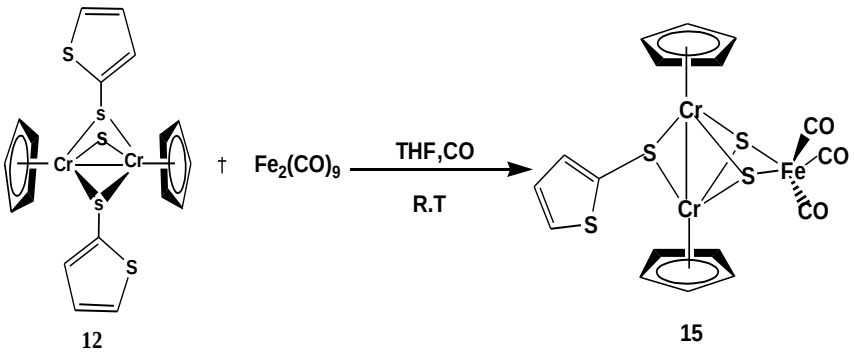

Scheme 16. Formation of $[Cp_2Cr_2(S_2C_4H_3)]S_2[Fe(CO)_3]$ (**15**)

2.5.2 Physical Properties of $[Cp_2Cr_2(S_2C_4H_3)]S_2[Fe(CO)_3]$ (15)

Complex **15** exists as dark purplish brown crystalline solid. It is soluble in *n*-hexane/toluene mixture to give a brownish purple solution. In the solid state, it is stable for a couple of days under an inert atmosphere. In solution, it is stable at ambient temperature under an inert atmosphere for a few hours.

2.5.3 Spectra Characteristics of $[Cp_2Cr_2(S_2C_4H_3)]S_2[Fe(CO)_3]$ (15)

2.5.3.1 I.R.spectra

$[Cp_2Cr_2(S_2C_4H_3)]S_2[Fe(CO)_3]$ (15)

$[Cp_2Cr_2(S_2C_4H_3)]S_2[Fe(CO)_3]$ (**15**) showed the ν_{CO} stretching frequency at 2021 m cm^{-1} and 1946 cm^{-1} in nujol and other peaks at 1216w, 1056sh, 1012w and 701w cm^{-1} (refer to Appendix I).

2.5.3.2 NMR spectra

$[Cp_2Cr_2(S_2C_4H_3)]S_2[Fe(CO)_3]$ (15)

The complex **15** is a heteronuclear complex with a $Fe(CO)_3$ fragment acting as an adduct. In the ^1H NMR spectrum (benzene-d_6), one Cp peak was recorded at δ 4.77, and $C_4H_3S_2$- peak were recorded as multiplets at δ 7.03, 7.12 and 7.70. In the ^{13}C NMR spectrum (benzene-d_6), one Cp peak was recorded as δ 97.51; the aromatic carbons for $C_4H_3S_2$- were recorded at δ 135.10, 135.40, 130.57 and 128.63.

2.5.3.3 Molecular structures

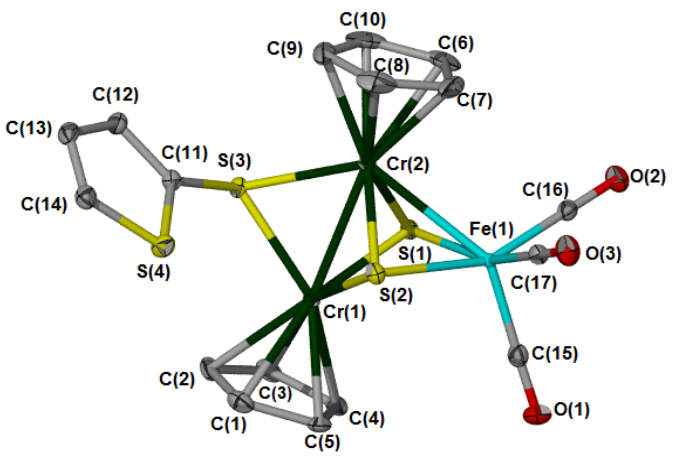

Figure 14. Molecular structure of $[Cp_2Cr_2(S_2C_4H_3)]S_2[Fe(CO)_3]$ (**15**)

The molecular structure of **15** is shown in Figure 14. The selected bond lengths (Å) and bond angles (º) of **15** are shown in Table 16. Complex **15** crystallizes in the triclinic system, space group P(-1). The structure of $[Cp_2Cr_2(S_2C_4H_3)]S_2[Fe(CO)_3]$ (**15**) contains a distorted tetragonal-bipyramidal Cr_2FeS_3 core. Two Cp_2Cr_2 fragments are linked by a direct Cr-Cr bond (2.686 Å) and by a thienyl and two sulfide bridges Cr-S(thiolate) and the average Cr-S(sulphide) bond lengths are 2.358 and 2.288 Å, respectively. Both sulphide sulfur, S1 and S2, are linked with the $Fe(CO)_3$ fragment (average Fe-S bond length is 2.301 Å). Although Cr(1) is not bonded directly to Fe, the Cp ring coordinated at Cr(1) occupies a close axial position with the other Cp ring coordinated at Cr(2).

Table 15. Bond lengths [Å] and angles [º] for $[Cp_2Cr_2(S_2C_4H_3)]S_2[Fe(CO)_3]$ (**15**)

Bond lengths			
Fe(1)-C(16)	1.792(3)	Cr(1)-S(1)	2.3116(9)
Fe(1)-C(17)	1.794(3)	Cr(1)-S(3)	2.3318(9)
Fe(1)-C(15)	1.808(3)	Cr(1)-Cr(2)	2.6861(7)
Fe(1)-S(2)	2.3045(9)	Cr(2)-S(2)	2.2882(9)
Fe(1)-S(1)	2.3100(8)	Cr(2)-S(1)	2.2888(9)
Fe(1)-Cr(2)	2.6879(6)	Cr(2)-S(3)	2.3582(8)
Fe(2)-S(6)	2.2964(9)	S(3)-C(11)	1.759(3)
Fe(2)-S(5)	2.3011(9)	O(1)-C(15)	1.146(4)
Fe(2)-Cr(6)	2.6921(7)	O(2)-C(16)	1.144(4)
Cr(1)-S(2)	2.2939(9)	O(3)-C(17)	1.135(4)
Bond angles			
C(16)-Fe(1)-C(17)	92.10(14)	C(4)-Cr(1)-S(1)	95.08(9)
C(16)-Fe(1)-C(15)	98.40(14)	S(2)-Cr(1)-S(1)	87.38(3)
C(16)-Fe(1)-S(2)	156.00(10)	C(4)-Cr(1)-S(3)	144.37(9)
C(17)-Fe(1)-S(2)	85.08(10)	C(3)-Cr(1)-S(3)	107.81(9)
C(15)-Fe(1)-S(2)	105.58(10)	S(2)-Cr(1)-S(3)	95.14(3)
C(16)-Fe(1)-S(1)	87.67(10)	S(1)-Cr(1)-S(3)	85.99(3)
C(17)-Fe(1)-S(1)	160.33(11)	S(2)-Cr(1)-Cr(2)	54.01(2)
C(15)-Fe(1)-S(1)	100.38(11)	S(1)-Cr(1)-Cr(2)	53.88(2)
S(2)-Fe(1)-S(1)	87.17(3)	S(3)-Cr(1)-Cr(2)	55.52(2)
C(16)-Fe(1)-Cr(2)	105.01(10)	C(9)-Cr(2)-S(2)	127.08(13)
S(2)-Fe(1)-Cr(2)	53.90(2)	C(9)-Cr(2)-S(1)	144.69(13)
C(4)-Cr(1)-S(2)	120.49(9)	S(2)-Cr(2)-S(1)	88.07(3)

C(8)-Cr(2)-S(3)	115.67(12)	C(9)-Cr(2)-S(3)	87.72(10)
C(7)-Cr(2)-S(3)	149.07(10)	Cr(1)-Cr(2)-Fe(1)	72.194(18)
C(10)-Cr(2)-S(3)	95.67(11)	Cr(2)-S(1)-Fe(1)	71.53(3)
C(6)-Cr(2)-S(3)	129.81(13)	Cr(2)-S(1)-Cr(1)	71.45(3)
S(2)-Cr(2)-S(3)	94.58(3)	Fe(1)-S(1)-Cr(1)	86.48(3)
S(1)-Cr(2)-S(3)	85.89(3)	Cr(2)-S(2)-Cr(1)	71.78(3)
S(2)-Cr(2)-Cr(1)	54.21(2)	Cr(2)-S(2)-Fe(1)	71.64(3)
S(1)-Cr(2)-Cr(1)	54.67(2)	Cr(1)-S(2)-Fe(1)	87.03(3)
S(3)-Cr(2)-Cr(1)	54.60(2)	Cr(1)-S(3)-Cr(2)	69.88(3)
C(9)-Cr(2)-Fe(1)	145.74(10)	Cr(6)-S(5)-Fe(2)	71.64(3)
S(2)-Cr(2)-Fe(1)	54.46(2)	C(13)-C(14)-S(4)	111.7(2)
S(1)-Cr(2)-Fe(1)	54.60(2)	O(1)-C(15)-Fe(1)	178.3(3)
S(3)-Cr(2)-Fe(1)	126.27(3)	O(2)-C(16)-Fe(1)	179.1(3)
O(3)-C(17)-Fe(1)	178.3(3)		

2.6 Electrochemical Studies

The presence of Mo-S bonds in a variety of redox enzymes has prompted synthetic and electrochemical studies of sulfur-containing complexes [27]. Thiolato-bridged complexes possess some desirable properties which make them useful as catalysts [42a].

Table 16. Cyclic Voltammetric Data Obtained using a Scan Rate of 0.1 Vs^{-1} at Pt Electrodes in CH_3CN with 0.2 M Bu_4NPF_6 as the Supporting Electrolyte

	Reduction processes [a]				Oxidation processes [a]			
Compd	$E_p^{red\ b}$/V	$E_p^{ox\ c}$/V	$E^r{}_{1/2}{}^d$/V	ΔE^e/mV	$E_p^{red\ b}$/V	$E_p^{ox\ c}$/V	$E^r{}_{1/2}{}^d$/V	ΔE^e/mV
6	-0.337	-0.125	-0.231	212				
8	-1.489				0.422			
9a	-0.0732	-0.0464	-0.0598	27				
9b					0.688	0.635	0.662	53
					0.0977	0.0513	0.0745	46
10					0.107	0.0410	0.074	66
11					0.540	0.435	0.487	105
12a	-1.415	-1.337	-1.376	78	0.485	0.309	0.0878	176
12b					0.354	0.295	0.649	59

[a] All potentials are relative to the Fc/Fc^+ redox couple.

[b] E_p^{red} = reductive peak potential.

[c] E_p^{ox} = oxidative peak potential.

[d] $E^r{}_{1/2}{}^d = (E_p^{red} + E_p^{ox})/2$

[e] $\Delta E = | E_p^{ox} - E_p^{red} |$

(a) $[CpCr(SC_6H_{11})]_2S$ (**6**)

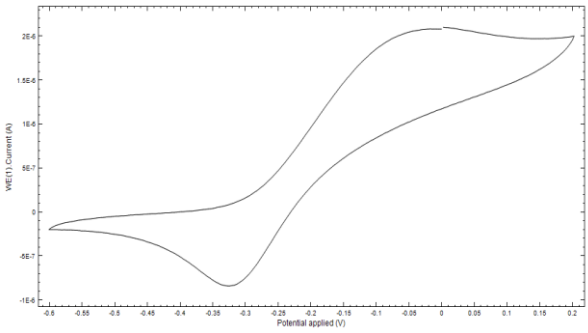

E/ V *vs*. Fc/Fc^+

(b) $[CpCr(S_2C_4H_3)]_2S$ (**12**)

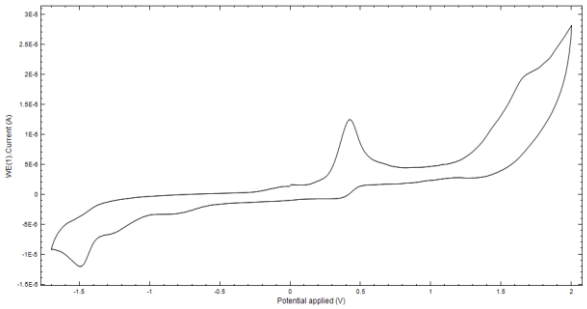

E/ V *vs*. Fc/Fc^+

Figure 15. Cyclic voltammograms of 0.5mM substrates recorded at Pt electrode in CH_3CN with 0.25 M Bu_4NPF_6 at a scan rate of 100 mV s^{-1}; (a) **6**, (b) **12**

The cyclic voltammogram of **6** showed a chemically reversible reduction process at around -0.3V vs. Fc/Fc^+. The anodic (E_p^{ox}) to cathodic (E_p^{red}) peak-to-peak separations ΔE_p were slightly wider, therefore, it is likely that the reduction process is affected by a slow rate of electron transfer. **12** displayed an irreversible reduction process at -1.4V vs. Fc/Fc^+. An irreversible oxidation process was observed at positive potential around + 0.3V vs. Fc/Fc^+ where the cathodic peak was particularly drawn out. The anodic peak current (i_p^{ox}) was much greater than the cathodic peak current (i_p^{red}), suggesting that more electrons were transferred during the oxidation process.

(c) *trans-syn* $[CpMo(CO)(SC_6H_{11})]_2$ (**8a**)

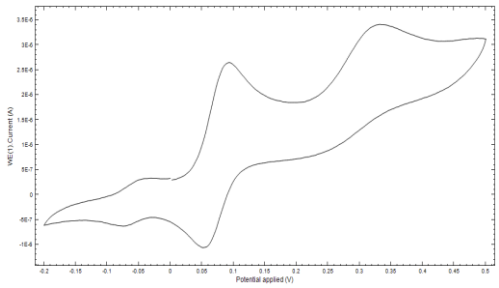

E/ V *vs*. Fc/Fc^+

(d) *trans-anti* $[CpMo(CO)(SC_6H_{11})]_2$ (**8b**)

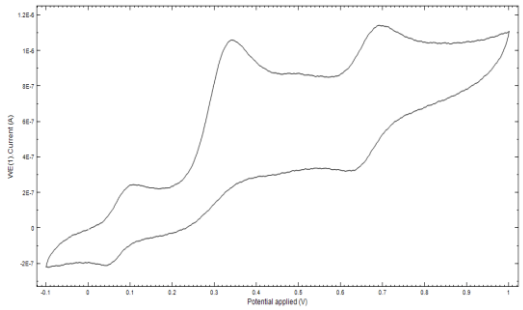

E/ V *vs*. Fc/Fc^+

(e) $[CpMo(SC_6H_{11})_2CO(O)]$ (**9**)

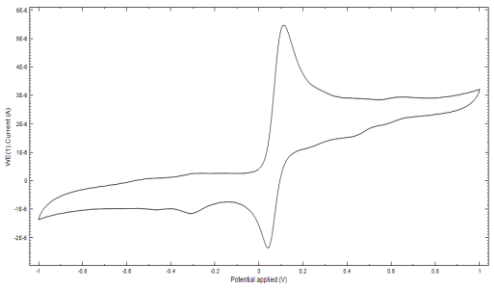

E/ V *vs*. Fc/Fc^+

(f) $[Cp_3Mo_3(CO)_4(O)(SC_6H_{11})]$ (**10**)

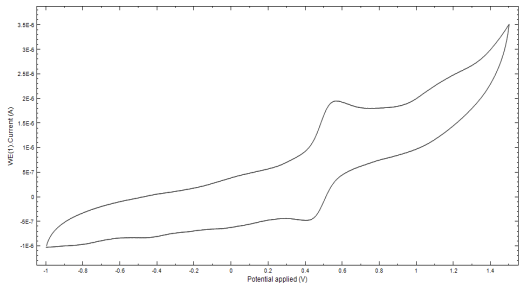

E/ V *vs*. Fc/Fc^+

Figure 16. Cyclic voltammograms of 0.5mM substrates recorded at Pt electrode in CH_3CN with 0.25 M Bu_4NPF_6 at a scan rate of 100 mV s^{-1}; (c) **8a**, (d) **8b**, (e) **9**, (f) **10**

Cyclic voltammogram of complex **8a** showed a reversible reduction process at potential around -0.05V vs. Fc/Fc^+ with a smaller i_p^{ox} and i_p^{red} value. The chemically reversible oxidation process is evident at potential around 0.06V vs. Fc/Fc^+ with a greater current magnitude than the first reduction process, indicating a higher number of electrons were transferred. An irreversible oxidation process at positive potentials (~ 0.3V) showed no reverse peak when the scan direction was reversed, suggesting chemical instability of the doubly bridged species, it might due to irreversible coordination of CH_3CN to the oxidized form of the compound. **8b** displayed two one-electron reversible oxidations and an irreversible oxidation processes. The small peak current observed on both reversible oxidation processes might be due to the slow rate of electron transferred. An irreversible oxidation process was evident at 0.34V with the current response approximately 2 times greater than the current obtained for the first, third oxidation processes, indicating a multiple-electron oxidation. The oxidation of **9** on Pt appears to be chemically reversible at a scan rate of 0.1 Vs^{-1} at potential around 0.04V vs. Fc/Fc^+. The i_p^{ox} value is at least twice of the i_p^{red} value observed for the oxidation process; it might due to the oxidation process which involves a higher number of electrons transferred. Complex **9** displayed one chemically irreversible reduction process; indicating that the reduced forms of **9** was chemically unstable.

Cyclic voltammogram of **10** showed an oxidation process at positive potentials with the oxidative (i_p^{ox}) to reductive (i_p^{red}) peak current ratio (i_p^{ox}/ i_p^{red}) is equal to unity on Pt. A much wider peak-to-peak separation indicates a slow electron transfer or a strong interaction with the electrode surface.

(g) *trans-syn* [CpMo(CO)($C_4H_3S_2$)]$_2$ **(13a)**

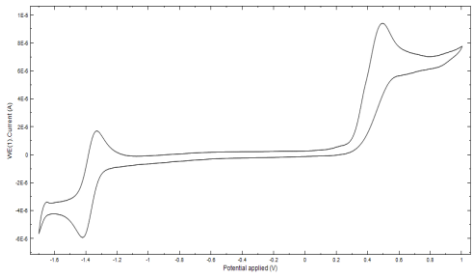

E/ V *vs*. Fc/Fc$^+$

(h) *trans-anti* [CpMo(CO)($C_4H_3S_2$)]$_2$ **(13b)**

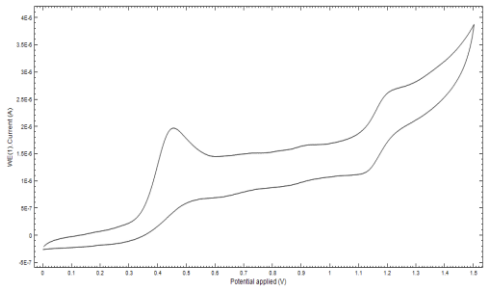

E/ V *vs*. Fc/Fc$^+$

Figure 17. Cyclic voltammograms of 0.5mM substrates recorded at Pt electrode in CH_3CN with 0.25 M Bu_4NPF_6 at a scan rate of 100 mV s^{-1}; (g) **13a**, (h) **13b**

CV experiment on *trans-syn* **13a** showed a chemically reversible reduction process at around -1.3V vs. Fc/Fc$^+$; reductive (i_p^{red}) peak to oxidative (i_p^{ox}) peak current ratio (i_p^{ox}/i_p^{red}) is equal to unity. An irreversible process was observed at positive potential which showed no reverse peak when the scan direction was reversed, suggesting instability of the reduced species. *Trans-anti* **13b** displayed a chemically reversible process at + 1.1V vs. Fc/Fc$^+$ with a small i_p^{ox} and i_p^{red} values. An oxidation process is evident at around + 0.4V vs. Fc/Fc$^+$ which showed no reverse peak when the scan direction was reversed; i_p^{ox} value observed was at least twice times higher indicating that the oxidation process involves the transfer of a higher number of electrons.

2.7 Conclusion

The study of $[CpM(CO)_3]_2$ [M=Cr(**1**) or Mo(**3**)] dimers and their M≡M bonded congeners $[CpM(CO)_2]_2$ [M=Cr(**2**) or Mo(**4**)] have shown high reactivity toward S-S bonded organic ligands. The reactivity demonstrates the facile S−S homolytic bond cleavage by these 17-electron organometallic species (**1A** or **3A**) or via the $[CpM(CO)_2]_2$ (M≡M) triply bonded complexes (**2** or **4**).

The homolytic S-S bond cleavage in dicylohexyl disulfide $(C_6H_{11}S)_2$ and thienyl disulfide $(C_4H_3S)_2S_2$ by the 15 or 17 electron $[CpCr(CO)_n]\cdot$ (n= 2, 3) has provided a facile route to the formation of $[CpCr(SC_6H_{11})]_2S$ (**6**) and $[CpCr(S_2C_4H_3)]_2S$ (**12**)

In addition, the susceptibility of the S-S bond cleavage leads to the formation of cyclopentadienyl thiolate-bridged dimolybdenum complexes. Most of the products formed in this reaction are diamagnetic since they are resulted from radical coupling. These organometallic complexes obey the 18-electron rule and are reasonably stable for a couple of days as solid state in air.

III Experimental

3.1 General Procedures

All reactions were carried out by using conventional Schlenk techniques under an inert atmosphere of nitrogen or under argon in a Vacumm Atmospheres Dribox which equipped with a HE-493 dri-train.

3.1.1 Physical Measurements

^{1}H and ^{13}C NMR spectra were measured on a JEOL Lambda FT 400MHz spectrometer or JEOL ECA 400 MHz Spectrometer. The chemical shifts for ^{1}H and ^{13}C referenced to residual C_6H_6 in benzene-d_6, to $(CH_3)_4Si$ in toluene-d_8. I.R. spectra in Nujols mulls were measured in the range 4000-400cm^{-1} by means of a Perkin-Elmer 2000 FTIR spectrophotometer. Elemental analyses were performed by in-house microanalytical laboratory using a Perkin-Elmer 2400 Series II CHNS/O System except Cr which was determined as CrO_4^{2-} according to the method by Haupt in our own laboratory [46]. Voltammetric experiments were conducted with Methrolm Autolab B.V. model with Pt as a working electrode. Potentials were referenced to the ferrocene/ferrocenium (Fc/Fc^{+}) redox couple, which was used as an internal standard. Tetrabutylammonium hexafluorophosphate was used as supporting electrolyte. The solutions were 0.2 M in $\{Bu_4N\}\{PF_6\}$ for CH_3CN. Mass spectrometric measurements were performed by direct injection using electrospray ionization (ESI) on an Agilent 6230 LCMS instrument. Electrospray (high resolution) mass spectrometric measurements were obtained on an Accurate Mass Q-Tof spectrometer. Single crystal X-ray diffractometry services were analyzed by the X-ray Crystallography Laboratory in our department.

3.1.2 Solvents and reagents

$M(CO)_6$ (M= Cr, Mo) and ligand (Diclyclohexyl disulfide and thienyl disulfide) were purchased from Sigma Aldrich Chemical Company and was used without any purification. Silica gel (Merck Kieselgel 60) and TLC plates (Merck Kieselgel $^{60}F_{254}$) were dried at 140 ºC overnight before chromatographic use. All solvents were distilled with sodium and benzophenone under nitrogen prior to use.

3.2 Preparation of starting complexes

3.2.1 Preparation of Dicyclopentadienylhexacarbonyldichromium and Dicyclopentadienylhexacarbonyldimolybdenum, $[CpM(CO)_3]_2$ [M=Cr(1), Mo(2)]

$[CpM(CO)_3]_2$ [M=Cr(**1**), Mo(**2**)] was synthesized using $M(CO)_6$ M=Cr, purchased from Fluka Ltd. according to Manning's method [45]. All reactions were carried out under an atmosphere of nitrogen. Diglyme was dried by distilling it with sodium and benzophenone under gas nitrogen prior to use. Sodium metal 0.434 g (18.87 mmol) was cut into small pieces and 4.5 mL (52.84 mmol) of freshly cracked cyclopentadiene solution was added to it in a 120 mL of dry diglyme in a 500 mL, three-necked, round-bottomed flask fitted with a Liebig condenser. After 30 min, metal dissolved in the solution to give a pale pink solution of sodium cyclopentadienide. 5.0g (18.87 mmol) of $M(CO)_6$ (M= Cr, Mo) was added to the mixture heated at reflux for 40 min. 30 mL of n-hexane was added to the solution to wash any sublimed $M(CO)_6$ M= Cr, Mo back into the reaction flask. During this period its color was bright yellow. Reaction mixture was cooled to room temperature and stirred using a magnetic stirrer. 4 mL of methanol was added slowly to destroy any unreacted sodium and 4 mL of water was added to destroy any unreacted sodium cyclopentadienide. Then a filtered solution in 189 mL of water and 12 mL of acetic acid of 15.1 g (37.74 mmol) of

hydrated iron(III) sulfate, $Fe_2(SO_4)_3.9H_2O$ was added. The color of the reaction mixture changed to green when M=Cr and purple when M=Mo, and fine crystals precipitated. These were filtered off using a 200 mL coarse sintered filter funnel layered with celite (1 cm). The filtered precipitate was washed with 189 mL of distilled water, 19 mL of cold methanol and 19 mL of pentane, and let to dry. Further purification could be effected by sublimation at *ca*. 120 ºC /0.1 mm Hg which gave a dark green crystalline product when M= Cr; 60-85% which was stored in the freezer of the Dribox; for M= Mo it filtered through filter funnel which will give a red crystalline product in a 90-98%. $[CpM(CO)_3]_2$ M= Cr, Mo caught fire in air easily, thus the filtration, washing and drying had to be carried out under N_2.

3.2.2 Preparation of Dicyclopentadienylhexacarbonyldichromium, $[CpCr(CO)_2]_2$

$[CpCr(CO)_2]_2$ was synthesized according to Hackett's method [11c]. A deep green suspension of $CpCr(CO)_3]_2$ (200mg, 0.497 mmol) in toluene (18mL) was reflux under stirring for 6 h. The resultant green solution was chromatographed on a silica gel column (1.5 cm x 5 cm) prepared in toluene. The eluate in toluene (30 mL) was then concentrated to *ca.* 5 mL and layered with n-hexane (ca. 1 mL). Cooling at -30ºC yielded fine deep green crystals of $[CpCr(CO)_2]_2$ (163 mg, 0.471 mmol, *ca*. 95% yield)

3.2.3 Preparation of Dicyclopentadienylhexacarbonyldimolybdenum, $[CpMo(CO)_2]_2$

$[CpMo(CO)_2]_2$ was synthesized according to Curtis *et al.*'s method [46]. A reddish purple suspension of $[CpMo(CO)_3]_2$ (1.0 g, 2.04 mmol) in toluene (20 mL) was heated at 120 ºC with vigorous stirring for 24 h. The resultant dark brownish red solution was chromatographed on a silica gel column (2 cm x 8 cm) prepared in n-hexane. The eluate in toluene (35 mL) was then evaporated to dryness under *vacuo*

yielding dark brownish red crystalline solids of $[CpMo(CO)_2]_2$ (0.869 g, 2.00 mmol, *ca*.98.04% yield)

3.2.4 Preparation of Diiron Enneacarbonyl, $Fe_2(CO)_9$

$Fe_2(CO)_9$ was synthesized according to R.B.King's method [47]. A mixture of iron pentacarbonyl (20 mL, 29.2 g, 0.149 mol) and glacial acetic acid (40 mL) was irradiated with an ultra-violet light source using a 125 W mercury high pressure lamp in a Hanovia photochemical reactor. The solution was magnetically stirred, and cooled with running water during irradiation. The photochemical reactor was placed in a container carefully lined on the sides and bottom with aluminium foil and the temperature was maintained between 20-25 ºC by means of running water. After 24 h of irradiation, the precipitated diiron enneacarbonyl was filtered out of solution. The orange crystalline product (22.5 g, 0.062 mol, 83% yield) was first washed with ethanol followed by ether, and then dried in *vacuo*.

3.3 Reaction of $[CpCr(CO)_3]_2$ (1) with Dicyclohexyl Disulfide

3.3.1 At 60ºC

$[CpCr(CO)_3]_2$ (200 mg, 0.497 mmol) was added to an equimolar of dicyclohexyl disulfide (0.11 mL, 0.497 mmol). Reaction mixture was magnetically stirred and heated in a silicone oil bath. Reaction mixture was allowed to stir overnight until the color of the mixture changed to dark purplish brown. Total reaction time is 60hrs of stirring. Reaction mixture was spotted by using TLC plate developed from 2*n*-hexane: 1 toluene: 1/3 ether which 2 spots were observed. Yellowish brown and purple in a Rf value of 5.8 cm and 1.5 cm.

The reaction mixture was put into the freezer. Next day the reaction mixture was concentrated to ca. 2 mL. The concentrated mixture was then chromatographed onto a silica gel packed column (1.5 cm x 12 cm) prepare in *n*-hexane.

Elution under slight pressure gave 2 fractions.

(i) A yellowish brown solution eluted with with *n*-hexane: toluene mixture (4: 1, 30 mL) which upon concentration to dryness gave $[CpCr(CO)_2]_2$ S (**5**) (33 mg, 0.102 mmol, 20.6% yield)

(ii) Dark purple solution eluted with *n*-hexane: toluene mixture (1: 2, 35 mL) which yielded fine purple crystals of $[CpCr(SC_6H_{11})]_2S$ (**6**). (109 mg, 0.219 mmol, 44.1 % yield). Anal. Found : ^{1}H NMR (Benzene-d_6): δ 0.89-1.41 (m, C_6H_{11}), δ 14.09 (br, Cp, $\nu_{1/2}$ = 59 Hz). ^{13}C NMR (Benzene-d_6): δ 27.60, 29.95, 38.46, 40.02 (C_6H_{11}), δ 91.57 (C_5H_5). I.R. : 1259m, 1093w, 1017w, 800m cm^{-1} (nujol). Anal. Calcd. for $C_{22}H_{32}S_3Cr_2$: C, 56.25; H, 4.68; Cr, 20.31; S, 18.75. Found: C, 56.57; H, 4.15; Cr, 19.59; S, 18.31%. A greenish blue fraction remained uneluted at the top of the column.

3.3.2 Thermolysis reaction

(i) Thermolysis of $[CpCr(SC_6H_{11})]_2S$ (6)

A deep purple solution of **6** (10 mg, 0.020 mmol) in deuterated toluene (ca. 1 mL) in a serum-capped 5 mm NMR tube was maintained at 100ºC and its NMR spectrum was monitored at regular intervals. From the spectra, **6** with δ 14.09 (41%) and $Cp_4Cr_4S_4$ (**7**) with δ 4.90 (34 %) were found after 15 h of reaction.

3.3.3 Reactivity studies of $[CpCr(CO)_2]_2$ (2) with Dicyclohexyl Disulfide

A stirred deep green solution of **2** (100 mg, 0.289 mmol) in toluene (15 mL) containing dicyclohexyl disulfide (0.0636 mL, 0.289 mmol) was stirred for 13h at 110ºC. The resultant purple solution was concentrated and loaded onto a silica gel column (1.5 x 10 cm) prepared in *n*-hexane.

(i) A yellowish brown solution in *n*-hexane: toluene (4:1, 20 mL) was eluted out which when concentrated to dryness yielded $[CpCr(CO)_2]_2S$ (**5**) (7 mg, 0.0217 mmol, 7.5% yield)

(ii) A deep purple solution in toluene: ether (2:1, 35 mL) was eluted out; which when concentrated gave a dark purple crystalline solids of **6** (47 mg, 0.0946 mmol, 32.7% yield).

3.3.4 Reactivity studies of $[CpCr(CO)_2]_2S$ (5) with Dicyclohexyl Disulfide

A dirty green mixture of **5** (20 mg, 0.062 mmol) and dicyclohexyl disulfide (0.014 mL, 0.062 mmol) prepared in deuterated toluene in a 5mm NMR tube was reacted at 60 ºC under an oil bath, and its proton NMR spectra were monitored at regular intervals. After 10 h, **5** (13.3%), **6** (45.6 %) and **7** (4.7%) were found in the NMR spectra.

3.4 Reaction of $[CpMo(CO)_2]_2$ (4) with Dicyclohexyl disulfide

3.4.1 At 70°C

A stirred suspension of $[CpMo(CO_2)_2]$ (**4**) (200 mg, 0.46 mmol) with an equimolar of dicyclohexyl disulfide (0.10 mL, 0.46 mmol) in toluene (15 mL) was refluxed for 104h. The resultant dark greenish brown reaction mixture was absorbed onto ca. 2 g of silica gel and concentrated under reduced pressure. It was then transferred and loaded onto a silica gel column (1.5 x 15.0 cm) prepared in *n*-hexane. The following fractions were eluted:

(i) A red color solution in a mixture of *n*-hexane: toluene (4: 1, 20 mL) which when concentrated to dryness yielded unreacted $[CpMo(CO)_2]_2$ (**4**) (37 mg, 0.0852 mmol, 18.5% yield)

(ii) A yellowish brown in *n*-hexane: toluene (1: 2, 45 mL) which when evaporated under reduced pressure, yielded dark green crystalline solids of *trans-syn* $[CpMo(CO)(SC_6H_{11})]_2$ (**8a**) (48 mg, 0.079 mmol, 17.17% yield). Anal. Found : ^{1}H NMR (Benzene-d_6) : δ 0.97- 1.68 (m, C_6H_{11}) ,δ 4.95, 5.05 (s, C_5H_5). ^{13}C NMR (Benzene-d_6) : 26.98, 27.32, 37.40 (C_6H_{11}), δ 90.56, 90.91 (C_5H_5), δ 247.19, 251.60 (CO). I.R. υ(CO) at 1852vs, 1843vs ; other bands, 1255w, 1026w, 887m, 530w, 478w cm^{-1} (nujol). Anal. Calcd. for $C_{24}H_{32}Mo_2O_2S_2$: C, 45.6; H, 3.8; Mo, 30.4; S,20.3. Found :C,45.6; H, 3.4; Mo, 30.7; S, 19.8%.

(iii) A yellowish green in *n*-hexane: toluene (1:2, 35 mL) which upon concentration to dryness under *vacuo* gave green crystallines solids of *trans-anti*$[CpMo(CO)(SC_6H_{11})]_2$ (**8b**) (36 mg, 0.059 mmol, 12.83% yield). Anal. Found : ^{1}H NMR (Benzene-d_6) : δ 0.97-1.68 (m, C_6H_{11}) , δ 5.12 (s, C_5H_5). ^{13}C NMR (Benzene-d_6) : 26.98, 27.32, 37.40 (C_6H_{11}), δ 91.40 (C_5H_5), δ 250.22 (CO). I.R. υ(CO) at 1858vs, 1819sh ; other bands, 1255w, 887w, 480w cm^{-1} (nujol). Anal. Calcd. for $C_{24}H_{32}Mo_2O_2S_2$: C, 44.7; H, 3.5; Mo, 31.2; S,20.7. Found: C, 44.7; H, 3.3; Mo, 31.1; S, 18.6%.

(iv) A purple fraction in a mixture of toluene: ether (1: 0.5, 50 mL) which when evaporated under reduced pressure yielded fine dark purple crystals of $[(CpMoSC_6H_{11})_2 CO(O)]$ (**9**) (37 mg, 0.062 mmol, 10.46% yield). Anal. Found : ^{1}H NMR (Benzene-d_6) : δ 0.89- 1.29 (m, C_6H_{11}), δ 5.22, 5.78 (s, C_5H_5). ^{13}C NMR (Benzene-d_6) : δ 26.85, 27.65, 44.47 (C_6H_{11}) , δ 88.74, 106.90 (C_5H_5) , δ 270.37 (CO). I.R. υ(CO) at 1814s; υ(Mo=O) at 883s; other bands, 1258m, 1186w, 996m, 816w, 788w cm^{-1} (nujol). Anal. Calcd. for $C_{23}H_{32}O_2S_2Mo_2$: C, 47.6; H, 3.7; Mo, 29.3; S, 14.6. Found: C, 47.5; H, 3.8; Mo, 30.2; S, 14.9%.

(v) A brown fraction in a mixture of ether: THF (1: 0.5, 40 mL) which when evaporated under reduced pressure, yielded dark brown crystalline solids of

$[Cp_3Mo_3(CO)_4(O)(SC_6H_{11})]$ (**10**) (19 mg, 0.026 mmol, 5.68% yield). Anal. Found : ^{1}H NMR (Benzene-d_6) : δ 0.88- δ 0.97 (m,C_6H_{11}), δ 4.87, 4.77, 4.21 (s, C_5H_5). ^{13}C NMR (Benzene-d_6) : δ 26.14, 36.78 (C_6H_{11}), δ 94.02, 95.52, 111.22 (C_5H_5), δ 253.53, 269.95, 272.71, 273.34 (CO). I.R. υ(CO) at 1946m, 1927m, 1814m, 1759m, other bands ,1096m, 821w, 723vw cm^{-1} (nujol). Anal. Calcd. for $C_{25}H_{26}Mo_3O_5S$: C, 49.4; H, 3.5; Mo, 28.2; S, 9.4. Found : C,49.5; H, 3.6; Mo, 25.8; S, 9.3%.

A brown layer remained uneluted at the top rim of the column.

3.4.2 At 110 ºC

A stirred suspension of $[CpMo(CO_2)_2]$ (**4**) (200 mg, 0.46 mmol) with an equimolar of dicyclohexyl disulfide (0.10 mL, 0.46 mmol) in toluene (15 mL) was refluxed for 90 h. The resultant dark brown reaction mixture was filtered through a disk of Celite (1 x 1.5 cm) and concentrated to ca.2-3 mL. It was then transferred and loaded onto a silica gel column (1.5 x 15.0 cm) prepared in *n*-hexane. The following fractions were eluted:

(i) A red color solution in a mixture of *n*-hexane: toluene (4:1, 20 mL) which when concentrated to dryness yielded unreacted $[CpMo(CO)_2]_2$ (**3**) (8 mg, 0.0184 mmol, 4% yield)

(ii) A dark greenish brown in *n*-hexane: toluene (1:2, 25 mL) which when evaporated under reduced pressure, yielded dark green crystalline solids of *trans-syn* $[CpMo(CO)(SC_6H_{11})]_2$ (**8a**) (45 mg,0.074 mmol, 16.09% yield). Anal. Found : ^{1}H NMR (Benzene-d_6) : δ 0.97- 1.68 (m, C_6H_{11}) ,δ 4.95, 5.05 (s, C_5H_5). ^{13}C NMR (Benzene-d_6) : 26.98, 27.32, 37.40 (C_6H_{11}), δ 90.56, 90.91 (C_5H_5), δ 247.19, 251.60 (CO). I.R. υ(CO) at 1852vs, 1843vs ; other bands, 1255w, 1026w, 887m, 530w, 478w cm^{-1} (nujol). Anal. Calcd. for $C_{24}H_{32}Mo_2O_2S_2$: C, 45.6; H, 3.8; Mo, 30.4; S,20.3. Found :C,45.6; H, 3.4; Mo, 30.7; S, 19.8%.

(iii) A yellowish green in *n*-hexane: toluene (1:2, 18 mL) which upon concentration to dryness under *vacuo* gave green crystallines solids of *trans-anti*-$[CpMo(CO)(SC_6H_{11})]_2$ (**8b**) (47 mg,0.077 mmol, 16.74% yield). Anal. Found : ^{1}H NMR (Benzene-d_6) : δ 0.97-1.68 (m, C_6H_{11}) , δ 5.12 (s, C_5H_5). ^{13}C NMR (Benzene-d_6) : 26.98, 27.32, 37.40 (C_6H_{11}), δ 91.40 (C_5H_5), δ 250.22 (CO). I.R. υ(CO) at 1858vs, 1819sh ; other bands, 1255w, 887w, 480w cm^{-1} (nujol). Anal. Calcd. for $C_{24}H_{32}Mo_2O_2S_2$: C, 44.7; H, 3.5; Mo, 31.2; S,20.7. Found :C,44.7; H, 3.3; Mo, 31.1; S, 18.6%.

(iv) A purple fraction in a mixture of toluene: ether (1:0.5, 50 mL) which when evaporated under reduced pressure yielded fine dark purple crystals of $[(CpMoSC_6H_{11})_2 CO(O)]$ (**9**) (49 mg, 0.0821 mmol, 17.8% yield). Anal. Found : ^{1}H NMR (Benzene-d_6) : δ 0.89- 1.29 (m, C_6H_{11}), δ 5.22, 5.78 (s, C_5H_5). ^{13}C NMR (Benzene-d_6) : δ 26.85, 27.65, 44.47 (C_6H_{11}) , δ 88.74, 106.90 (C_5H_5) , δ 270.37 (CO). I.R. υ(CO) at 1814s; υ(Mo=O) at 883s; other bands, 1258m, 1186w, 996m, 816w, 788w cm^{-1} (nujol). Anal. Calcd. for $C_{23}H_{32}O_2S_2Mo_2$: C, 47.6; H, 3.7; Mo, 29.3; S, 14.6. Found: C, 47.5; H, 3.8; Mo, 30.2; S, 14.9%

(v) A brown fraction in a mixture of ether: THF (1: 0.5, 40 mL) which when evaporated under reduced pressure, yielded dark brown crystalline solids of $[Cp_3Mo_3(CO)_4(O)(SC_6H_{11})]$ (**10**) (34 mg, 0.0468 mmol, 10.17% yield). Anal. Found : ^{1}H NMR (Benzene-d_6) : δ 0.88- δ 0.97 (m,C_6H_{11}), δ 4.87, 4.77, 4.21 (s, C_5H_5). ^{13}C NMR (Benzene-d_6) : δ 26.14, 36.78 (C_6H_{11}), δ 94.02, 95.52, 111.22 (C_5H_5), δ 253.53, 269.95, 272.71, 273.34 (CO). I.R. υ(CO) at 1946m, 1927m, 1814m, 1759m, other bands ,1096m, 821w, 723vw cm^{-1} (nujol). Anal. Calcd. for $C_{25}H_{26}Mo_3O_5S$: C, 49.4; H, 3.5; Mo, 28.2; S, 9.4. Found : C,49.5; H, 3.6; Mo, 25.8; S, 9.3%. A brown layer remained uneluted at the top rim of the column.

3.4.3 Thermolysis reactions

(i) Thermolysis reaction of $[CpMo(CO)(SC_6H_{11})]_2$ (8)

A yellowish green solution of **8** (20 mg, 0.0329 mmol) in deuterated benzene (ca. 1 mL) in a 5 mm. NMR tube was maintained at 70 ºC and its ^1H NMR spectrum (δ 5.12) was monitored at intervals. After 2 h, there was observed an approximate 3% of **8a** together with unconverted of **8b** (97%)**.** At 4 h, **8b** is converted to other secondary products of $[(CpMoSC_6H_{11})_2CO(O)]$ (**9**) (2% yield), $Cp_3Mo_3(CO)_4(O)(SC_6H_{11})]$ (**10**) (1% yield), and its *trans-syn* isomer, **8a** (31% yield) and the unconverted **8b** (57% yield). After 10 h, the final solution contained $[(CpMoSC_6H_{11})_2CO(O)]$ (**9**) (7% yield), $Cp_3Mo_3(CO)_4(O)(SC_6H_{11})]$ (**10**) (4% yield) and also found unconverted **8b** (47%) but the yield for trans-syn$[CpMo(CO)(SC_6H_{11})]_2$ (**8a**) (6% yield) was decreased.

(ii) Thermolysis reaction of $[(CpMoSC_6H_{11})_2CO(O)]$ (9)

A purple solution of **9** (20 mg, 0.0335 mmol) in deuterated benzene (ca. 1 mL) in a 5 mm. NMR tube was maintained at 70 ºC for 10 h. Its ^1H NMR spectrum showed that the resultant dark brownish purple solution consists of $[(CpMoSC_6H_{11})_2CO(O)]$ (**9**) (31% yield) , $[Cp_3Mo_3(CO)_4(O)(SC_6H_{11})]$ (**10**) (27% yield) together with some uncharacterized precipitates.

(iii) Thermolysis reaction of $[Cp_3Mo_3(CO)_4(O)(SC_6H_{11})]$ (10)

A dark brown solution of $[Cp_3Mo_3(CO)_4(O)(SC_6H_{11})]$ (**10**) (7 mg, 0.0097 mmol) in $C_6D_5CD_3$ (~ 0.5 mL) in a 5 mm septum capped NMR tube was thermolyzed at 100 ºC for 10 h. The reaction was monitored by ^1H NMR at regular intervals. After 8 h, weak resonances **10** (δ 4.87, 4.77, 4.21) were present in the solution. Total decomposition as indicated by the complete disappearance of the Cp resonances took place after 10 h. From the spectra, an organic fragment was left in the solution.

3.5 Reaction of $[CpCr(CO)_3]_2$ (1) with Thienyl Disulfide

3.5.1 At room temperature

A deep green suspension of $[CpCr(CO)_3]_2$ (**1**) (200 mg, 0.497 mmol) in toluene (15 mL) containing thienyl disulfide $[C_4H_3S_2]_2$ (115 mg, 0.497 mmol) was stirred at room temperature. After 20 min, a homogeneous reddish brown solution was obtained, but the reaction was allowed to proceed for 2 h. The resultant reddish brown solution was concentrated to ca. 2 mL in vacuo and then loaded onto a silica gel column (1.5 x 12 cm). The following fractions were eluted:

(i) A orangy brown fraction in toluene: ether (2: 1, 35 mL) which when concentrated to dryness yielded $CpCr(CO)_3H$ (**11**) (90 mg, 0.445 mmol, 89.5% yield)

(ii) A yellowish brown fraction in *n*-hexane: toluene (4: 1, 20 mL) which when concentrated to dryness yielded deep green crystalline solids of $[CpCr(CO)_2]_2S$ (**5**) (23 mg, 0.0714 mmol, 14.4% yield). A greenish blue layer remained uneluted at the top rim of the column.

3.5.2 At 60°C

A deep green suspension of $[CpCr(CO)_3]_2$ (**1**) (200 mg, 0.497 mmol) in toluene (15 mL) containing thienyl disulfide $[C_4H_3S_2]_2$ (115 mg, 0.497 mmol) was stirred at 60°C for 30 min. A dark purple solution was obtained. The resultant purple solution was concentrated to ca. 2 mL and loaded onto a silica gel column (1.5 x 10 cm) prepared in *n*-hexane.

The following fractions were eluted:

(i) A yellowish brown fraction in *n*-hexane: toluene (2: 1, 10 mL) which when concentrated to dryness yielded green crystalline solids of $[CpCr(CO)_2]_2S$ (**5**). (25 mg, 0.0776 mmol, 15.6% yield)

(ii) A deep purple fraction in toluene: ether (2: 1, 40 mL) which when concentrated to dryness yielded dark purple crystalline solids of $[CpCr(S_2C_4H_3)]_2S$ (**12**). (150 mg, 0.302 mmol, 60.8% yield). Anal. Found : ^1H NMR (Benzene-d_6) : δ 12.72 (br, Cp, $\nu_{1/2}$ = 30 Hz) δ 7.12, 7.36 (m, $C_4H_3S_2$). ^{13}C NMR (Benzene-d_6) : δ 101.04 (C_5H_5), δ131.24, δ 132.83, δ 134.84, δ 135.12 ($C_4H_3S_2$). I.R.: 1052w, 1015w, 839vw, 804m, 722w cm^{-1} (nujol). Anal. Calcd. for $C_{18}H_{16}Cr_2S_5$: C, 43.09; H, 2.76; Cr, 14.36; S, 9.6. Found: C, 43.37; H, 2.58; Cr, 14.39; S, 9.5%.

3.5.3 Thermolysis reactions

(i) Thermolysis reaction of $[CpCr(S_2C_4H_3)]_2S$ (12)

A dark purple solution of **12** (20 mg, 0.0403 mmol) in deuterated toluene was maintained at 100 ºC under an oil bath, its NMR spectra was monitored at intervals time. After 12 h it completely changed to **7**.

3.5.4 Reactivity studies of $[CpCr(CO)_2]_2$ (2) with Thienyl Disulfide

A deep green solution of **2** (100 mg, 0.289 mmol) in toluene (15 mL) containing thienyl disulfide (66.5 mg, 0.289 mmol) was stirred for 3h at 110ºC. The resultant purple solution was concentrated and loaded onto a silica gel column (1.5 x 10 cm) prepared in *n*-hexane. The following fractions were eluted out:

(i) A yellowish brown fraction in *n*-hexane: toluene (2: 1, 8 mL) which when concentrated to dryness gave a green crystalline solids of $[CpCr(CO)_2]_2S$ (**5**). (13 mg, 0.0403 mmol, 13.9%)

(ii) A deep purple solution in toluene: ether (2: 1, 30 mL) was eluted out; which when concentrated gave a dark purple crystalline solids of **12** (83 mg, 0.167 mmol, 57.8%).

3.5.5 Reactivity studies of $[CpCr(CO)_2]_2S$ (5) with Thienyl Disulfide

A dirty green mixture of **5** (20 mg, 0.0621 mmol) and thienyl disulfide (14.3 mg, 0.0621 mmol) prepared in deuterated benzene in a 5mm NMR tube was reacted at 60 ºC under an oil bath for 20 h. **5** (8 mg, 39.9 %), **12** (5 mg, 16.1 %) were found.

3.6 Reaction of $[CpMo(CO)_2]_2$ (4) with Thienyl disulfide

3.6.1 At 70 °C

A solution of $[CpMo(CO)_2]_2$ (**2**) (300 mg, 0.691 mmol) in toluene (20 mL) was reacted with an equimolar of thienyl disulfide $[C_4H_3S_2]_2$ (159 mg, 0.691 mmol) and stirred for 4 h at 70 °C. The resultant dark brownish red reaction mixture was concentrated to ca. 2-3 mL. Then the filtrate was transferred and loaded onto a silica gel column (1.5 x 13 cm) prepared in *n*-hexane. The following fractions were eluted:

(i) A dark red fraction in n-hexane (30 mL) which when concentrated to dryness yielded unreacted $[CpMo(CO)_2]_2$ (**2**) (37 mg, 0.0852 mmol, 12.33% yield)

(ii) A greenish brown fraction in *n*-hexane: toluene (1: 2, 48 mL) which when evaporated under reduced pressure yielded dark brown crystalline solids of $[CpMo(CO)(C_4H_3S_2)]_2$ (**13a**) (74 mg, 0.122 mmol, 17.66 % yield). Anal. Found : ^{1}H NMR (Benzene-d_6) : δ 4.92, 5.31 (s, C_5H_5), δ 6.69, 6.78, 6.90, 7.02 (m, $C_4H_3S_2$). ^{13}C NMR (Benzene-d_6) : 92.45, 92.48 (d, C_5H_5), δ126.26, 127.88, 129.67, 130.06 ($C_4H_3S_2$), δ 245.65, 246.73 (CO). I.R. υ(CO) at 1830s, 1865s; other bands, 1418w, 1218w, 1210vw, 1062w, 807w, 694w cm^{-1} (nujol). Anal. Calcd. for $C_{20}H_{16}Mo_2O_2S_4$: C, 50.01; H, 3.87; Mo, 30.73; O, 5.12; S,10.27. Found : C, 49.88; H, 3.96; Mo, 31.02; O, 5.63; S, 10.83%.

(iii) A yellowish green fraction in *n*-hexane: toluene (1: 3, 35 mL) which when concentrate to dryness under *vacuo* gave green crystalline solids of *trans-anti*-$[CpMo(CO)(C_4H_3S_2)]_2$ (**13b**) (62 mg, 0.102 mmol, 14.76% yield). Anal. Found : ^{1}H NMR (Benzene-d_6) : δ 5.09 (s, C_5H_5), δ 6.69, 6.78, 6.90, 7.02 (m, $C_4H_3S_2$). ^{13}C NMR (Benzene-d_6): δ 91.75 (s, C_5H_5), δ126.26, 127.88, 129.67, 130.06 ($C_4H_3S_2$), δ 242.09 (CO). I.R. υ(CO) at 1909vs, other bands, 1418w, 1218w, 1210vw, 1062w, 807w, 694w cm^{-1} (nujol). Anal. Calcd. for $C_{20}H_{16}Mo_2O_2S_4$: C, 50.03; H, 3.85; Mo, 30.80; O, 5.30; S,10.40. Found: C, 50.01; H, 3.85; Mo, 30.96; O, 5.78; S, 10.53%.

(iv) A purple fraction in toluene: ether (2: 0.5, 15 mL) which was obtained as a purple crystalline solids of $[CpMo(O)(C_4H_3S_2)]_2O$ (**14**) (27 mg, 0.044 mmol, 6.37% yield). Anal. Found: ^1H NMR (Benzene-d_6) : δ 4.79, δ 4.95 (s, C_5H_5), δ7.03, 7.12, 7.70 (m, $C_4H_3S_2$). ^{13}C NMR (Benzene-d_6) : δ 91.48, 95.51(C_5H_5), δ 135.10, 135.40, 130.57, 128.63($C_4H_3S_2$). I.R. υ(CO) at 1953m, 1826m, other bands, 1060w, 809w, 723w, 702w cm^{-1} (nujol). Anal. Calcd. for $C_{18}H_{16}Mo_2O_3S_4$: C, 45.6; H, 3.8; Mo, 30.4; O, 5.67; S, 14.6. Found: C,45.0, H, 3.8; Mo, 30.4; O, 5.63; O, 5.67, S, 20.5%.

3.6.2 At 110 ºC

A solution of $[CpMo(CO)_2]_2$ (**2**) (300 mg, 0.691 mmol) in toluene (20 mL) was reacted with an equimolar of thienyl disulfide $[C_4H_3S_2]_2$ (159 mg, 0.691 mmol) and stirred for 1.5 h at 70 °C. The resultant dark brown reaction mixture was then filtered via a sintered glass funnel to remove an uncharacterized insoluble black residue (97 mg). The filtrate was then concentrated onto ca. 2 mL and loaded onto a silica gel column (1.5 x 15 cm) prepared in *n*-hexane. The following fractions were eluted:

(i) A red solution eluted in *n*-hexane (30 mL) which when concentrated to dryness yielded unreacted $[CpMo(CO)_2]_2$ (**2**) (13 mg, 0.0299 mmol, 4.33 %)

(ii) A greenish brown fraction in *n*-hexane: toluene (1: 2, 35 mL) which when evaporated under reduced pressure yielded dark brown crystalline solids of $[CpMo(CO)(C_4H_3S_2)]_2$ (**13a**) (54 mg, 0.0887 mmol, 12.84% yield). Anal. Found : ^1H NMR (Benzene-d_6) : δ 4.92, 5.31 (s, C_5H_5), δ 6.69, 6.78, 6.90, 7.02 (m, $C_4H_3S_2$). ^{13}C NMR (Benzene-d_6) : 92.45, 92.48 (d, C_5H_5), δ126.26, 127.88, 129.67, 130.06 ($C_4H_3S_2$), δ 245.65, 246.73 (CO). I.R. υ(CO) at 1830s, 1865s; other bands, 1418w, 1218w, 1210vw, 1062w, 807w, 694w cm^{-1} (nujol). Anal. Calcd. for $C_{20}H_{16}Mo_2O_2S_4$: C, 50.01; H, 3.87; Mo, 30.73; O, 5.12; S,10.27. Found : C, 49.88; H, 3.96; Mo, 31.02; O, 5.63; S, 10.83%.

(iii) A yellowish green fraction in *n*-hexane: toluene (1: 3, 28 mL) which when concentrate to dryness under *vacuo* gave green crystalline solids of *trans-anti* $[CpMo(CO)(C_4H_3S_2)]_2$ (**13b**) (64 mg, 0.105 mmol, 15.20% yield). Anal. Found : ^{1}H NMR (Benzene-d_6) : δ 5.09 (s, C_5H_5), δ 6.69, 6.78, 6.90, 7.02 (m, $C_4H_3S_2$). ^{13}C NMR (Benzene-d_6): δ 91.75 (s, C_5H_5), δ126.26, 127.88, 129.67, 130.06 ($C_4H_3S_2$), δ 242.09 (CO). I.R. υ(CO) at 1909vs, other bands, 1418w, 1218w, 1210vw, 1062w, 807w, 694w cm^{-1} (nujol). Anal. Calcd. for $C_{20}H_{16}Mo_2O_2S_4$: C, 50.03; H, 3.85; Mo, 30.80; O, 5.30; S,10.40. Found: C, 50.01; H, 3.85; Mo, 30.96; O, 5.78; S, 10.53%.

(iv) A purple fraction in toluene: ether (2: 0.5, 15 mL) which was obtained as an purple crystalline solids of $[CpMo(O)(C_4H_3S_2)]_2O$ (**14**) (31 mg, 0.0503 mmol, 7.28% yield). Anal. Found: ^{1}H NMR (Benzene-d_6) : δ 4.79, δ 4.95 (s, C_5H_5), δ7.03, 7.12, 7.70 (m, $C_4H_3S_2$). ^{13}C NMR (Benzene-d_6) : δ 91.48, 95.51(C_5H_5), δ 135.10, 135.40, 130.57, 128.63($C_4H_3S_2$). I.R. υ(CO) at 1953m, 1826m, other bands, 1060w, 809w, 723w, 702w cm^{-1} (nujol). Anal. Calcd. for $C_{18}H_{16}Mo_2O_3S_4$: C, 50.01; H, 3.87; Mo, 30.73; O, 5.12; S, 10.27. Found : C,49.88, H, 3.96; Mo, 31.02; O, 5.63; S, 10.83%.

3.6.3 Thermolysis reactions

(i) Thermolysis reaction of $[CpMo(CO)(C_4H_3S_2)]_2$ (13)

A greenish yellow solution of **13** (20 mg, 0.0328 mmol) in C_6D_6 (0.5 mL) in a 5 mm NMR tube was thermolyzed at 70ºC for 9 h. After 2 h, an approximate of 6% of **13a** together with unconverted of **13b (**94%) were present in the solution. At 3 h, **13b** is converted to other secondary products of $[CpMo(O)(C_4H_3S_2)]_2O$ (**14**) (9.7% yield), and its *trans-syn* isomer **13a** (29% yield) and the unconverted **13b** (43% yield). After 9 h, the final solution consisted of $[CpMo(O)(C_4H_3S_2)]_2O$ (**14**) (14.3% yield) together with unconverted **13b** (33% yield) but the yield for trans-syn **13a** (9% yield) was decreased.

(ii) Thermolysis reaction of $[CpMo(O)(C_4H_3S_2)]_2O$ (14)

The complex $[CpMo(O)(C_4H_3S_2)]_2O$ (8 mg, mmol) were dissolved in C_6D_6 in (0.5 mL) in a 5mm NMR tube. The purple solution was thermolyzed at 70 ºC and was monitored *via* ^1H NMR at regular intervals of 2 h. After 22 h, the resultant dark brown solution consists of **14** (9.7%) together with some uncharacterized dark brown precipitates.

3.7 Formation of specific transition metal carbonyl fragments adduct of $[CpCr(S_2C_4H_3)]_2S$

3.7.1 Reaction of $[CpCr(S_2C_4H_3)]_2S$ (12) with 2 mole equivalent of $Fe_2(CO)_9$ at room temperature

A mixture of $[CpCr(S_2C_4H_3)]_2S$ (**12**) (100 mg, 0.201 mmol) and $Fe_2(CO)_9$ (146.53 mg, 0.403 mmol) were dissolved in THF in a Schlenk flask. The reaction was stirred at room temperature under a CO atmosphere. The color of the solution was changed from dark purple to brownish purple after 15 h of vigorous stirring. The reaction mixture was concentrated to dryness and the residue redissolved in toluene (ca. 2 mL) and chromatographed on a silica gel column (1.5 cm x 12 cm) prepared in *n*-hexane. Two fractions were eluted:

(i) An unreacted orange brown solution was eluted out with *n*-hexane: toluene (3: 1, 10 mL) which when concentrated to dryness yielded $Fe_2(CO)_9$ (8 mg, 0.022 mmol, 10.95% yield).

(ii) A brownish purple fraction was eluted with *n*-hexane: toluene (2: 1, 25 mL) which on concentration to ca. 2 mL and slow crystallization at -28 ºC for 4 days yielded fine dark purplish brown crystals of $[Cp_2Cr_2(S_2C_4H_3)]S_2[Fe(CO)_3]$ (**15**) (38 mg, 0.0687 mmol, 34.18% yield). Anal. Found: ^{1}H NMR (Benzene-d_6) : δ 4.77(s, C_5H_5), δ7.03, 7.12, 7.70 (m, $C_4H_3S_2$). ^{13}C NMR (Benzene-d_6): δ 97.51(C_5H_5), δ 135.10, 135.40, 130.57, 128.63($C_4H_3S_2$). I.R. υ (CO) at 2021m, 1946m, other bands, 1216w, 1056sh, 1012w, 701w cm^{-1} (nujol). Anal. Calcd. for $C_{17}H_{13}Cr_2FeO_3S_4$: C, 42.79; H, 3.05; Cr, 18.52; Fe, 9.95; O, 8.55; S, 17.14. Found: C, 43.16; H, 3.11; Cr, 18.55; Fe, 9.98; O, 8.69; S, 16.96

(iii) A brownish green fraction was eluted with toluene (18 mL) which when concentrated to dryness yielded an uncharacterized dark brown precipitate (12 mg).

(iv) An unreacted dark purple fraction was eluted out with toluene: ether (1:1/2, 10 mL) which when concentrated to dryness yielded $[CpCr(S_2C_4H_3)]_2S$ (**12**) (6 mg, 0.012 mmol, 5.97% yield).

A dark greenish brown rim remained on top of the column.

3.8 Crystal Structure Determinations

3.8.1 Structure determination of $[CpCr(SC_6H_{11})]_2S$ (6) and $[CpCr(S_2C_4H_3)]_2S$ (12)

Diffraction quality single crystals of **6** obtained as dark purple rod shape which were grown from THF layered with ether after 3 weeks at -28ºC.

Diffraction quality single crystals of **12** obtained as dark purple block which were grown in THF layered with ether after 1 week at -28ºC.

Both crystals were coated with low temperature oil to prevent decomposition in air. Details of crystal parameters, data collection, and structure refinement were given in Table 17 and 18.

Method of Determination

The crystals are mounted on quartz fibers. X-ray data were collected on a Bruker APEX-II diffractometer equipped with a CCD area detector using Mo Kα radiation (λ = 0.71073 Å). The structure was solved by direct methods with SHELXL-97 and refinements were from SHELXL-97[48]. The structure of **6** refined to R= 0.0671 for the 6350 reflections, and **12** to R= 0.0502 for 4289 reflections.

3.8.2 Structure determination of $[CpMo(CO)(SC_6H_{11})]_2$ (8b) , $[(CpMoSC_6H_{11})_2CO(O)]$ (9) and $[Cp_3Mo_3(CO)_4(O)(SC_6H_{11})]$ (10)

Diffraction quality single crystals of **8b** obtained as crystalline dark green in block shape which were grown from THF layered with ether after 3 days at ambient temperature. Complex **9** was obtained as crystalline dark purple rod shape; which were grown from a saturated solution toluene/THF after 4 days at ambient temperature. Complex **10** was obtained as dark brown crystals which were grown from THF layered with ether after 2 days at ambient temperature. Details of crystal parameters, data collection, and structure refinement were given in Table 19, 20 and 21.

Method of Determination

Diffractions measurements were carried out at -173 ºC for **8b**, **9** and **10** on a Bruker APEX-II diffractometer equipped with Mo Kα radiation. Structures solution and refinement were carried out with the Bruker-SHELXTL programs [49].

3.8.3 Structure determination of $[CpMo(CO)(C_4H_3S_2)]_2$ (13b) and $[CpMo(O)(C_4H_3S_2)]_2O$ (14)

Diffraction quality single crystals of **13** obtained as crystalline dark green rod shape from THF/ether mixture after 5 days at ambient temperature; Complex **14** was obtained as dark brown crystals; crystallized from a saturated solution toluene/THF after 1 week. Details of crystal parameters, data collection, and structure refinement were given in Table 22 and 23.

Method of Determination

The crystals are mounted on quartz fibers. X-ray data were collected on a Bruker APEX-II diffractometer equipped with a CCD area detector using Mo Kα radiation (λ = 0.71073 Å). The structure was solved by direct methods with SHELXL-97 and

refinements were from SHELXL-97 [48]. The structure of **13** refined to R= 0.0208 for the 9463 reflections, and **14** to R= 0.0206 for 9328 reflections.

3.8.4 Structure determination of $[Cp_2Cr_2(S_2C_4H_3)]S_2[Fe(CO)_3]$ (**15**)

Diffraction quality single crystals of **15** obtained as crystalline dark brownish purple blocks grown from *n*-hexane/toluene mixture after 4 days at -28 ºC. Details of crystal parameters, data collection, and structure refinement were given in Table 24.

Method of Determination

The crystals are mounted on quartz fibers. X-ray data were collected on a Bruker APEX-II diffractometer equipped with a CCD area detector using Mo Kα radiation (λ = 0.71073 Å). The structure was solved by direct methods with SHELXL-97 and refinements were from SHELXL-97 [48]. The structure of **15** refined to R= 0.0342 for the 18833 reflections.

Table 17. Crystal data and processing parameters of $[CpCr(SC_6H_{11})]_2S$ (**6**).

Complex	$[CpCr(SC_6H_{11})]_2S$ (**6**)
Empirical formula	$C_{22}H_{31.75}Cr_2S_3$
Formula weight	496.40
Temperature (K)	100(2) K
Wavelength (Å)	0.7107
Crystal system	Orthorhombic
Space group	Pna21
Unit cell dimension	
a (Å)	18.4262(3)
b (Å)	13.7686(2)
c (Å)	17.4883(3)
α (º)	90
β (º)	90
γ (º)	90
Volume $Å^3$	4436.83(12)
Z	8
Density (Mg m^{-3})	1.486
Absorption coefficient (mm^{-1})	1.267
F(000)	2078
Crystal size	0.13 x 0.1x 0.04 mm
θ range for data collection	1.85 to 23.25 º
Limiting indices	-20<=h<=20 -15<=k<=15 -19<=l<=18
Reflections collected / unique	24403 / 6350 [R(int) = 0.0573]
Data / restraints / parameters	6350 / 399 / 524
Goodness-of-fit on F^2	1.078
Final R indices [I>2σ(I)]	R1 = 0.0671 wR2 = 0.1672
R indices (all data)	R1 = 0.0755 wR2 = 0.1764
Largest diff. peak and hole (eA^{-3})	1.975 and -0.544 eA^{-3}

Table 18. Crystal data and processing parameters of $[CpCr(S_2C_4H_3)]_2S$ (**12**).

Complex	$[CpCr(S_2C_4H_3)]_2S$ (**12**)
Empirical formula	$C_{18}\ H_{16}\ Cr_2\ S_5$
Formula weight	496.61
Temperature (K)	100(2) K
Wavelength (Å)	0.71073 A
Crystal system	Monoclinic
Space group	P21/n
Unit cell dimensions	
a (Å)	9.6040(4)
b(Å)	9.8300(4)
c (Å)	20.8497(10)
α (º)	90
β (º)	102.835(5)
γ (º)	90
Volume $Å^3$	1919.18(14)
Z	4
Density (Mg m^{-3})	1.719
Absorption coefficient (mm $^{-1}$)	1.675
F(000)	1008
Crystal size	0.30 x 0.05 x 0.05
θ range for data collection	2.30 to 27.50 deg.
Limiting indices	-11<=h<=12 -12<=k<=12 -20<=l<=27
Reflections collected / unique	9582 / 4289 [R(int) = 0.0340]
Data / restraints / parameters	4289 / 28 / 227
Goodness-of-fit on F^2	1.109
Final R indices [I>2 σ (I)]	R1 = 0.0502 wR2 = 0.1234
R indices (all data)	R1 = 0.0632 wR2 = 0.1310
Largest diff. peak and hole (eA^{-3})	1.094 and -0.607 eA^{-3}

Table 19. Crystal data and processing parameters of $[CpMo(CO)(SC_6H_{11})]_2$ (**8b**).

Complex	$[CpMo(CO)(SC_6H_{11})]_2$ (**8b**)
Empirical formula	$C_{24}\,H_{32}\,Mo_2\,O_2\,S_2$
Formula weight	608.50
Temperature (K)	100(2) K
Wavelength (Å)	0.71073 A
Crystal system	Triclinic
Space group	P(-1)
Unit cell dimensions	
a (Å)	7.74770(10)
b (Å)	9.62470(10)
c(Å)	10.51620(10)
α (º)	107.6079(9)
β (º)	106.9781(8)
γ (º)	112.2333(7)
Volume $Å^3$	614.076(12)
Z	1
Density (Mg m^{-3})	1.645
Absorption coefficient (mm^{-1})	1.209
F(000)	308
Crystal size	0.40 x 0.05 x 0.1 mm
θ range for data collection	2.29 to 27.50 deg.
Limiting indices	-10<=h<=9 -12<=k<=12 -13<=l<=13
Reflections collected / unique	5823 / 2799 [R(int) = 0.0164]
Data / restraints / parameters	2799 / 0 / 136
Goodness-of-fit on F^2	1.153
Final R indices [I>2sigma(I)]	R1 = 0.0205 wR2 = 0.0634
R indices (all data)	R1 = 0.0225 wR2 = 0.0674
Largest diff. peak and hole (eA^{-3})	0.357 and -0.433 eA^{-3}

Table 20. Crystal data and structure refinement for $[(CpMoSC_6H_{11})_2CO(O)]$ (**9**).

Complex	$[(CpMoSC_6H_{11})_2CO(O)]$ (**9**)
Empirical formula	$C_{23}\ H_{32}\ Mo_2\ O_2\ S_2$
Formula weight	596.49
Temperature K	100(2) K
Wavelength (Å)	0.71073 A
Crystal system	monoclinic
Space group	P21
Unit cell dimensions	
a (Å)	9.8247(2)
b (Å)	20.5313(5)
c(Å)	11.5389(3)
α (º)	90
β (º)	92.5720(10)
γ (º)	90
Volume $Å^3$	2325.21(10)
Z	2
Calculated density (Mg m^{-3})	1.704
Absorption coefficient (mm^{-1})	1.275
F(000)	1208
Crystal size	0.60 x 0.20 x 0.04
θ range for data collection	1.77 to 27.50
Limiting indices	-12<=h<=12 -26<=k<=26 -14<=l<=14
Reflections collected / unique	22116 / 10091 [R(int) = 0.0691]
Data / restraints / parameters	10091 / 121 / 488
Goodness-of-fit on F^2	0.986
Final R indices [I>2σ (I)]	R1 = 0.0509 wR2 = 0.0830
R indices (all data)	R1 = 0.0871 wR2 = 0.0933
Largest diff. peak and hole (eA^{-3})	1.159 and -0.852 eA^{-3}

Table 21. Crystal data and structure refinement for $[Cp_3Mo_3(CO)_4(O)(SC_6H_{11})]$ (**10**).

Complex	$[Cp_3Mo_3(CO)_4(O)(SC_6H_{11})]$ (**10**)
Empirical formula	$C_{25}\ H_{26}\ Mo_3\ O_5\ S$
Formula weight	723.45
Temperature K	100(2) K
Wavelength (Å)	0.71073 A
Crystal system	monoclinic
Space group	P21/n
Unit cell dimensions	
a (Å)	11.6441(7)
b (Å)	15.0388(9)
c (Å)	16.4414(10)
α (º)	90
β (º)	98.0690(10)
γ (º)	90
Volume $Å^3$	2850.6(3)
Z	4
Calculated density (Mg m^{-3})	1.860
Absorption coefficient (mm^{-1})	1.415
F(000)	1592
Crystal size	0.25 x 0.20 x 0.15 mm
θ range for data collection	1.84 to 27.50 º
Limiting indices	-15<=h<=14 -19<=k<=19 -21<=l<=21
Reflections collected / unique	26785 / 6540 [R(int) = 0.0403]
Data / restraints / parameters	6540 / 80 / 397
Goodness-of-fit on F^2	0.990
Final R indices [I>2σ(I)]	R1 = 0.0287 wR2 = 0.0574
R indices (all data)	R1 = 0.0454 wR2 = 0.0631
Largest diff. peak and hole (eA^{-3})	0.781 and -0.549 eA^{-3}

Table 22. Crystal data and structure refinement for $[CpMo(CO)(C_4H_3S_2)]_2$ (**13b**).

Complex	$[CpMo(CO)(C_4H_3S_2)]_2$ (**13b**)
Empirical formula	$C_{20}H_{16}Mo_2O_2S_4$
Formula weight	608.45
Temperature K	100(2) K
Wavelength (Å)	0.71073 A
Crystal system	Monoclinic
Space group	P2(1)/c
Unit cell dimensions	
a (Å)	8.44150(10)
b (Å)	16.1804(2)
c (Å)	7.58040(10)
α (º)	90
β (º)	99.7477(5)
γ (º)	90
Volume $Å^3$	1020.43(2)
Z	2
Calculated density (Mg m^{-3})	1.980
Absorption coefficient (mm^{-1})	1.653
F(000)	600
Crystal size	0.33 x 0.25 x 0.04 mm
θ range for data collection	2.45 to 27.50 º
Limiting indices	-10<=h<=10 -21<=k<=21 -9<=l<=9
Reflections collected / unique	9463 / 2336 [R(int) = 0.0163]
Data / restraints / parameters	2336 / 38 / 140
Goodness-of-fit on F^2	1.001
Final R indices [I>2σ(I)]	R1 = 0.0208 wR2 = 0.0510
R indices (all data)	R1 = 0.0228 wR2 = 0.0521
Largest diff. peak and hole (eA^{-3})	0.538 and -0.553 eA^{-3}

Table 23. Crystal data and structure refinement for $[CpMo(O)(C_4H_3S_2)]_2O$ (**14**).

Complex	$[CpMo(O)(C_4H_3S_2)]_2O$ (**14**)
Empirical formula	$C_{18}\ H_{16}\ Mo_2\ O_3\ S_4$
Formula weight	600.43
Temperature K	100(2) K
Wavelength (Å)	0.71073 A
Crystal system	Monoclinic
Space group	P2(1)/c
Unit cell dimensions	
a(Å)	9.54440(10)
b(Å)	11.9273(2)
c(Å)	9.72480(10)
α (º)	90
β (º)	112.2440(6)
γ (º)	90
Volume $Å^3$	1024.67(2)
Z	2
Calculated density (Mg m^{-3})	1.946
Absorption coefficient (mm^{-1})	1.648
F(000)	592
Crystal size	0.35 x 0.18 x 0.10 mm
θ range for data collection	2.31 to 27.49 º
Limiting indices	-12<=h<=12 -15<=k<=15 -12<=l<=12
Reflections collected / unique	9328 / 2349 [R(int) = 0.0182]
Data / restraints / parameters	2349 / 44 / 140
Goodness-of-fit on F^2	1.040
Final R indices [I>2σ(I)]	R1 = 0.0206 wR2 = 0.0530
R indices (all data)	R1 = 0.0238 wR2 = 0.0547
Largest diff. peak and hole (eA^{-3})	1.011 and -0.370 eA^{-3}

Table 24.Crystal data and structure refinement for $[Cp_2Cr_2(S_2C_4H_3)]S_2[Fe(CO)_3]$ (**15**).

Complex	$[Cp_2Cr_2(S_2C_4H_3)]S_2[Fe(CO)_3]$ (**15**)
Empirical formula	$C_{17}\,H_{13}\,Cr_2\,Fe\,O_3\,S_4$
Formula weight	553.36
Temperature	100(2) K
Wavelength (Å)	0.71073 A
Crystal system	Triclinic
Space group	P(-1)
Unit cell dimensions	
a(Å)	10.20820(10)
b(Å)	11.3952(2)
c(Å)	19.4010(3)
α (º)	102.6930(10)
β (º)	95.0050(10)
γ (º)	113.7580(10)
Volume $Å^3$	1975.65(5)
Z	4
Calculated density (Mg m^{-3})	1.860
Absorption coefficient (mm^{-1})	2.243
F(000)	1108
Crystal size	0.30x 0.13 x 0.2 mm
θ range for data collection	2.02 to 27.50 º
Limiting indices	-13<=h<=13 -14<=k<=14 -25<=l<=25
Reflections collected / unique	18833 / 8988 [R(int) = 0.0225]
Data / restraints / parameters	8988 / 0 / 487
Goodness-of-fit on F^2	1.059
Final R indices [I>2σ(I)]	R1 = 0.0342 wR2 = 0.0881
R indices (all data)	R1 = 0.0457 wR2 = 0.0944
Largest diff. peak and hole (eA^{-3})	0.514 and -0.408eA^{-3}

IV. References

1. (a) Baird, M. C. Chem. Rev. 1988, 88, 1217.

   (b) Tyler, D. R. Prog. Inorg. Chem.1988, 36, 125.

2. Adams, R. D.; Collins, D. E.; Cotton, F. A. J. Am. Chem. Soc. 1974, 96, 749.

3. McLain, S. J. J. Am. Chem. Soc. 1988, 110, 643.

4. (a) Madach, T.; Vahrenkamp, H. Z. Naturforsch. B. 1978, 33b, 1310.

   (b) Rieger, P.H. Coord. Chem. Rev. 1994, 135, 203.

5. (a) Goh, L. Y.; Lim, Y. Y. J. Organomet. Chem. 1991, 402, 209.

   (b) Goh, L. Y.; Khoo, S. K.; Lim, Y. Y. J. Organomet. Chem. 1990, 399, 115.

6. (a) Halpern, J. Pure Appl. Chem. 1986, 58, 575. (b) Kochi, J. K. Organometallic Mechanisms and Catalysis, Academic Press, New York, 1978.

7. Gonzalez, A. A.; Hoff, C. D. Inorg. Chem. 1989, 28, 4295.

8. Ju, T. D.; Lang, R. F.; Roper, G. C.; Hoff, C. D. J. Am. Chem. Soc. 1996, 118, 5328.

9. Capps, K. B.; Bauer, A.; Ju, T. D.; Hoff, C. D. Inorg. Chem. 1999, 38, 6130.

10. Ju, T. D.; Capps, K. B.; Lang, R. F.; Roper, G. C.; Hoff, C. D. Inorg. Chem. 1997, 36, 614.

11. (a) King, R. B.; Organomet. Synth. 1965, 1, 109.

    (b) Keppie, S. A.; Lappert, M. F. J.Chem. Soc. A 1971, 3216.

    (c) Hackett, P.; O'Neill, P. S.; Manning, A. R. J. Chem. Soc. Dalton Trans. 1974, 1625.

    (d) Manning, A. R.; Hackett, P.; Birdwhistell, R.; Soye, P. Organomet. Synth. 1990, 28, 148.

12 Cooley, N. A.; Watson, K. A.; Fortier, S.; Baird, M. C.; Organometallics 1986, 5, 2563.

13 (a) Goh, L. Y.; D'aniello Jr., M. J.; Slater, S; Muetterties, E. L.; Tavanaiepour, I.;Chang, M. I.; Fredrich, M. F.; Day, V. W. Inorg. Chem. 1979, 18, 192.

   (b) Cooley,N. A.; MacConnachie, P. T. F.; Baird, M. C. Polyhedron 1988, 7, 1965.

(c) O'Callaghan, K. A. E.; Brown, S. J.; Page, J. A.; Baird, M. C. Organometallics 1991, 10, 3119.

14. M.D. Curtis, W.M. Butler, J.Organomet. Chem. 155 (1978) 131.

15. a) F.C.Wilson, D.P. Shoemaker, J. Chem. Phys.27 (1957) 809.

b) R.D. Adams, D.M. Collins, F. A. Cotton, Inorg. Chem. 13 (1974) 1086.

16. P.R. Drake, M.C. Baird, J.Organomet. Chem. 363 (1989) 131.

17. R.C. Job, M.D. Curtis, Inorg. Chem., 12 (1973) 2510.

18. D.S. Ginley, M.S. Wrighton, J. Am.Chem.Soc., 97 (1975) 3533.

19. M.D. Curtis, R.J. Klingler., J. Organomet. Chem., 161 (1978) 23.

20. R.J. Klinger, W. M. Butler, M.D. Curtis, J. Am.Chem. Soc. 1978,100,5024.

21. R.B. King, J. Am. Chem. Soc. 85 (1963) 1587

22. (a) L.Y. Goh, T.W. Hambley, G.B. Robertson, J. Chem. Soc. Chem. Commun. (1983) 1458.

(b) L.Y. Goh, T.W. Hambley, G.B. Robertson, Organometallic, 6 (1987)1051.

(c) L.Y. Goh, W. Chen, E. Sinn, J. Chem. Soc. Chem. Commun. (1985) 462.

(d) L.Y. Goh, W.Chen, E. Sinn, Organometallics 7 (1988) 2020.

23. L.Y. Goh, M.S. Tay, T.C.W. Mak, R.J. Wang, Organometallics 11 (1992) 1711.

24. L.Y. Goh, Y.Y. Lim, M.S. Tay, T.C.W. Mak, Z.Y. Zhou, J.Chem. Soc. Dalton Trans. (1992) 1239.

25. L.Y. Goh, M.S. Tay, W. Chen, Organometallics 13 (1994) 1813.

26. J.L. Kice, in: A. Senning (Ed.), In Sulfur in Organic and Inorganic Chemistry, Marcel Dekker, New York, Vol 1 (1971) p.153.

27. P.M. Treichel, J. H. Morris, F. G.A. Stone, J. Chem. Soc., (1963) 720.

28. P.M. Treichel, G. R. Wilkes., Inorg. Chem. 7 (1966) 1182.

29. E.W. Tillay, E.D. Schermer, W.H. Baddley., Inorg. Chem. 7(9) (1968) 1925.

30. I.B. Benson, S.D. Killops, S.A.R. Knox, A.J. Welch., J.C.S. Chem. Comm. (1980) 1137.

31. H. Rakoczy, M. Schollenberger, B.Nuber, M.L. Ziegler., J. Organomet. Chem. 467 (1994) 217.

32. L.C. Song, J.Q. Wang, Q.M. Hu, R.J. Wang, T.C.W. Mak, Inorg. Chim. Acta. 256 (1997) 129.

33. L.C. Song, Y.C. Shi, Q.M. Hu, F. Du, X.A. Mao. Polyhedron 18 (1999) 19.

34. L.C. Song, Y.C. Shi, Q.M. Hu, Y. Chen, J. Sun, J. Organomet. Chem. 626 (2001) 192.

35. P. Schollhammer, F. Y. Pétillon, R. Pichon, S.P. Guilou, J. Talarmin, K.W. Muir, S. E. Girdwood, J. Organomet. Chem. 486 (1995) 183.

36. P. Schollhammer, F. Y. Pétillon, R. Pichon, S.P. Guilou, J. Talarmin, K.W. Muir, L.M. Muir. Organometallics 14 (1995) 2277.

37. R.C.S. Wong, M. L. Ooi, C.F. Chee, G.H. Tan. Inorganica Chimica Acta 358 (2005) 1269- 1273.

38. Z.Q. Weng , L.Y. Goh, Acc.Chem.Res. 37(2004) 187-199.

39. M.A. Alvarez, M. E. Garcia, V. Riera, M.A. Ruiz, C. Bois, Y. Jeannin., J.Am. Chem. Soc., 117 (1995) 1324.

40. C.P. Gibson, A.D. Rae, D.R. Tomchick and L.F. Dahl. J.Organometal.Chem. 340 (1988) C23-C30.

41. R.H Crabtee, M.Lavin. Inorg.Chem. 1986, 25, 805-812.

42.
(a) T. Nagno, K. Arakane, M. Hirobe, Tetrahedron Lett. 21 (1980) 5021;

(b) J. Cuomo, J.H. Merrifield, J.F.W. Keana, J. Am. Chem. Soc. 45 (1980) 4216.

43. (a) J.C. Coupez, M. Guéguen, J.E. Guerchais, F.Y. Pétillon, J. Talarmin., J.Organomet. Chem. 312 (1986) 81 and references cited therein.

(b) J. C. Coupez, J. E. Guerchais, F. Y. Pétillon, J. Talarmin., J. Chem. Soc. Trans. (1986) 1917 and references cited therein.

44. G.W. Haupt, J. Res.Natl.Bur.Stand. USA 48 (1952) 414.

45. R. Birdwhistell, P. Hackett, A.R. Manning, J. Organometal. Chem. 157 (1978) 239.

46. R. Klingler, W.M. Butler, M.D. Curtis, J. Am. Chem. Soc. 97 (1975) 3533.

47. King, R. B. Organometallic Synthesis. Volume 1 Transition-Metal Compounds; Academic Press : New York, 1965. ISBN 0-444-42607-8

48. G.M. Sheldrick, SHELXS97 and SHELXL97, University of Göttingen (1997).

49. G.M. Sheldrick, SADABS, Bruker Nonius area detector scaling and absorption correction V2.05, University of Gottingen, Germany(1999).

50. D. Saurenz, F. Demirhan, P. Richard, R. Poli, H.Sitzmann. Eur. J. Inorg. Chem. 2002 (1415-1424).